NASA-CR-197725

INTERIM
IN-35-CR
Circ
47893
p. 101

DEPARTMENT OF AEROSPACE ENGINEERING
COLLEGE OF ENGINEERING & TECHNOLOGY
OLD DOMINION UNIVERSITY
NORFOLK, VIRGINIA 23529

HOT-WIRE CALIBRATION IN SUBSONIC/TRANSONIC FLOW REGIMES

By

K. A. Nagabushana

and

Robert L. Ash, Principal Investigator

Summary of Research
For the period November 18, 1993 through November 17, 1994

Prepared for
National Aeronautics and Space Administration
Langley Research Center
Hampton, VA 23681-0001

Under
Research Grant NAG-1-1552
Dr. Gregory Jones, Technical Monitor
FLDMD-Experimental Methods Branch

April 1995

N95-25699
Unclas
G3/35 0047893

(NASA-CR-197725) HOT-WIRE CALIBRATION IN SUBSONIC/TRANSONIC FLOW REGIMES Research Report, 18 Nov. 1993 - 17 Nov. 1994 (Old Dominion Univ.) 101 p

Old Dominion University Research Foundation

DEPARTMENT OF AEROSPACE ENGINEERING
COLLEGE OF ENGINEERING & TECHNOLOGY
OLD DOMINION UNIVERSITY
NORFOLK, VIRGINIA 23529

HOT-WIRE CALIBRATION IN SUBSONIC/TRANSONIC FLOW REGIMES

By

K. A. Nagabushana

and

Robert L. Ash, Principal Investigator

Summary of Research
For the period November 18, 1993 through November 17, 1994

Prepared for
National Aeronautics and Space Administration
Langley Research Center
Hampton, VA 23681-0001

Under
Research Grant NAG-1-1552
Dr. Gregory Jones, Technical Monitor
FLDMD-Experimental Methods Branch

Submitted by the
Old Dominion University Research Foundation
P.O. Box 6369
Norfolk, VA 23518

April 1995

HOT-WIRE CALIBRATION IN SUBSONIC/TRANSONIC FLOW REGIMES

by
K.A. Nagabushana and R.L. Ash
Old Dominion University
Department of Aerospace Engineering
Norfolk, VA 23529

Abstract

A different approach for calibrating hot-wires, which simplifies the calibration procedure and reduces the tunnel run-time by an order of magnitude was sought. In general, it is accepted that the directly measurable quantities in any flow are velocity, density, and total temperature. Very few facilities have the capability of varying the total temperature over an adequate range. However, if overheat temperature parameter, a_w, is used to calibrate the hot-wire then the directly measurable quantity, voltage, will be a function of the flow variables and the overheat parameter i.e., $E = f(u,\rho,a_w,T_w)$ where a_w will contain the needed total temperature information. In this report, various methods of evaluating sensitivities with different dependent and independent variables to calibrate a 3-wire hot-wire probe using a constant temperature anemometer (CTA) in subsonic/transonic flow regimes is presented. The advantage of using a_w as the independent variable instead of total temperature, T_o, or overheat temperature parameter, τ, is that while running a calibration test it is not necessary to know the recovery factor, the coefficients in a wire resistance to temperature relationship for a given probe. It was deduced that the method employing the relationship $E = f(u,\rho,a_w)$ should result in the most accurate calibration of hot wire probes. Any other method would require additional measurements. Also this method will allow calibration and determination of accurate temperature fluctuation information even in atmospheric wind tunnels where there is no ability to obtain any temperature sensitivity information at present. This technique greatly simplifies the calibration process for hot-wires, provides the required calibration information needed in obtaining temperature fluctuations, and reduces both the tunnel run-time and the test matrix required to calibrate hot-wires. Some of the results using the above techniques are presented in an appendix.

Nomenclature

a_w $\frac{R_w - R_{adw}}{R_{adw}}$, Overheat temperature parameter

d_w Wire diameter

E Mean voltage across wire

Kn Knudsen number

k_t Thermal conductivity of air at T_o

ℓ Wire length

M Mach number

m Mass of fluid flow

Nu_t Nusselt number

P_w Power to hot-wire

Q_w Heat transfer rate

R_{ref} Resistance of wire at reference temperature T_{ref}

Re_t Reynolds number based on viscosity evaluated at T_o and wire diameter

R_w Resistance of wire

S_u Velocity sensitivity

S_ρ Density sensitivity

S_{T_o} Total temperature sensitivity

T_{adw} Recovery temperature of wire

T_o Total temperature

T_{ref} Reference temperature

T_w Wire temperature

u Velocity

α & β Coefficients in wire resistance to temperature relationship

η $\frac{T_{adw}}{T_o}$, Recovery temperature ratio

ρ Density

γ Ratio of specific heats

θ $\frac{T_w}{T_o}$, Temperature parameter

τ $\frac{T_w - T_{adw}}{T_o}$, Temperature parameter

Introduction

The heat transfer from heated wires in fluid flows has been investigated for many years for various reasons. One of the main reasons in fluid mechanics is the application of the results to hot wire anemometry. The early work in this field was performed by Boussinesq (1905)[1] and King (1914)[2]. Even though "*King's law*" was derived over 75 years ago, it is still being used, in various forms, to predict the heat transfer from heated wires in subsonic incompressible flows. From King's law it can be shown that the heat transfer parameter, Nusselt number, is a function only of Reynolds and Prandtl numbers.

In the 1950's, it was shown that the Nusselt number can be a function of Mach number for Mach numbers as low as 0.10, indicating that King's law does not apply[3,4]. The reason for this disagreement was determined by Spangenberg[5] to be due to gas rarefaction effects. Spangenberg found that $Nu_t = f(Re_t, M, Kn)$, where the apparent Mach number or compressibility effect was a slip flow or Knudsen number effect. Since the Knudsen number is related to the Reynolds and Mach numbers, only two of the three quantities in the relationship for the Nusselt number are required. Experimental results obtained by King and others indicate that the Nusselt number is also a function of a temperature parameter. The functional relationships expressed for Nusselt number are $Nu_t = f(M, Re_t, \theta)$[6] or $Nu_t = f(M, Kn, \tau)$[7,8]. From the

above functional relationship, it has been shown that the mean voltage measured across the heated wire is $E = f(u,\rho,T_o,T_w)$[6].

Theoretical Consideration

To obtain the sensitivity relationships for use in hot wire anemometry, the following heat transfer equation is usually used to describe the heat loss from a heated wire mounted normal to the flow:

$$Q_w = 2\pi\ell k_t (T_w - \eta T_o) Nu_t \tag{1}$$

For steady state conditions the electrical power supplied to the wire is equal to the heat loss from the wire $(P_w = Q_w)$. Differentiating this equation in terms of its logarithmic derivatives yields:

$$d\log Q_w = d\log Nu_t - \frac{\eta}{\tau} d\log T_o + \frac{\theta}{\tau} d\log T_w - \frac{\eta}{\tau} d\log \eta + d\log k_t \tag{2}$$

where $d\log T_w = 0$ for a constant temperature anemometer (CTA).

For sensitivities depending on $Nu_t = f(M,Kn,\tau)$:

Equations were re-derived for the sensitivities of heated wires operated in compressible flow and powered by a constant temperature anemometer using the heat transfer relationship for the variables $Nu_t = f(M,Kn,\tau)$. The sensitivity equations derived by Baldwin[7] and Sandborn[8] are incomplete for several reasons. In these references the velocity sensitivity includes a $\partial T_o/\partial u$ term under the constraint that $T_o = constant$. There are other terms missing

in the equations due to an incomplete partial differentiation process. Following the assumptions[7,8] that $Nu_t = f(M, Kn, \tau)$, the change in Nusselt number is:

$$d\log Nu_t = \frac{\partial \log Nu_t}{\partial \log M} d\log M + \frac{\partial \log Nu_t}{\partial \log Kn} d\log Kn + \frac{\partial \log Nu_t}{\partial \log \tau} d\log \tau \qquad (3)$$

The Mach number is a function of u and T_o. Thus:

$$d\log M = \frac{\partial \log M}{\partial \log u} d\log u + \frac{\partial \log M}{\partial \log T_o} d\log T_o \qquad (4)$$

$$d\log M = \left(1 + \frac{\gamma - 1}{2} M^2\right) d\log u - \frac{1}{2}\left(1 + \frac{\gamma - 1}{2} M^2\right) d\log T_o \qquad (5)$$

The Knudsen number is a function of only density for a given wire diameter, and can be expressed as[7]:

$$Kn = \frac{1.587x10^{-8}}{\rho d_w} \quad \text{or} \quad d\log Kn = -d\log \rho \qquad (6)$$

The recovery temperature ratio, η, is assumed to be a function of M and Kn. Then:

$$d\log \eta = \frac{\partial \log \eta}{\partial \log M} d\log M + \frac{\partial \log \eta}{\partial \log Kn} d\log Kn \qquad (7)$$

The thermal conductivity for air is evaluated at T_o, giving:

$$d\log k_t = \frac{\partial \log k_t}{\partial \log T_o} d\log T_o \qquad (8)$$

The power to the heated wire can be written as:

$$d\log P_w = d\log E_w - d\log R_w \tag{9}$$

For a constant temperature anemometer:

$$d\log R_w = 0 \tag{10}$$

The quantity $\tau = \frac{T_w - \eta T_o}{T_o}$, therefore, the change in τ is:

$$d\log \tau = -\frac{\theta}{\tau} d\log T_o - \frac{\eta}{\tau} d\log \eta \tag{11}$$

Equations (5-11) can be substituted into (2) to give:

$$d\log E_w = S_u\, d\log u + S_\rho\, d\log \rho + S_{T_o}\, d\log T_o \tag{12}$$

where

$$S_u = \frac{1}{2}\left\{\left(1+\frac{\gamma-1}{2}M^2\right)\left[\frac{\partial \log Nu_t}{\partial \log M} - \frac{\eta}{\tau}\frac{\partial \log \eta}{\partial \log M}\left(\frac{\partial \log Nu_t}{\partial \log \tau}+1\right)\right]\right\} \tag{13}$$

$$S_\rho = \frac{1}{2}\left\{-\frac{\partial \log Nu_t}{\partial \log Kn} + \frac{\eta}{\tau}\frac{\partial \log \eta}{\partial \log Kn}\left(\frac{\partial \log Nu_t}{\partial \log \tau}+1\right)\right\} \tag{14}$$

$$S_{T_o} = \frac{1}{2}\left\{-\frac{1}{2}S_u - \left(1+\frac{\eta}{\tau}\right)\frac{\partial \log Nu_t}{\partial \log \tau} - \frac{\eta}{\tau} + \frac{\partial \log k_t}{\partial \log T_o}\right\} \tag{15}$$

The sensitivity equations as derived by Baldwin in reference 7 using functional relationship $Nu_t = f(M, Kn, \tau)$ are as follows:

$$\frac{dI}{I} = \frac{1}{2}\left\{\begin{array}{l}\left[\left(1+\frac{\gamma-1}{2}M^2\right)\left(\frac{\partial \log Nu_t}{\partial \log M} - \frac{M}{\tau}\frac{\partial \eta}{\partial M}\right) - \frac{\eta}{\tau}(\gamma-1)M^2\right]\frac{dU}{U} \\ -\frac{\partial \log Nu_t}{\partial \log Kn}\frac{d\rho}{\rho} + \left(\frac{\partial \log k_t}{\partial \log T_o} - \frac{\eta}{\tau} - \frac{\tau+\eta}{Nu_t}\frac{\partial Nu_t}{\partial M}\right)\frac{dT_o}{T_o}\end{array}\right\} \qquad (16)$$

These equations (13-15) for velocity, density and total temperature sensitivities are different from equation (16) for several reasons. In equation (16) the velocity was differentiated with respect to T_o under the assumption that $T_o = constant$. Also, the differentiation processes in was incomplete.

The re-derived equations were used to obtain the velocity, density and total temperature sensitivities for hot-wires and are compared with the sensitivities computed using the functional relationship $E = f(u, \rho, T_o, T_w)$. The constraints required by calculus and the functional form of the equation dictated by the data were met by both methods for computing sensitivities. These results are presented in the enclosed appendix.

<u>For sensitivities depending on</u> $Nu_t = f(M, Kn, a_w)$:

Following the assumptions that $Nu_t = f(M, Kn, a_w)$, the change in Nusselt number is:

$$d\log Nu_t = \frac{\partial \log Nu_t}{\partial \log M} d\log M + \frac{\partial \log Nu_t}{\partial \log Kn} d\log Kn + \frac{\partial \log Nu_t}{\partial \log a_w} d\log a_w \qquad (17)$$

The quantity $a_w = \frac{R_w - R_{adw}}{R_{adw}}$ and $R_{adw} = f(M, Kn, T_o)$. Therefore, the change in a_w is:

$$d\log a_w = -\frac{\theta}{a_w}\left\{\begin{array}{l} \dfrac{\partial \log R_{adw}}{\partial \log M}\left[\left(1+\dfrac{\gamma-1}{2}M^2\right)\left(d\log u-\dfrac{1}{2}d\log T_o\right)\right] \\ \\ -\dfrac{\partial \log R_{adw}}{\partial \log Kn}d\log\rho+\dfrac{\partial \log R_{adw}}{\partial \log T_o}d\log T_o \end{array}\right\} \quad (18)$$

Substituting equations (5-10), (17) and (18) in equation (2) leads to equation (12) where

$$S_u = \frac{1}{2}\left\{\left(1+\frac{\gamma-1}{2}M^2\right)\left[\frac{\partial \log Nu_t}{\partial \log M}-\frac{\eta}{\tau}\frac{\partial \log \eta}{\partial \log M}\frac{\partial \log R_{adw}}{\partial \log M}-\frac{\theta}{a_w}\frac{\partial \log Nu_t}{\partial \log M}\right]\right\} \quad (19)$$

$$S_\rho = \frac{1}{2}\left\{-\frac{\partial \log Nu_t}{\partial \log Kn}+\frac{\eta}{\tau}\frac{\partial \log \eta}{\partial \log Kn}+\frac{\theta}{a_w}\frac{\partial \log Nu_t}{\partial \log a_w}\frac{\partial \log R_{adw}}{\partial \log Kn}\right\} \quad (20)$$

$$S_{T_o} = \frac{1}{2}\left\{-2S_u-\frac{\theta}{a_w}\frac{\partial \log Nu_t}{\partial \log a_w}-\frac{\eta}{\tau}+\frac{\partial \log k_t}{\partial \log T_o}\right\} \quad (21)$$

For sensitivities depending on $E = f(M, Kn, a_w)$:

If we use the relationship $E = f(M, Kn, a_w)$ then the change in voltage is:

$$d\log E = \frac{\partial \log E}{\partial \log M}d\log M+\frac{\partial \log E}{\partial \log Kn}d\log Kn+\frac{\partial \log E}{\partial \log a_w}d\log a_w \quad (22)$$

Substituting equations (5) through (10) and (18) in equation (22) leads to equation (12) where

$$S_u = \left(1+\frac{\gamma-1}{2}M^2\right)\left[\frac{\partial \log E}{\partial \log M}-\frac{\theta}{a_w}\frac{\partial \log E}{\partial \log a_w}\frac{\partial \log R_{adw}}{\partial \log M}\right] \quad (23)$$

$$S_\rho = \left\{ -\frac{\partial \log E}{\partial \log Kn} + \frac{\theta}{a_w} \frac{\partial \log E}{\partial \log a_w} \frac{\partial \log R_{adw}}{\partial \log Kn} \right\} \tag{24}$$

$$S_{T_o} = \left\{ -\frac{1}{2} S_u - \frac{\theta}{a_w} \frac{\partial \log E}{\partial \log a_w} \frac{\partial \log R_{adw}}{\partial \log T_o} \right\} \tag{25}$$

Resistance to temperature relationship can be written as:

$$R_w = R_{ref} \left\{ 1 + \alpha (T_w - T_{ref}) + \beta (T_w - T_{ref})^2 \right\} \tag{26}$$

Using equation (26) the quantity $\partial \log R_{adw} / \partial \log T_o$ can be obtained as:

$$\frac{\partial \log R_{adw}}{\partial \log T_o} = \frac{T_{adw} \left[\alpha + 2\beta (T_{adw} - T_{ref}) \right]}{\left[1 + \alpha (T_{adw} - T_{ref}) + (T_{adw} - T_{ref})^2 \right]} \tag{27}$$

For sensitivities depending on $E = f(u, \rho, T_o)$:

For a constant temperature anemometer (CTA), the change in voltage across the wire can be expressed as $E = f(u, \rho, T_o)$. Once the wire is calibrated and functional relationships are defined, the sensitivities can be evaluated by taking the partial change in E with respect to u , ρ and T_o in turn. The equations for sensitivities can be written as:

$$S_u = \left(\frac{\partial \log E}{\partial \log u} \right)_{\rho, T_o, T_w} \tag{28}$$

$$S_\rho = \left(\frac{\partial \log E}{\partial \log \rho} \right)_{u, T_o, T_w} \tag{29}$$

$$S_{T_o} = \left(\frac{\partial \log E}{\partial \log T_o} \right)_{u,\rho,T_w} \tag{20}$$

This method of obtaining sensitivities is the direct method since the output voltage, which is a directly measurable quantity, is a function of velocity, density and total temperature which are in turn directly measurable quantities.

For sensitivities depending on $Nu_t = f(M_\infty, Re_t, \theta)$:

For the sake of completeness, the sensitivity equations for constant current anemometers (CCA) using the functional relationship of $Nu_t = f(M_\infty, Re_t, \theta)$, as derived by Morkovin[5], are repeated here. They are:

$$S_u = \frac{1}{2}\left\{ \left(1 + \frac{\gamma - 1}{2} M^2\right) \left[\frac{\partial \log Nu_t}{\partial \log M}\bigg|_{Re_t,\theta} - \frac{\eta}{\tau_w} \frac{\partial \log \eta}{\partial \log M}\bigg|_{M,\theta} \right] + S_\rho \right\} \tag{31}$$

$$S_\rho = \frac{1}{2}\left\{ \frac{\partial \log Nu_t}{\partial \log \mathrm{Re}_t}\bigg|_{M,\theta} - \frac{\eta}{\tau_w} \frac{\partial \log \eta}{\partial \log \mathrm{Re}_t}\bigg|_{M,\theta} \right\} \tag{32}$$

$$S_{T_o} = \frac{1}{2}\left\{ S_u + S_\rho(2m_t - 1) - \frac{\partial \log Nu_t}{\partial \log \theta}\bigg|_{M,Re_t} - \frac{\eta}{\tau_w} + \frac{\partial \log k_t}{\partial \log T_o} \right\} \tag{33}$$

Experimental Description:

The data were collected using the "*Probe Calibration Tunnel*" (PCT) at NASA Langley research center which is an open jet tunnel in which velocity, density and total temperature can be controlled independently. The combination of a staged pressure system, low mass flow rates through the facility and the availability of large vacuum systems enables this facility to run

continuously. It has two interchangable, subsonic and transonic nozzles, having diameters of 1.50 and 2.25 inches respectively, that yields a continuous flow capability over the Mach number range of 0.05 to 1.0. Tunnel stagnation pressure and temperature can be varied from a minimum of 0.20 atmospheres to a maximum of 10 atmospheres and from 500°R to 600°R, respectively. This corresponds to a Reynolds number range of $1 x 10^6 < Re/ft < 51 x 10^6$ for a Mach number of 1. The 3-wire hot-wire probe utilized three different diameters of Platinum coated Tungsten wires (diameters of 0.0001, 0.0002 and 0.0003 inch) and was used to obtain most of the calibration data. The test matrix consisted of 12 velocities, 7 densities and 5 total temperatures for the cases where $E = f(u,\rho,a_w,T_w)$. For $E = f(M,Kn,a_w)$, the test matrix consisted of 12 Mach numbers, 7 Knudsen numbers and 8 overheats. The lower and upper bounds of the test matrix for the two methods are given in Tables I and II. In this study all Knudsen numbers were greater than 0.01, indicating that all the data were in the slip flow regime based on the definition of the slip flow.

Parameter	Minimum	Maximum
Total pressure, psi	3.40306	46.2992
Static pressure, psi	2.83727	31.5238
Velocity, ft/sec	113.785	950.953
Mach number	0.0982	0.941
Total temperature, °R	500	600
Static temperature, °R	417.33	579.73
Reynolds number/foot	0.3×10^6	12.3×10^6
Density	0.01875	0.14693
Mass flow, lb/sec	0.012832	1.71468

Table I. Minimum and Maximum Test Conditions of Test Matrix for Functional Relationship $E = f(u,\rho,a_w,T_w)$.

Parameter	Minimum	Maximum
Total pressure, psi	3.675	29.4
Static pressure, psi	3.44859	26.2216
Mach number	0.1	0.95
Total temperature, °R	540	540
Static temperature, °R	457.433	539.73
Reynolds number/foot	0.5×10^6	13.3×10^6
Knudsen number	0.00494	0.10369
Overheat ratio	0.3	1.0
Density	0.01875	0.13333
Mass flow, lb/sec	0.013103	1.7193

Table II. Minimum and Maximum Test Conditions of Test Matrix for Functional Relationship $E = f(M, Kn, a_w)$.

Discussion:

To illustrate the complexity of the sensitivity equations, consider the relationship between voltage across a wire mounted normal to the flow and the quantities u, ρ and T_O for the constant temperature anemometer. Utilizing a small perturbation assumption we can write:

$$\frac{e'}{E} = S_u \frac{u'}{u} + S_\rho \frac{\rho'}{\rho} + S_{T_o} \frac{T_o'}{T_o} \tag{34}$$

Evaluating the partial derivatives in the above sensitivity equations requires care when carrying out the mean flow calibration. For example, consider equations (31-33). The evaluation of $\left.\frac{\partial \log Nu_t}{\partial \log Re_t}\right|_{M,\theta}$ must be obtained by varying P_O only and the Mach number and the total temperature must be held constant. Also, the evaluation of $\left.\frac{\partial \log Nu_t}{\partial \log M}\right|_{Re_t,\theta}$ requires that the total pressure be changed when the Mach number is varied in order to maintain Reynolds number constant. Similar constraints must be observed when $\left.\frac{\partial \log \eta}{\partial \log Re_t}\right|_{M}$ and $\left.\frac{\partial \log \eta}{\partial \log M}\right|_{Re_t}$ are evaluated. Care must also be taken in evaluating the partial derivatives when using other *dependent and independent variables. This method of obtaining sensitivities is time consuming* when conducting experiments in large wind tunnels since the Mach number and the total pressures must be varied in order to maintain the prescribed non-varying independent variable at a constant level when the variation of the remaining dependent variables being sought.

If $Nu_t = f(M_\infty, Re_t, \theta)$ and the above described constraint is applied, the operational envelope for the facility must be considered, since there is a skewing of the Nu_t vs. Re_t curves for constant Mach numbers because $Re_t = f(u,\rho)$[9]. Due to this skewing, the region over which the partial derivatives can be evaluated will reduce rapidly. The advantage of using the suggested functional relationship i.e., $E_b = f(m, T_o, T_w)$ or $E_b = f(m, a_w, T_w)$ can be seen by *plots of Nu_t vs. Kn for constant Mach number where the data are not as skewed and a more* complete set of derivatives can be evaluated from a given number of data points[5]. This efficient use of data with the wire voltage correlated in terms of these primitive variables cannot be ignored and that will reduce the amount of data needed for calibration by an order of magnitude. Eventually, that attribute leads to better accuracy in the calibration process.

The effect of wire temperature is complicated due to its nonlinear variation and because it is not fully understood. In the literature several methods based on various heat transfer

relationships, using different dependent and independent variables for a given type of anemometer, are available to compute hot-wire sensitivities. Among these, the most extensively used correlations are $Nu_t = f(M_\infty, Kn, \tau_w)$ and $Nu_t = f(M_\infty, Re_t, \theta)$. All these methods should give identical results for the sensitivity of a given hot-wire at given test conditions. Hot-wire calibrations have been performed as part of the PCT facility flow quality investigation, in various flow regimes. At higher speeds, where compressible flow effects occur, it has been found that King's Law is not valid[1,2,10]. Hence, those flow regimes have been investigated.

In the 1950's, Kovasznay[11,12] extended hot-wire anemometry to compressible flows where it was found experimentally that in supersonic flow the heated wire was sensitive only to mass flow and total temperature. Kovasznay developed a graphical technique to obtain these fluctuations, which is used primarily in supersonic and hypersonic flows. Kovasznay's[12] compressible flow results showed that there was a significant difference between the heat transfer in compressible and incompressible flows. In subsonic compressible, transonic and low supersonic flows, effects due to compressibility influence the heat transfer from a wire. In high supersonic and hypersonic flows a strong shock occurs ahead of the wire and the heat transfer from the wire is influenced by subsonic flow downstream of the shock front. Because of this, it was found experimentally that in supersonic/hypersonic flows $Nu_t = f(Re_t, \theta)$ only, and the heat transfer from the wire was again a function of mass flow, total temperature, and wire temperature. For this reason some understanding of subsonic flow while studying supersonic or hypersonic flow, becomes essential.

In continuum flow the mean free path of the particles is less than the diameter of the wire and conventional heat transfer theories are applicable. When the diameter of the wire approaches a few mean free paths between the particles, the flow does not behave as a continuum, but exhibits some effects of the finite spacing between the particles. These effects have been studied[13,14] by assuming finite velocity and temperature jump boundary conditions.

This gas rarefaction regime was noted as slip flow. In free molecular flow the fluid is assumed to be composed of individual particles and the distance between the particles is sufficiently large that their impact with and reflection from a body is assumed to occur without interaction between the particles.

Conclusions

The following conclusions have been made:

- The equation obtained for a constant temperature anemometer (CTA) based on the assumption that $E = f(u,\rho,T_o)$ resulted in an equation in which neither wire length nor the coefficients in the wire resistance vs. temperature relationship were required. This should result in a more accurate method for calibrating hot-wire probes in facilities where total temperature can be varied.

- The equation obtained for a constatnt current anemometer (CCA) based on the assumption that $E = f(u,\rho,T_o,T_w)$ results in an equation that requires the variation of four independent variables and is believed to be too complicated for routine use. The equation also requires evaluation of β who's elimiation was desired.

- The equation obtained for a CCA and CTA under the assumption that $Nu_t = f(M,Kn,a_w)$ and T_o = constant resulted in an equation where α and β occured in only one term in the equation for the total temperature sensitivity. Consequently, this calibration of wires should be more accurate than those obtained using conventional methods.

- The sensitivities computed based on the methods presented using the data obtained in the "*Probe Calibration Tunnel*" are comparable. However, differences in S_{T_o} are more significant than for S_u and S_ρ.

- In general, the velocity sensitivity ranges from 0.05 to 0.40, density sensitivity ranges from 0.10 to 0.40 and total temperature sensitivity ranges from -0.2 to -1.0.

- The equations (13-15) for the sensitivities of a constant temperature anemometer are different from those in references 7 and 8. In those references, the velocity sensitivity has a term for $\frac{\partial \log T_o}{\partial \log u}$ under the constraints that T_o = constant. There are other terms missing in the equations due to the incomplete partial differentiation process.

References

1. Boussinesq, J. 1905: "*An Equation for the Phenomena of Heat Convection and an Estimate of the Cooling Power of Fluids,*" Journal de Mathematiques, Vol. 1, pp. 285-332, also Comptes Rendus, Vol. 133, pp. 257.

2. King, L.V. 1914: "*On the Convection of Heat from Small Cylinders in a Stream of Fluid,*" Phil. Trans. of Roy. Soc. (London), Ser. A. Vol. 214, No. 14, pp. 373-432.

3. Laurence, J.C.; and Landes, L.G. 1952: "*Auxiliary Equipment and Techniques for Adapting the Constant-Temperature Hot-Wire Anemometer to Specific Problems in Air-Flow Measurements,*" NACA TN 2843.

4. Lowell, H.H. 1950: "*Design and Application of Hot-Wire Anemometers for Steady-State Measurements at Transonic and Supersonic Airspeeds,*" NACA TN 2117.

5. Spangenberg, W.G. 1955: "*Heat Loss Characteristics of Hot-Wire Anemometers at Various Densities in Transonic and Supersonic Flows,*" NACA TN 3381.

6. Morkovin, M.V. 1956: "*Fluctuations and Hot-Wire Anemometry in Compressible Flows,*" NATO AGARDograph 24.

7. Baldwin, L.V. 1958: "Slip-Flow Heat Transfer From Cylinders in Subsonic Airstreams," NACA TN 4369.

8. Sandborn, V.A. 1972: "*Resistance Temperature Transducers,*" Metrology Press, Fort Collins, Colorado.

9. Davies, P.O.A.L., and Fisher, M.J., 1964, "*Heat Transfer from Electrically Heated Cylinders,*" Proceedings of the Royal Society, Series A, Mathematical and Physical Sciences, Vol. 280, No. 1383, pp. 486-527.

10. Dryden, H.L., and Kuethe, A.M., 1929, "*The Measurement of Fluctuations of Air Speed by the Hot-Wire Anemometer,*" NACA-TR-320.

11. Kovasznay, L.S.G., 1950, "*The Hot-Wire Anemometer in Supersonic Flows,*" Journal of the Aeronautical Sciences, Vol. 17, No. 9, pp. 565-584.

12. Kovasznay, L.S.G., 1953, "*Turbulence in Supersonic Flow,*" Journal of the Aeronautical Sciences, Vol. 20, No. 10, pp. 657-674.

13. Sauer, F.M., and Drake, Jr., R.M., 1953, "*Forced Convection Heat Transfer from Horizontal Cylinders in a Rarefied Gas,*" Journal of the Aeronautical Sciences, Vol. 20, pp. 175-180, 209.

14. Weltmann, R.N., and Kuhns, P.W., 1960, "*Heat Transfer to Cylinders in Crossflow in Hypersonic Rarefied Gas Streams,*" NASA-TND-267.

Appendix

NIS

AIAA 94-2536

A Rational Technique for Calibrating Hot-Wire Probes in Subsonic to Supersonic Speeds

K.A. Nagabushana
Old Dominion University
Norfolk, VA 23508

P.C. Stainback
NASA Langley Research Center
Hampton, VA 23681

and

G.S. Jones
NASA Langley Research Center
Hampton, VA 23681

18th AIAA Aerospace Ground Testing Conference

June 20-23, 1994 / Colorado Spring, CO

For permission to copy or republish, contact the American Institute of Astronautics and Aeronautics
370 L'Enfant Promenade, S.W. Washington, D.C. 20024

A Rational Technique for Calibrating Hot-Wire Probes from Subsonic to Supersonic Speeds

K.A. Nagabushana†
Research Associate
Old Dominion University
Norfolk, VA 23508

P.C. Stainback
Distinguished Research Associate
NASA Langley Research Center
Hampton, VA 23681

and

G.S. Jones
Aerospace Engineer
NASA Langley Research Center
Hampton, VA 23681

Abstract

Hot-wire anemometry is a well developed technique for measuring fluctuations in flowing fluids where its application depends on the mean flow calibration of the heated wire. The conventional technique usually used to calibrate hot-wire probes is based on the determination of Nusselt number and wire recovery temperature ratio as functions of Reynolds number and Mach number. This method requires the measurement of the wire length and the coefficients in the temperature - resistance equation for the wire material. The accurate measurement of these quantities are difficult to make, particularly the wire length and the coefficient of the second degree term in the temperature - resistance equation. The lack of accurate values for these two quantities are possible sources of error in the determination of the sensitivities for the heated wire to heat transfer from the wire. A technique is proposed that reduces the dependency of the sensitivities of wires to these quantities.

Nomenclature

a'_w	$(R_w - R_{a_w})/R_{a_w}$
A	$\left[1 - \frac{\theta}{a'_w}(1+\varepsilon)\frac{\partial \log E}{\partial \log a'_w}\right]^{-1}$
c_p	specific heat at constant pressure
c_v	specific heat at constant volume
d_w	diameter of the hot-wire
dA_w	elemental surface area of the wire
e'	fluctuating voltage across the sensor
E	mean voltage across the sensor
h	heat transfer coefficient
I	current across the sensor
k	thermal conductivity of air evaluated at subscript temperature
K	$\partial \log T_w / \partial \log R_w$
Kn	Knudsen number
ℓ	hot-wire length
m_t	$\partial \log \mu_t / \partial \log T_o$
M	Mach number
Nu	Nusselt number evaluated at subscript temperature
P	electrical power to the hot-wire
q	dynamic pressure

Copyright © 1994 by K.A. Nagabushana. Published by the American Institute of Aeronautics and Astronautics, Inc. with permission.

†Formerly contract research engineer at Fluid Mechanics Division, NASA Langley Research Center through ViGYAN Inc., Hampton, VA 23666.

AIAA 94-2536, 18th AIAA 19th Ground Test Conference
Colorado Springs, Colorado, July 20-23, 1994

Q	forced convective heat transfer
r	radius of the hot-wire
R	resistance
Re	Reynolds number
s	distance along circumference of the wire
S_u	velocity sensitivity
S_ρ	density sensitivity
S_{T_o}	total temperature sensitivity
T	temperature
u	velocity
x	distance along the length of wire
α	$\left(1+\frac{\gamma-1}{2}M^2\right)^{-1}$
α_1 & β_1	coefficients in temperature - resistance relationship
ε	finite circuit factor, $-(\partial \log I/\partial \log E)$
η	recovery temperature ratio, T_{adw}/T_o
θ	temperature parameter, R_w/R_{adw}
μ	absolute viscosity of air evaluated at subscript temperature
Λ	sweep angle
γ	specific heat ratio, c_p/c_v
ρ	density
τ_w	temperature loading parameter, $(T_w - T_{adw})/T_o$
φ	angle in polar co-ordinate system
ϕ'	normalized voltage fluctuation ratio = $\left(e'/E\right)/S_{T_o}$
$'$	indicates instantaneous value

Subscript

adw	adiabatic wall condition
ave	average condition
l	local value
*M*1	method I referred to $E = f(u,\rho,T_o,T_w)$
*M*2	method II referred to $E = f(M,Kn,a'_w)$
o	total condition
ref	reference conditions, $T_0 = 0°C$
w	wire condition
∞	free stream or static condition

Introduction

Historically, much hot-wire data were analyzed by using equations derived by Morkovin[1] to obtain the sensitivities of the heated wire to changes in velocity, density, and total temperature. This is particularly true for wires operating in the compressible flow regime. The use of these equations requires a knowledge of the wire length, α_1 and β_1 in the temperature - resistance relationship for the wire material. The operation of wires at high temperatures requires a knowledge of β_1 values. The calibration of the wire at elevated temperature places a severe demand on the construction of the probe to withstand these temperatures. Because of this, values for β_1 are often not obtained from calibration but from handbooks.

The length of the wire must also be known and for wires having slack it is difficult to accurately measure their lengths. Since the wire is heated, the length measured when cold will differ from the value when the wire is hot. The approximate values of β_1 and errors in measuring the length of the wire can lead to error in the calibrated values of the mean flow sensitivities. The mean flow calibration is also constrained by the average values used and the approximations made for the heat transfer equation. The use of general functional relationships for heat transfer from the heated wire should lead to more accurate mean flow calibrations.

Two methods are proposed for calibrating the sensitivities of heated wires to flow variables. One method eliminates the need to measure the wire length or α_1 and β_1. In the second method, the quantities α_1 and β_1 affect only the total temperature sensitivity of the wire to a minor degree. Equations, based on these techniques, will be presented for constant temperature and constant current anemometers (CTA and CCA). Calibration data for a constant temperature anemometer will be presented based on these two calibration techniques.

Theoretical Consideration

Rational for using Functional Relationships

Consider the heat transfer from a heated wire with slack as shown in figure 1. For this problem the general heat transfer equation due to forced convection can be written in integral form as:

$$Q = \int h(T_w - T_{adw})dA_w \qquad (1)$$

where

$$dA = dxds = rdxd\varphi \qquad (2)$$

Using equation (2) we can write equation (1) as:

$$Q = 2r\ell \int_{-x/\ell}^{x/\ell} \int_{0}^{\pi} h(T_w - T_{adv}) \frac{dx}{\ell} d\varphi \tag{3}$$

Here h, T_w and T_{adv} are local values. Using stagnation values of these quantities to normalize the above equation along with the stagnation values at zero sweep, the above equation can be rewritten as:

$$Q = 2r\ell h_{o,\Lambda=0}(T_w - T_{adv})_{o,\Lambda=0} \int_{-\frac{x}{\ell}}^{\frac{x}{\ell}} \int_{0}^{\pi} \frac{h_{o,\Lambda}}{h_{o,\Lambda=0}} \frac{(T_w - T_{adv})_{o,\Lambda}}{(T_w - T_{adv})_{o,\Lambda=0}} \frac{h}{h_{o,\Lambda}} \frac{(T_w - T_{adv})}{(T_w - T_{adv})_{o,\Lambda}} \frac{dx}{\ell} d\varphi \tag{4}$$

where Λ, T_w and $T_{w,o,\Lambda}$ are $f(x)$. T_{adv} and $T_{adv,o,\Lambda}$ are $f(M, Kn, T_o, \Lambda)$. Mach number and Reynolds number are $f(\varphi)$. $h/h_{o,\Lambda} = f(\varphi) = f(M_l, Kn_l)$ and $h_{o,\Lambda}/h_{o,\Lambda=0} = f(M_\infty, Kn_\infty, \Lambda) = f(x)$. The quantities that are $f(x)$ are due to conduction to the supports and to the local sweep. This is a more complex equation than the usual heat transfer equation used to derive hot-wire equations.

The conventional heat transfer equation due to forced convection can be written as:

$$Q = \pi \ell d_w h_{ave} (T_{w,ave} - T_{adv,ave}) \tag{5}$$

Nondimensionalizing equation (5) similar to that done in equation (4) gives:

$$Q = \pi \ell d_w h_{o,\Lambda=0} (T_w - T_{adv})_{o,\Lambda=0} \frac{h_{ave}}{h_{o,\Lambda=0}} \frac{(T_{w,ave} - T_{adv,ave})}{(T_w - T_{adv})_{o,\Lambda=0}} \tag{6}$$

Here equation (4) and (6) represent the same quantity but approached in a different way. Evaluating the terms in equations (4) and (6) are difficult. However, note that both equations can be represented in terms of functional relationship to basic flow quantities as:

$$Q = f(u, \rho, T_o, T_w) \tag{7}$$

which can be used to evaluate the sensitivities of the wire to heat transfer more accurately than equation (4) or (5) or (6) as far as the hot-wire application is concerned.

Derivation of Sensitivity Equations

The functional relationship given by Morkovin that governs the voltage measured across a heated wire was obtained from equation (5) and results in:

$$E = f(u, \rho, T_o, T_w) \tag{8}$$

The change in voltage with respect to the independent variables is:

$$d\log E = \frac{\partial \log E}{\partial \log u} d\log u + \frac{\partial \log E}{\partial \log \rho} d\log \rho + \frac{\partial \log E}{\partial \log T_o} d\log T_o + \frac{\partial \log E}{\partial \log T_w} d\log T_w \tag{9}$$

For a constant current anemometer the change in wire temperature must be considered. The temperature of the wire should be obtained from the wire resistance using the following equation:

$$\frac{R_w}{R_{ref}} = 1 + \alpha_1 (T_w - T_{ref}) + \beta_1 (T_w - T_{ref})^2 \tag{10}$$

Equation (10) is required to relate T_w to R_w. For $T_w = f(R_w)$ the following equation can be written:

$$d\log T_w = K \; d\log R_w \tag{11}$$

Ohm's law gives:

$$d\log R_w = d\log E - d\log I \tag{12}$$

Using equation (11) and (12), equation (9) can be written as:

$$\left[1 - K \frac{\partial \log E}{\partial \log T_w}(1+\varepsilon)\right] d\log E = \frac{\partial \log E}{\partial \log u} d\log u + \frac{\partial \log E}{\partial \log \rho} d\log \rho + \frac{\partial \log E}{\partial \log T_o} d\log T_o \tag{13}$$

The final equation for the change in E becomes:

$$d\log E = S_u d\log u + S_\rho d\log \rho + S_{T_o} d\log T_o \tag{14}$$

where

$$S_u = \frac{\partial \log E / \partial \log u}{\left[1 - K \frac{\partial \log E}{\partial \log T_w}(1+\varepsilon)\right]}; \quad S_\rho = \frac{\partial \log E / \partial \log \rho}{\left[1 - K \frac{\partial \log E}{\partial \log T_w}(1+\varepsilon)\right]}; \quad S_{T_o} = \frac{\partial \log E / \partial \log T_o}{\left[1 - K \frac{\partial \log E}{\partial \log T_w}(1+\varepsilon)\right]} \tag{15}$$

For a CTA, $dT_w = 0$ and the final equation for the change in E is same as equation (14) where:

$$S_u = \frac{\partial \log E}{\partial \log u};\quad S_\rho = \frac{\partial \log E}{\partial \log \rho};\quad S_{T_o} = \frac{\partial \log E}{\partial \log T_o} \tag{16}$$

Equation (15) is not recommended for calibrating a CCA since the flow variables of u, ρ, T_o and T_w must be varied. This makes the calibration process too lengthy. The term K, in equation (11) also requires values of α_1 and β_1. However, equation (14) and (16) for a CTA does not require the knowledge of wire length or α_1 and β_1.

It is not often possible to vary T_o in wind tunnels. To overcome this problem, the following functional relationship is suggested:

$$E = f(M, Kn, a'_w) \tag{17}$$

where T_o is constant. Using equation (17), the change in the voltage across the heated wire is:

$$d\log E = \frac{\partial \log E}{\partial \log M} d\log M + \frac{\partial \log E}{\partial \log Kn} d\log Kn + \frac{\partial \log E}{\partial \log a'_w} d\log a'_w \tag{18}$$

From the definition of a'_w, the change in a'_w is :

$$d\log a'_w = \frac{\theta}{a'_w}\left(d\log R_w - d\log R_{adw}\right) \tag{19}$$

One possible functional relationship for R_{adw} is:

$$R_{adw} = f(M, Kn, T_o) \tag{20}$$

From which the change in R_{adw} is:

$$d\log R_{adw} = \frac{\partial \log R_{adw}}{\partial \log M}\left[\frac{1}{\alpha}\left(d\log u - \frac{1}{2} d\log T_o\right)\right] - \frac{\partial \log R_{adw}}{\partial \log Kn} d\log \rho + \frac{\partial \log R_{adw}}{\partial \log T_o} d\log T_o \tag{21}$$

Using equation (21) in (19), substituting $d\log a'_w$ into equation (18), and rearranging leads to:

$$d\log E = S'_u d\log u + S'_\rho d\log \rho + S'_{T_o} d\log T_o + \frac{\theta}{a'_w}\frac{\partial \log E}{\partial \log a'_w} d\log R_w \tag{22}$$

Finally, Ohm's law can be used to express the wire resistance in terms of the voltage across the wire as follows:

$$d\log R_w = (1+\varepsilon) d\log E \tag{23}$$

Using equation (23) in (22), the final equation for the change in E is same as equation (14) where:

$$S_u = AS'_u = \frac{A}{\alpha}\left\{\frac{\partial \log E}{\partial \log M} - \frac{\theta}{a'_w}\frac{\partial \log E}{\partial \log a'_w}\frac{\partial \log R_{adw}}{\partial \log M}\right\} \tag{24}$$

$$S_\rho = AS'_\rho = A\left\{\frac{\theta}{a'_w}\frac{\partial \log E}{\partial \log a'_w}\frac{\partial \log R_{adw}}{\partial \log Kn} - \frac{\partial \log E}{\partial \log Kn}\right\} \tag{25}$$

$$S_{T_o} = AS'_{T_o} = A\left[\frac{\theta}{a'_w}\frac{\partial \log E}{\partial \log a'_w}\left(\frac{1}{2\alpha}\frac{\partial \log R_{adw}}{\partial \log M} - \frac{\partial \log R_{adw}}{\partial \log T_o}\right) - \frac{\partial \log E}{\partial \log M}\right] \tag{26}$$

$$A = \left[1 - \frac{\theta}{a'_w}(1+\varepsilon)\frac{\partial \log E}{\partial \log a'_w}\right]^{-1} \tag{27}$$

Using equation (10) the quantity $\partial \log R_{adw}/\partial \log T_o$ can be obtained as:

$$\frac{\partial \log R_{adw}}{\partial \log T_o} = \frac{T_{adw}\left[\alpha_1 + 2\beta_1\left(T_{adw} - T_{ref}\right)\right]}{\left[1 + \alpha_1\left(T_{adw} - T_{ref}\right) + \beta_1\left(T_{adw} - T_{ref}\right)^2\right]} \tag{28}$$

The evaluation of $\partial \log R_{adw}/\partial \log T_o$, requires values for α_1 and β_1 and the latter should be obtained from the temperature-resistance calibration of the wire. The values for α_1 can be easily obtained, however, it is often necessary to use handbook values for β_1. In any case, the values of α_1 and β_1 occur in only one term in the equation for the sensitivity of the wire to total temperature and any error in β_1 would be limited to this sensitivity. The possible error in evaluating $\partial \log R_{adw}/\partial \log T_o$ by neglecting the value for β_1 can be obtained from:

$$\frac{\left[\frac{\partial \log R_{adw}}{\partial \log T_o}\right]_{\alpha_1,\beta_1}}{\left[\frac{\partial \log R_{adw}}{\partial \log T_o}\right]_{\alpha_1}} = \frac{\left\{T_{adw}\left[\alpha_1 + 2\beta_1\left(T_{adw} - T_{ref}\right)\right]\right\}_{\alpha_1,\beta_1}}{\left\{\alpha_1 T_{adw}\right\}_{\alpha_1}} \tag{29}$$

where

$$[T_{adw}]_{\alpha_1,\beta_1} = \frac{-(\alpha_1 - 2\beta_1 T_{ref})}{2\beta_1} \pm \sqrt{\frac{\alpha_1^2}{4\beta_1^2} + \frac{1}{\beta_1}\left(\frac{R_{adw}}{R_{ref}} - 1\right)} \qquad (30)$$

and

$$[T_{adw}]_{\alpha_1} = \frac{1}{\alpha_1}\left[\frac{R_{adw}}{R_{ref}} - 1\right] + T_{ref} \qquad (31)$$

For a CTA $d\log R_w = 0$, and equations (24) - (26) are valid with $A = 1$.

Facility and Description of Present Work

The "*Probe Calibration Tunnel*" (PCT)[2] is an open jet tunnel with the ability to independently control velocity, density and total temperature. The primary purpose of this facility is to economically calibrate probes for NASA's major test facilities at the Langley Research Center. Typical operational cost for the PCT is 1% of the cost of operating a major facility[2]. The combination of the staged pressure system and low mass flow requirement of the facility and the large volume vacuum systems enables economic and accurate calibration of probes. Due to these feature, the flow in this facility is continuous. Schematic diagram of the facility is presented in figure 2.

The PCT has two interchangeable, subsonic and transonic, nozzles having diameter of 1.50 and 2.25 inches, that gives a continuous flow capability over Mach number range of 0.05 to 1.0. Tunnel stagnation pressure and temperature can be varied from a minimum of 0.20 atmosphere to a maximum of 10 atmospheres and 500°R to 600°R, respectively. This corresponds to a Reynolds number range of $1 \times 10^6 < Re/ft < 51 \times 10^6$ for a Mach number of 1.

A schematic diagram of the data acquisition system for this test is presented in figure 3. A three wire hot-wire probe consisting of three different diameters of Platinum coated Tungsten wire (diameters of 0.0001, 0.0002 and 0.0003 inch) was used to obtain the data. The 1.50 inch diameter nozzle was used in this test. The operational envelope of the tunnel with this nozzle is compared with few other facilities in figure 4, where similar[3-6] hot-wire measurements were performed at NASA Langley.

The test matrix consisted of 12 velocities, 7 densities and 5 total temperatures for the case where $E = f(u,\rho,T_o,T_w)$. For $E = f(M,Kn,a'_w)$, the test matrix consisted of 12 Mach numbers, 7 Knudsen numbers and 8 overheats. The lower and upper bounds of the test matrix for the two methods are given in Table I and II. The flow region of the present test as compared to earlier calibration tests are shown in figure 5. At selected test conditions, fluctuation data were obtained for future analysis. In this study, all the Knudsen number were greater than 0.01 indicating that all the data were in the slip flow regime based on the definition of the slip flow boundary in reference 7.

Parameter	Minimum	Maximum
Total Pressure, psi	3.40306	46.2992
Static Pressure, psi	2.83727	31.5238
Velocity, ft/sec	113.785	950.953
Mach Number	0.0982	0.941
q , psi	0.0064	14.328
Total Temperature, °R	500	580
Static Temperature, °R	417.33	579.73
Reynolds number/foot	0.3×10^6	12.3×10^6
Heater Power, Watts	32.5	4545
Density	0.01875	0.14693
Mass flow, lb/sec	0.012832	1.71468

Table I. Minimum and Maximum Test Conditions of Test Matrix for Functional Relationship $E = f(u,\rho,T_o,T_w)$; Method I.

Parameter	Minimum	Maximum
Total Pressure, psi	3.675	29.4
Static Pressure, psi	3.44859	26.2216
Mach Number	0.10	0.95
q , psi	0.0066	9.8543
Total Temperature, °R	540	540
Static Temperature, °R	457.433	539.73
Reynolds number/foot	0.5×10^6	13.3×10^6
Knudsen number	0.00494	0.10369
Heater Power, Watts	33.2	2985
Density	0.01875	0.13333
Mass flow, lb/sec	0.013103	1.1793
Overheat Ratio	0.3	1.0

Table II. Minimum and Maximum Test Conditions of Test Matrix for Functional Relationship $E = f(M,Kn,a'_w)$; Method II.

Results and Discussion

Data obtained in the "*Probe Calibration Tunnel*" was used to calculate the sensitivities of several hot-wires using the two methods developed for CTA. The data were obtained such that the partial derivatives of the functional relationship such as $E = f(u,\rho,T_o,T_w)$ and $E = f(M,Kn,a'_w)$ were satisfied as dictated by the calculus, i.e., while obtaining data by varying one independent variable, the other independent variables were held constant. Constant Temperature Anemometers (CTA) were used in obtaining the hot-wire data. Thus, the restriction of the calculus with respect to T_w was satisfied automatically and the first functional relationship reduces to $E = f(u,\rho,T_o)$. Polynomials of appropriate degree were chosen to give the "*best curve fit*" to the data to evaluate the partial derivatives required in the sensitivities equations.

The test conditions in this study for $E = f(u,\rho,T_o)$ case are presented in Table I. Examples of curve fits to the data are shown in figures 6 (a-b) where the dependent variable, measured voltage, is presented against each of the independent variable, while the other independent variables were held constant. Computing sensitivities in this case was simple and direct. The logarithmic derivative of the measured voltage to each independent variable gives the sensitivity of the hot-wire to corresponding variable as shown in equation (16).

In the second set of data, a'_w was chosen over T_o to demonstrate that even though many wind tunnels do not have the capability of varying total temperature, the limitations of the tunnel can be overcome by using a'_w. In obtaining the second set of data with respect to overheat ratio, all the hot-wires were operated at assigned overheat values. The test conditions for this case are given in Table II. The curve fit of measured voltage vs. various independent variables are presented in figure 7 (a-b). Here the sensitivities were computed using equations (24)-(26).

To obtain fluctuation quantities each hot-wire on the probe was assigned different overheat value in an attempt to make $S_u \neq S_\rho$, a necessary condition for obtaining fluctuations. However, no fluctuation quantities are presented in the present study.

Velocity Sensitivity:

As seen in figures 6-a and 7-a, the voltage increases rapidly at low velocities or Mach numbers and at transonic speed the slope of the curves tend to decrease. For the case $E = f(M,Kn,a'_w)$ there was a tendency for $dE/dM \rightarrow 0$ at intermediate Mach numbers before increase as $M \rightarrow 1$. Thus, in correlating E vs. M at transonic speeds might result in zero or negative slope. This variation was also observed in the data presented by other researchers[8,10,11]. In order to correlate these data higher order polynomials were required. This could lead to large difference in the sensitivities at higher Mach number due to poor curve fitting at the end points. Precautions need to be taken in using the proper degree of polynomials because they could lead to unreasonable values for the sensitivities. One such difficulty in using higher order polynomial was presented in reference 9 where it lead to a hairpin like variation of S_u with S_ρ.

Examples of the velocity sensitivity, S_u, for both sets of data are presented in figures 8 (a-b) and generally, S_u ranged from 0.05 to 0.40. In both cases S_u increased with increased u or M at low subsonic speeds and decreased at intermediate subsonic speeds. As S_u approached sonic velocity, the sensitivities increased rapidly.

A comparison of S_u for both the methods is presented in figure 9. It is expected that both methods, at identical test conditions, should give similar results. Most of the values for S_u agreed within about 25 percent, however, some of the differences shown may be due to different degree of polynomial curve fits used in each technique. Also, it may be due to the differences in the operation of the anemometer for each method. In the first method, T_w is held constant and T_o is varied. In the second method, T_o is held constant and T_w is varied. Due to this difference in the operation of the hot-wire the end-loss to the support could be different. This difference in end loss could contribute to differences in all the three sensitivities.

Density Sensitivity

The measured voltages across the hot wires monotonically increased or decreased with increasing density or Knudsen number, respectively. At higher Knudsen number the slope changed sign which was due to large change in Knudsen number and

insufficient data . A second degree polynomial was used to correlate the data. The density sensitivity, S_ρ, varies from 0.1 to 0.4 and an example of S_ρ for both the cases are presented in figures 10 (a-b). Except for the data where Knudsen number had a large change, the density sensitivities in both the cases were comparable with each other and a case is presented in figure 11.

A comparison of velocity sensitivity, S_u, with density sensitivity, S_ρ, is presented in figures 12 (a-b) and shows that $S_u \neq S_\rho$ for most of the data. However, few data points do approach $S_u = S_\rho$ and $S_u > S_\rho$ in some cases for $E = f(M,Kn,a'_w)$. The cases where $S_\rho > S_u$ indicates that the wire was in the slip flow regime. This observation is consistent with Spangenberg's data[8] as noted in reference 9. It was also noted that at higher Mach numbers and lower overheat ratio, a'_w, S_u approaches S_ρ. As a'_w was increased S_u became greater than S_ρ.

Total Temperature Sensitivity

For method II, the manufacturer's suggested values of α_1 and Morkovin[1] suggested values of β_1 for tungsten wire were used to compute S_{T_o}. α_1 was also computed using the data obtained during the test and this value was comparable with the manufacturer's provided value of α_1. The data obtained in the present study was not adequate to evaluate β_1.

An example of the data used to obtain the total temperature sensitivity, S_{T_o}, is presented in figures 6(b) and 7(b) and S_{T_o} ranges from -0.2 to -1.0. However, the total temperature sensitivity obtained using the first method was always larger than the values computed using the second method. A few examples of these variations are presented in figures 13 (a-b). This range of temperature sensitivity is consistent with the earlier studies[6,9] from the authors. The temperature sensitivities using the overheat parameter may be more accurate because better curve fits were possible since more data points were available when using the $E = f(u,\rho,T_o)$ method. This shows the possible advantage of using this method versus the other.

A comparison of total temperature sensitivity, S_{T_o}, between the two methods is presented in figure 14. There is a significant difference between the values of S_{T_o} for the two methods. This difference might be explained if the end losses are taken into account since they might be different due to the difference in the operation of the anemometer for each method.

In general, the range of data available from the present study is greater than those obtained from previous studies[3-6], particularly in regards to temperature information. In some of the earlier studies logarithmic functions were used to correlate the data which gave no variation of the sensitivity to its corresponding independent variable. Therefore, polynomial functions seem to be a better technique for correlating the data compared to logarithmic functions. However, careful analysis of the present data is required for a better understanding of the differences between the sensitivities, particularly the total temperature sensitivity, so that they could be applied for computing the fluctuation quantities.

Conclusion

Conventional methods for calibrating hot-wire probes use equations which include quantities that are difficult to evaluate. These quantities are wire length and β_1 in the temperature - resistance equation for the wire material. This could lead to possible errors in obtaining the sensitivities of the heated wire to changes in velocity, density and total temperature. Methods were developed that either eliminated the need for the measurement of ℓ and β_1, which are difficult to make accurately or reduced the effect of β_1. From a study of these methods the following conclusions can be made:

1. The equation obtained for a CTA based on the assumption that $E = f(u,\rho,T_o)$ resulted in an equation in which neither wire length or α_1 and β_1 are required. This should result in a more accurate method for calibrating hot-wire probes in facilities where T_o can be varied.

2. The equation obtained for a CCA based on the assumption that $E = f(u,\rho,T_o,T_w)$ results in an equation that requires the variation of four independent variables and is believed to be too complicated for routine use. The equation also requires the evaluation of β_1 who's elimination was desired.

3. The equation obtained for a CCA and CTA under the assumption that $E = f(M,Kn,a'_w)$ and

T_o = constant resulted in an equation where α_1 and β_1 occurred in only one term in the equation for the total temperature sensitivity. Because of this the calibration of wires should be more accurate than those obtained using conventional methods.

4. The sensitivities computed based on the methods presented using the data obtained in "*Probe Calibration Tunnel*" gives comparable results for S_u and S_ρ. However, there were significant differences in the values for S_{T_o}. The differences in the sensitivities could be due to different degree of the polynomial curve fits used in each technique or due to the differences in the operation of the anemometer in each method.

5. In general, the velocity sensitivity ranges from 0.05 to 0.40, density sensitivity ranges from 0.10 to 0.40 and total temperature sensitivity ranges from -0.2 to -1.0.

6. Polynomial functions seem to be better for correlating hot-wire data compared to logarithmic functions.

Acknowledgment

The first author acknowledge the support of this research by National Aeronautics and Space Administration under contract NAS1-18585 and grant NAG1-1552. The assistance of Mr. Ricky L. Clark in obtaining the data for this study is gratefully acknowledged. Also, the first author is grateful to Prof. Robert L. Ash for his continuous encouragement throughout this study.

References

1. Morkovin, M.V., 1956, "*Fluctuations and Hot-wire Anemometry in Compressible Flows,*" AGARDograph 24.

2. Jones G.S., 1994, "*Wind Tunnel Requirements for Hot-Wire Calibration,*" AIAA-94-2534.

3. Johnson, C.B., and Stainback, P.C., 1984, "*A Study of Dynamic Measurements Made in the Settling Chamber of the Langley 0.3-Meter Transonic Cryogenic Tunnel,*" AIAA-84-0596.

4. Jones, G.S., and Stainback, P.C., 1988, "*A New Look at Wind Tunnel Flow Quality for Transonic Flows,*" SAE 881452 Aerospace Technology Conference and Exposition, Anaheim, California.

5. Stainback, P.C., and Owen, F.K., 1984, "*Dynamic Flow Quality Measurements in the Langley Low Turbulence Pressure Tunnel,*" AIAA-84-0621.

6. Nagabushana, K.A., and Stainback, P.C., 1992, "*Heat Transfer From Cylinders in Subsonic Slip Flows,*" NASA-CR-4429.

7. Stadler, J.R., Goodwin, G., and Creager, M.O., 1951, "*A Comparison of Theory and Experiment for High-Speed Free-Molecule Flow,*" NACA Rep. 1032 (Supersedes NACA-TN-2244).

8. Spangenberg, W.G., 1955, "*Heat Loss Characteristics of Hot-Wire Anemometers at Various Densities in Transonic and Supersonic Flows,*" NACA-TN-3381.

9. Stainback, P.C., and Nagabushana, K.A., 1994, "*Hot-Wire Anemometry in Subsonic Slip and Transonic Flow Regimes,*" AIAA-94-2535.

10. Baldwin, L.V., 1958, "*Slip-Flow Heat Transfer From Cylinders in Subsonic Airstreams,*" NACA-TN-4369.

11. Igoe, W.B., 1994, "*Analysis of Fluctuating Static Pressure Measurements in a Large High Reynolds Number Transonic Cryogenic Wind Tunnel,*" Ph.D., dissertation, George Washington University.

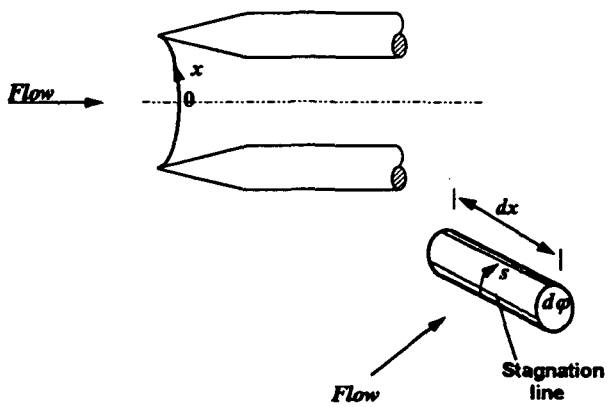

Figure 1. Schematic Diagram of Heated Wire.

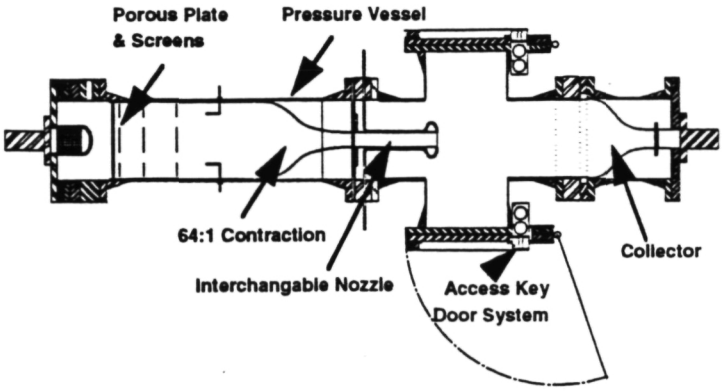

Figure 2. Schematic Diagram of "*Probe Calibration Tunnel*".

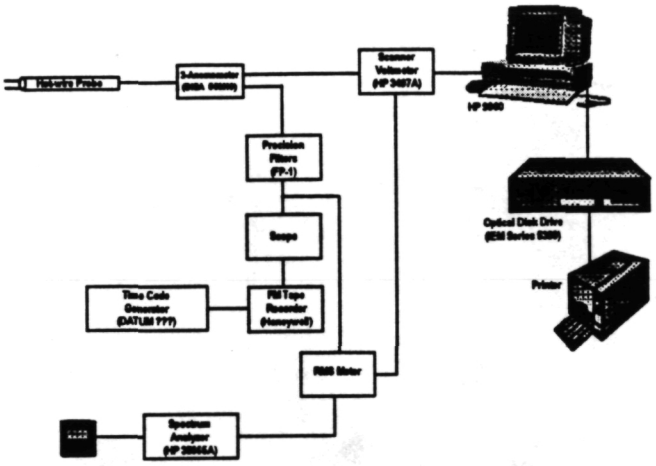

Figure 3. Schematic Diagram of Data Acquisition System.

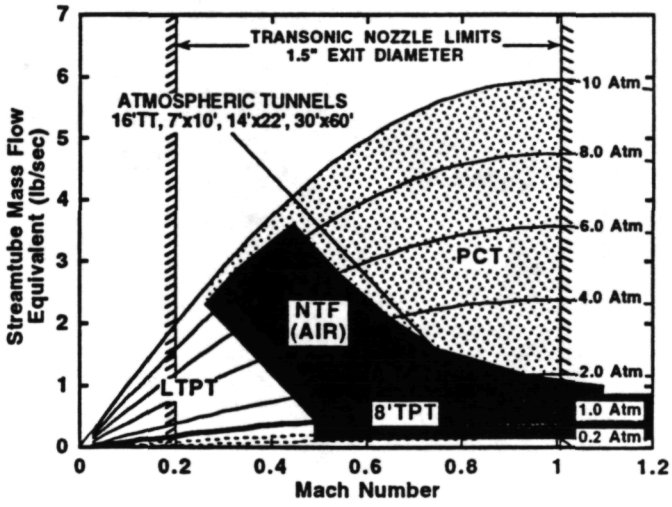

Figure 4. Operational Envelope of the "*Probe Calibration Tunnel*".

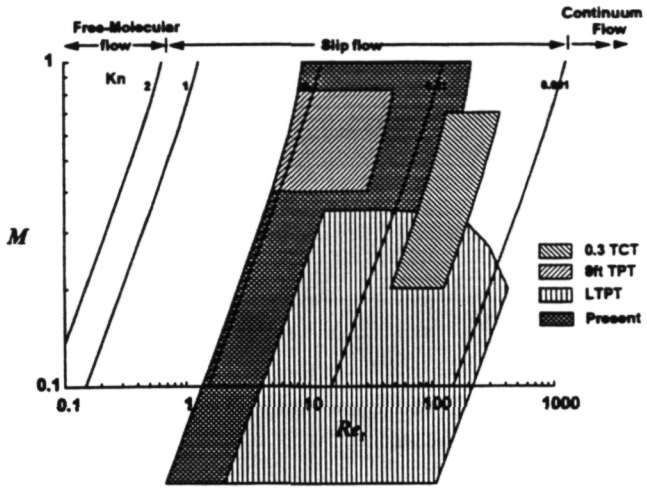

Figure 5. Comparison of Present Test Range with Earlier Calibration Tests.

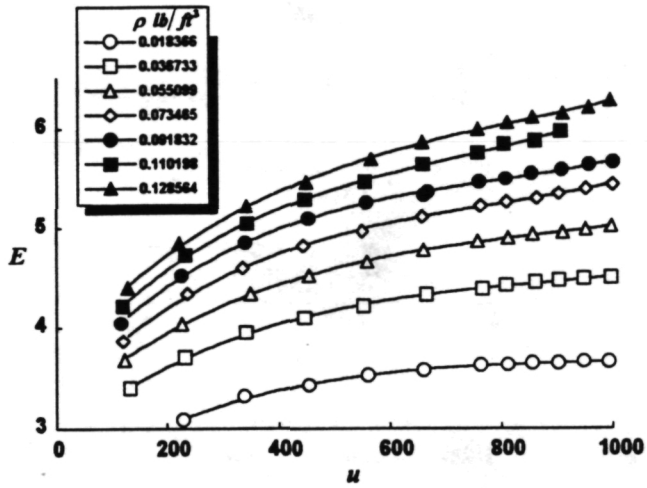

(a) E vs. u ; $T_o = 540°R$

Figure 6. Data Correlated as $E = f(u, \rho, T_o)$; $d_w = 0.0001$ *inch*.

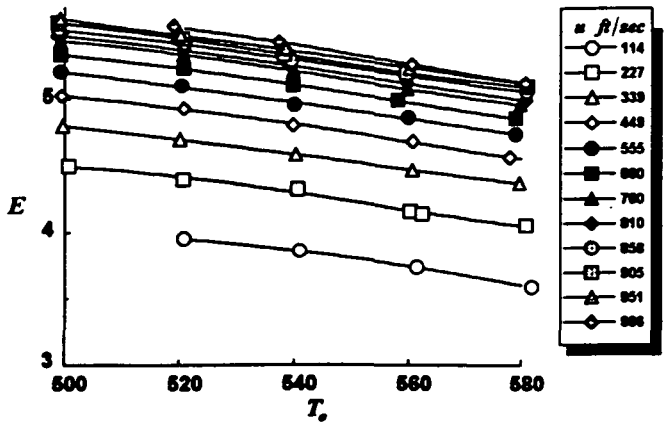

(b) E vs. T_e; $\rho = 0.073465\ lb/ft^3$

Figure 6. Concluded.

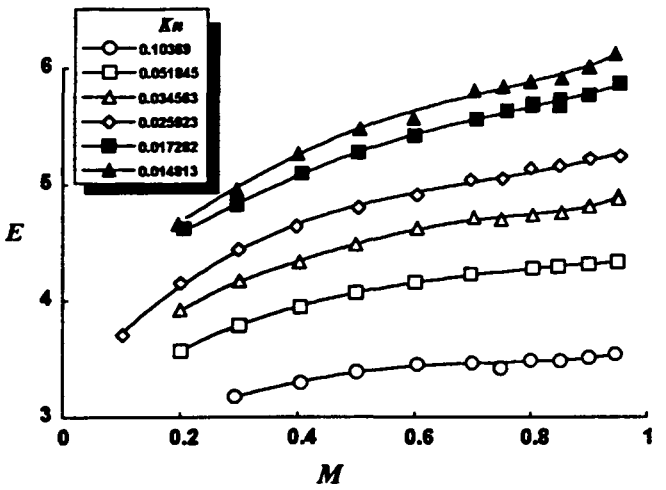

(a) E vs. M; $a'_w = 0.6$

Figure 7. Data Correlated as $E = f(M, Kn, a'_w)$; $T_e = 540°R$; $d_w = 0.0001\ inch$.

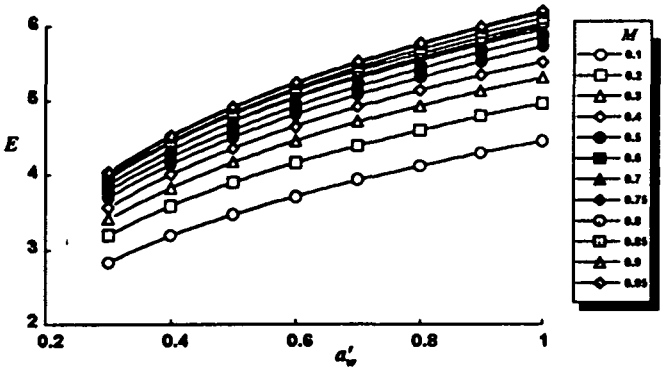

(b) E vs. a'_w; $Kn = 0.025923$

Figure 7. Concluded.

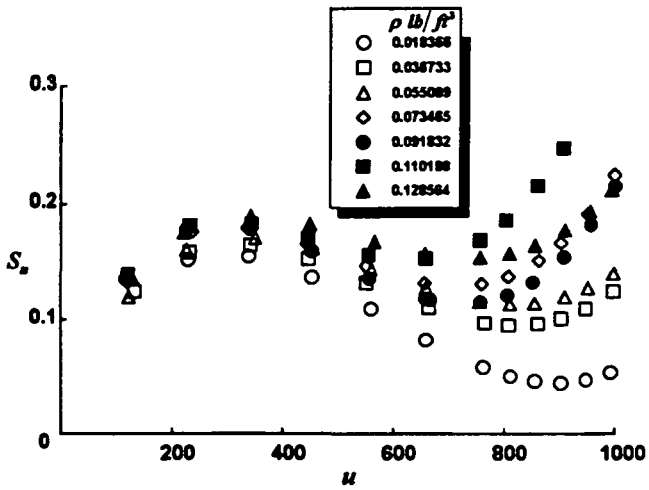

(a) For the case of $E = f(u, \rho, T_e)$

Figure 8. Velocity Sensitivity, S_u; $T_e = 540°R$; $d_w = 0.0001\ inch$.

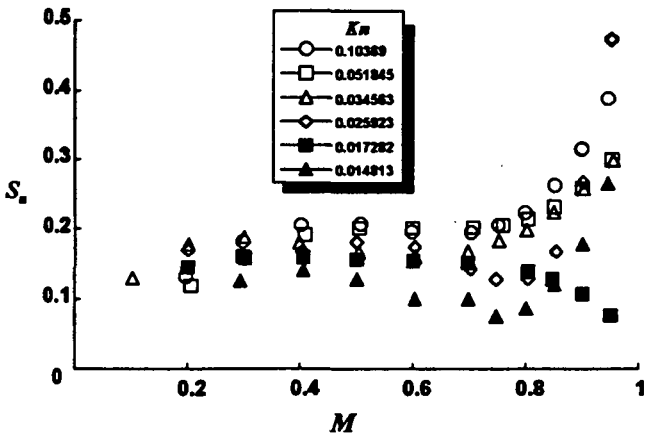

(b) For the case of $E = f(M, Kn, a'_w)$; $a'_w = 0.6$

Figure 8. Concluded.

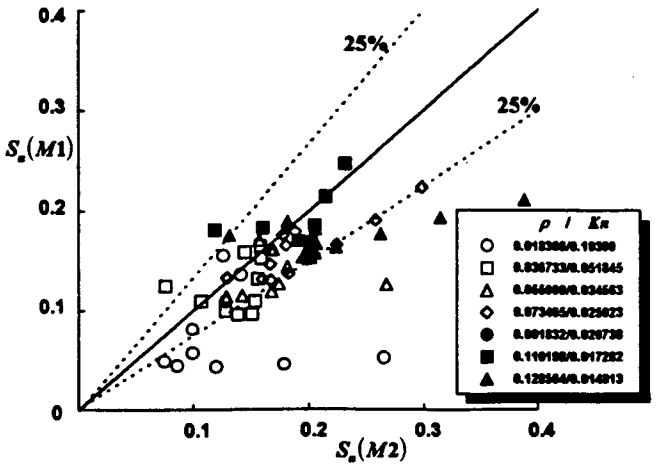

Figure 9. Comparison of S_u for both methods; $T_e = 540°R$; $d_w = 0.0001$ *inch*.

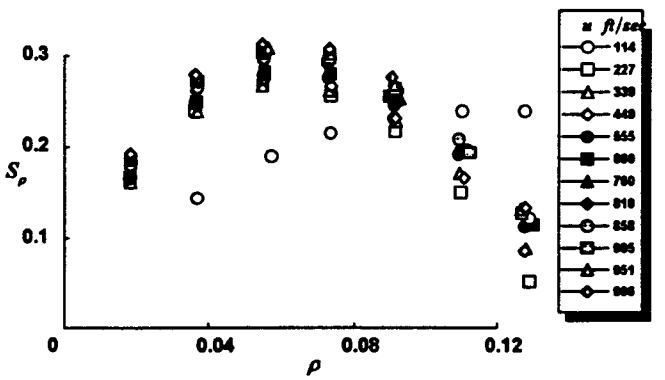

(a) For the case of $E = f(u, \rho, T_e)$

Figure 10. Density Sensitivity, S_ρ; $T_e = 540°R$; $d_w = 0.0001$ *inch*.

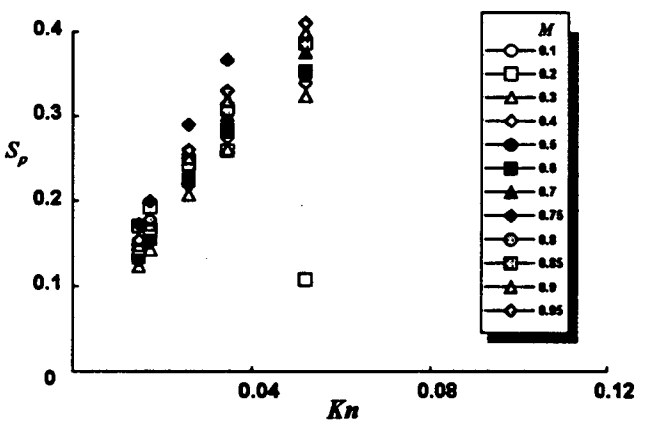

(b) For the case of $E = f(M, Kn, a'_w)$; $a'_w = 0.6$.

Figure 10. Concluded.

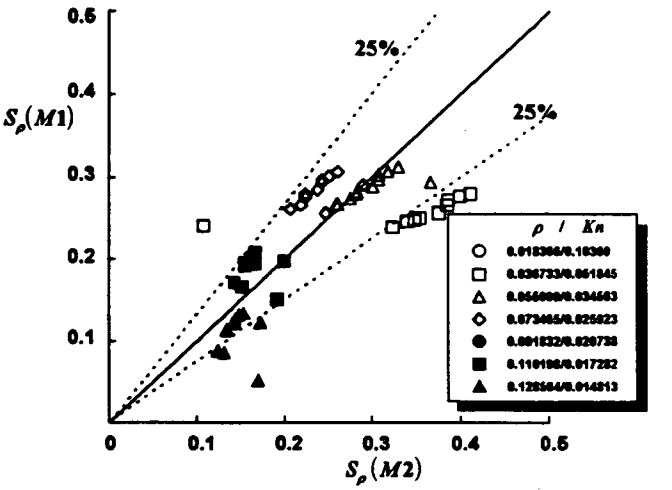

Figure 11. Comparison of S_ρ for both methods; $T_e = 540°R$; $d_w = 0.0001$ *inch*.

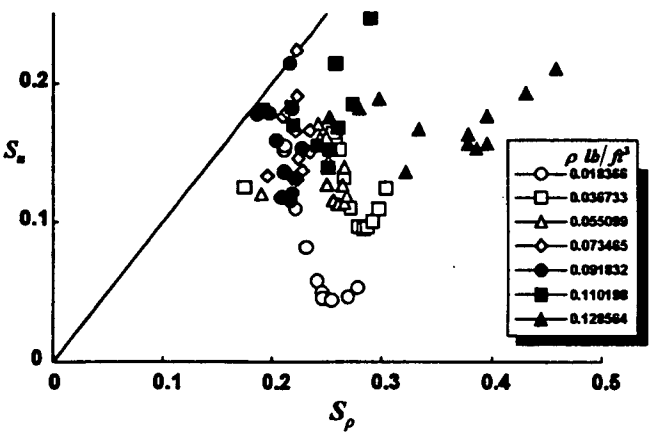

(a) For the case of $E = f(u, \rho, T_e)$

Figure 12. Comparison of S_u vs. S_ρ; $T_e = 540°R$; $d_w = 0.0001$ *inch*.

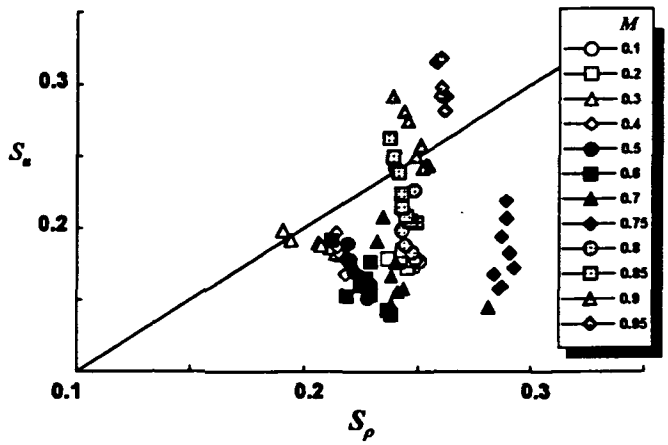

(b) For the case of $E = f(M, Kn, a'_w)$; $Kn = 0.025923$

Figure 12. Concluded.

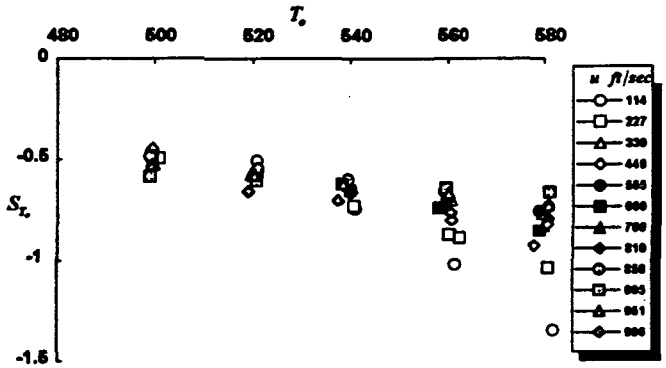

(a) For the case of $E = f(u, \rho, T_o)$; $\rho = 0.073465\ lb/ft^3$

Figure 13. Total Temperature Sensitivity, S_{T_o}; $d_w = 0.0001\ inch$.

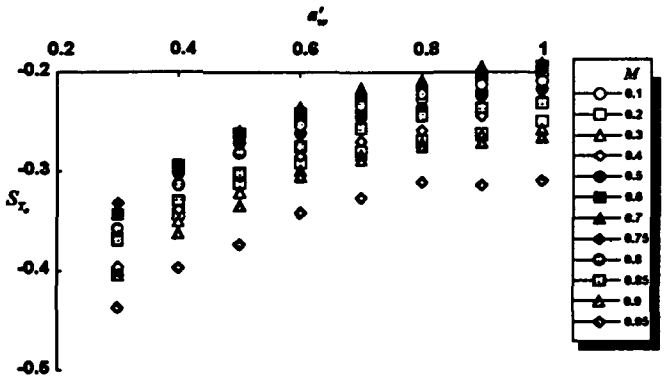

(b) For the case of $E = f(M, Kn, a'_w)$; $T_o = 540°R$; $Kn = 0.025923$

Figure 13. Concluded.

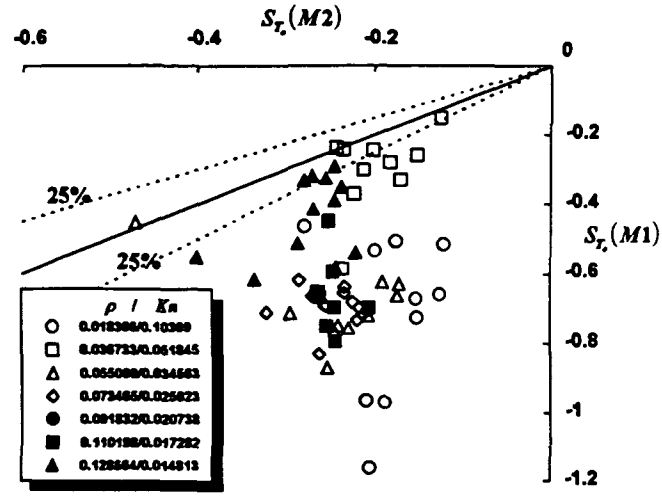

Figure 14. Comparison of S_{T_o} for both methods; $T_o = 540°R$; $d_w = 0.0001\ inch$.

AIAA 94-2535
Hot-Wire Anemometry in Subsonic Slip and Transonic Flow Regimes

P.C. Stainback
NASA Langley Research Center
Hampton, VA 23681

and

K.A. Nagabushana
Old Dominion University
Norfolk, VA 23508

18th AIAA Aerospace Ground Testing Conference

June 20-23, 1994 / Colorado Spring, CO

For permission to copy or republish, contact the American Institute of Astronautics and Aeronautics
370 L'Enfant Promenade, S.W. Washington, D.C. 20024

AIAA 94-2535, 18th AIAA 19th Ground Test Conference
Colorado Springs, Colorado, July 20-23, 1994

Hot-Wire Anemometry in Subsonic Slip and Transonic Flow Regimes

P.C. Stainback
Distinguished Research Associate
NASA Langley Research Center
Hampton, VA 23681

and

K.A. Nagabushana
Research Associate
Old Dominion University
Norfolk, VA 23508

Abstract

Much has been written about the improbability and impossibility of obtaining solutions to the mean square equation for constant current anemometry in subsonic slip and transonic flows. For these flow conditions, the fluctuating voltage across a wire mounted normal to the flow is a function of velocity, density, and total temperature. In principal, the fluctuations of these quantities can be measured, however, to date there are no known acceptable solutions to the mean square equation in these flow regimes. In this study, data presented in the 1950's by Spangenberg were used to show that, for a large region in the Nusselt number - Reynolds number or Nusselt number - Knudsen number regimes, there exists the possibility of obtaining solutions to the mean square hot-wire equation. These data were used to compute the sensitivities of the heated wire to changes in velocity, density, and total temperature; indicate regions where the velocity and density sensitivities were different (a condition required for a solution to the mean square equation); and show a second, necessary condition for a solution. Examples of fluctuation and mode diagrams for subsonic compressible and subsonic slip flows are also presented under the assumption that there are solutions to the hot-wire anemometry equation.

Nomenclature

$a_0 _ a_n$	coefficients in equations (22) - (27)
$b_0 - b_n$	coefficients in equations (24) - (26)
$c_0 - c_n$	coefficients in equation (26)
a,b,c &d	constants in equation (A-4)
A	quantity given by equation (20)
c_p	specific heat at constant pressure
c_v	specific heat at constant volume
d	wire diameter
e'	fluctuating voltage across the sensor
E_w	mean voltage across sensor
f,g,h	constants in equation (A-4)
h	coefficient of heat transfer
I_w	current through the wire
k_o	thermal conductivity of air based on $T_0 = 0°C$
K	$\partial \log T_w / \partial \log R_w$
Kn	Knudsen number
ℓ	wire length
L	characteristic length
m	mean mass flow
M	Mach number
Nu	Nusselt number
n	number of data points
P_w	electrical power to wire
Q_w	heat transfer from wire
q	sensitivity ratio = S_u/S_{T_t}
R_w	resistance of wire
R_{wf}	wire resistance at reference temperature
r	sensitivity ratio = S_m/S_{T_t}
s	sensitivity ratio = S_ρ/S_{T_t}
S_m	mass sensitivity
S_u	velocity sensitivity
S_ρ	density sensitivity
S_{T_t}	total temperature sensitivity
T	temperature
T_t	total temperature
u	velocity
V	general dependent variable

This paper is declared a work of the U.S. Government and is not subject to copyright protection in the United States..

x,y,z	general independent variables
ε	$-(\partial \log I_w / \partial \log R_w)$
α	$\left(1+\frac{\gamma-1}{2}M^2\right)^{-1}$
α_1	linear temperature - resistance coefficient of wire
β	$\alpha(\gamma-1)M^2$
β_1	second degree temperature - resistance coefficient of wire
λ	mean free path
η	recovery temperature ratio, T_{adw}/T_o
θ	temperature parameter, T_w/T_o
θ	angle between probe axis and plane sound wave
γ	specific heat ratio, c_p/c_v
ρ	density
τ_w	temperature loading parameter, $(T_w - T_{adw})/T_o$
ϕ'	normalized fluctuation voltage ratio = $\left(e'/E_w\right)/S_{\tau_w}$

Superscript

$'$	indicates instantaneous value
$\sim$	RMS value
$\overline{\ }$	mean value

Subscript

adw	adiabatic wall condition
w	wire condition
∞	free stream or static condition
o	based on $T = 0°C$
ref	reference condition at $T_0 = 0°C$
ω	vorticity
σ	entropy
sf	far field sound

Introduction

Constant current anemometry (CCA) has been extensively used to measure fluctuations in incompressible and compressible flows[1-3]. In compressible flow the heated wire is, in general, sensitive to changes in velocity, density, and total temperature and fluctuations in these quantities can, in principal, be measured[4]. In supersonic flow it has been found experimentally that the mean voltage measured across a heated wire is only a function of changes in mass flow and total temperature[5]. Using this result for supersonic flow, Kovasznay developed a graphical technique for determining fluctuations of mass flow, total temperature, and their correlation[6]. Very few attempts have been made to measure fluctuations in subsonic compressible flow using a CCA because of the complexity that exists when the heat transfer from the wire is a function of three independent variables.

Some efforts have been made to measure fluctuations in subsonic compressible flow using a constant temperature anemometer (CTA). For these investigations a three-wire probe was used and the voltages across the wires were digitized and a system of three equations solved to obtain the instantaneous changes in velocity, density, and total temperature as a function of time. Statistical techniques were then used to obtain fluctuations and correlations of interest[7].

For compressible flow; where the wire is sensitive to velocity, density, and total temperature; equations for CCA are usually derived using mean square values. This results in a single equation with six unknowns. Much has been written about the improbability[4] and impossibility[8] of obtaining solutions to this mean square equation. Solutions to this equation requires that the velocity and density sensitivities of the heated wire be sufficiently different. In this report, data published in the 1950's by Spangenberg[9] was used to show that there exist a large region in the Nusselt number-Reynolds number or Nusselt number-Knudsen number regimes where the velocity and density sensitivities appeared to be sufficiently different to permit suitable solutions to the mean square equation. It was further shown that solutions were possible only when the velocity and density sensitivities were non-linearly related in specific manners. Again Spangenberg's data were used to show that this second condition can often be satisfied, further indicating that solutions to the mean square equation are possible. Examples of fluctuation and mode diagrams for subsonic compressible and subsonic slip flows are also presented under the assumption that there are solutions to the hot-wire anemometry equation.

Spangenberg's Data

Spangenberg's data were presented in terms of $Nu_\infty = f(M,\rho,\tau_w)$ for $T_o = constant$. Data were presented for several wire diameters and wire lengths. The data to be considered herein were obtained using a Pt-10% Rh wire having a diameter of 0.00015 inch and a length of 2.80 mm. Data were limited to the following conditions:

$$0.05 < M < 0.95$$
$$0.0004 < \rho,\ gm/cm^3 < 0.0012$$
$$0.221 < \tau_w < 2.192$$

The Nusselt numbers presented were corrected for heat loss to the supports of the wire. This corrected Nusselt number, Nu_∞, is suitable for comparing heat transfer results from different experiments using different wire materials and different ℓ/d's. For computing fluctuations, the sensitivities of the wire must be obtained using the uncorrected Nusselt number, Nu_o. For the results presented herein, Nu_∞ values were converted to Nu_o values using the method presented by Spangenberg.

Examples of Spangenberg's data are presented in figure 1. In figure 1a the uncorrected Nusselt number is presented as a function of Mach number for various values of density for a given value of τ_w. The Nusselt number increases rapidly with Mach number at very low values. The slopes of the curves decrease somewhat as the Mach number increases. At the higher Mach numbers ($0.6 < M < 0.95$) the Nusselt number often reaches a peak prior to decreasing. This variation of Nu_o with M at the higher Mach numbers often results in zero or negative slopes for Nu_o vs M. The Mach numbers at which the slopes of the curves reach zero increase with increasing density. This variation of Nu_o vs M was also observed in data presented in references 10 and 11. Polynomials were used to fit curves to the data from which the required derivatives were obtained, and a fourth degree equation was required to obtain "*good*" fits. The variation of Nu_o with ρ, shown in figure 1b, is monotonically increasing with increasing density. A second degree equation was used to fit curves to the Nu_o vs ρ data.

The variation of Nusselt number with respect to τ_w is presented in figure 1c and this variation of Nu_o is rather complex and nonlinear. The Nusselt number can often increase then decrease with increasing values of τ_w. A closer look at Nu_o vs τ_w data revealed that, for most of the data, the values of Nu_o decreased from $0.629 \le \tau_w \le 1.629$ but most often increased or tended to increase from $1.629 \le \tau_w \le 2.192$. This variation of Nu_o over this later interval of τ_w was present in about 80 percent of the data and had a profound affect on the relationship between the velocity and density sensitivities. It is not known if this variation can be supported by the limited amount of data which is available. If third degree curves were fitted to the data, there was a significant change in the derivatives for most of the data at the higher values of τ_w. Because of these changes, the values of Nu_o were fitted to values of τ_w using both second and third degree equations. The results obtained using these two curve fits on the variation of the velocity and density sensitivities will be presented subsequently.

Data presented by Baldwin in Ref. 10 also showed a similar variation of the Nusselt number with τ_w. This complex and nonlinear variation of Nusselt number with τ_w or overheat is probably the reason that solutions to the mean square equation for CCA might exist.

In general, the scatter in the values of Nu_o with respect to M and ρ are acceptably small; the apparent scatter of Nu_o with respect to τ_w is somewhat larger. This is probably due to the relatively small change in Nu_o with respect to τ_w or the limited number of values of τ_w that are available.

Theoretical Considerations

Because of the manner in which Spangenberg presented his data, equations must be derived for the change in voltage across the wire in terms of the sensitivity of the wire to changes in velocity, density, and total temperature. The equation for the heat transfer from the heated wire is generally given as:

$$Q = \pi d \ell h (T_w - T_{aw}) \tag{1}$$

For steady state conditions, power supplied to the heated wire equals the aerodynamic heat transfer from the wire. Therefore:

$$P_w = I_w^2 R_w = \pi \ell k_o (T_w - \eta T_o) Nu_o \tag{2}$$

Making the small perturbation assumption, the change in R_w can be expressed as:

$$(1 - 2\varepsilon) d\log R_w = d\log Nu_o + d\log \tau_w + d\log T_o \tag{3}$$

where:

$$\varepsilon = -\frac{\partial \log I_w}{\partial \log R_w} \tag{4}$$

For Spangenberg's data:

$$Nu_o = f(M, \rho, \tau_w) \tag{5}$$

Note that there is a direct relationship between density and Knudsen number. Therefore, the Knudsen number could be used as independent variable. The change in Nu_o is:

$$d\log Nu_o = \frac{\partial \log Nu_o}{\partial \log \rho} d\log \rho + \frac{\partial \log Nu_o}{\partial \log M} d\log M + \frac{\partial \log Nu_o}{\partial \log \tau_w} d\log \tau_w \qquad (6)$$

It is desired to obtain the final equation in the following form:

$$E_w = f(u, \rho, T_o) \qquad (7)$$

The change in M is:

$$d\log M = \frac{1}{\alpha}\left(d\log u - \frac{1}{2} d\log T_o\right) \qquad (8)$$

and

$$d\log \tau_w = \frac{\theta}{\tau_w} d\log T_w - \frac{\eta}{\tau_w} d\log \eta - \frac{\eta}{\tau_w} d\log T_0 \qquad (9)$$

The recovery temperature ratio can be written as:

$$\eta = f(\rho, M) \qquad (10)$$

and the change in η is:

$$d\log \eta = \frac{\partial \log \eta}{\partial \log \rho} d\log \rho + \frac{1}{\alpha} \frac{\partial \log \eta}{\partial \log M}\left(d\log u - \frac{1}{2} d\log T_o\right) \qquad (11)$$

The temperature of the wire must be obtained from the measured resistance using:

$$\frac{R_w}{R_{wf}} = 1 + \alpha_1 (T_w - T_{wf}) + \beta_1 (T_w - T_{wf})^2 \qquad (12)$$

Therefore:

$$T_w = f(R_w) \qquad (13)$$

and

$$d\log T_w = K\, d\log R_w \qquad (14)$$

Finally, Ohm's law can be used to express the wire resistance in terms of the voltage across the wire as follows:

$$d\log R_w = \frac{d\log E_w}{(1+\varepsilon)} \qquad (15)$$

Morkovin[4] gives the following equation for the changes in E_w due to changes in u, ρ and T_o for a CCA:

$$d\log E_w = -S_u d\log u - S_\rho d\log \rho + S_\tau d\log T_o \qquad (16)$$

For the present case the sensitivities can be obtained using equations (3) - (15) and are given by:

$$S_u = \frac{A}{\alpha}\left[\frac{\partial \log Nu_o}{\partial \log M} - \frac{\eta}{\tau_w} \frac{\partial \log \eta}{\partial \log M}\left(\frac{\partial \log Nu_o}{\partial \log \tau_w} + 1\right)\right] \qquad (17)$$

$$S_\rho = A\left[\frac{\partial \log Nu_o}{\partial \log \rho} - \frac{\eta}{\tau_w} \frac{\partial \log \eta}{\partial \log \rho}\left(\frac{\partial \log Nu_o}{\partial \log \tau_w} + 1\right)\right] \qquad (18)$$

$$S_\tau = A\left[-\frac{1}{2\alpha} \frac{\partial \log Nu_o}{\partial \log M} + \frac{\eta}{\tau_w}\left(\frac{\partial \log Nu_o}{\partial \log \tau_w} + 1\right)\left(\frac{1}{2\alpha} \frac{\partial \log \eta}{\partial \log M} - 1\right) - \frac{\partial \log Nu_o}{\partial \log \tau_w}\right] \qquad (19)$$

where

$$A = \frac{(1+\varepsilon)}{\left[(1-2\varepsilon) - \frac{\theta K}{\tau_w}\left(\frac{\partial \log Nu_o}{\partial \log \tau_w} + 1\right)\right]} \qquad (20)$$

For Spangenberg's data η varied with M and plots of η vs M were presented in his report. The values for α_1 and β_1 for the wire material were also presented. Therefore, after the partial derivatives in equation (17) - (20) were determined the sensitivities to changes in u, ρ, and T_o could be calculated.

The value of ε cannot be evaluated from Spangenberg's data because the voltage of the battery used is unknown and there are several variable resistors, having unknown resistances, in the electrical circuit. Because of these problems the absolute values of the sensitivities could not be obtained. The values of ε does not, however, influence the ratio of the sensitivities, the important parameters, since the quantity A cancels out when the ratios are formed.

The Partial Derivatives

Spangenberg's data were measured and tabulated in a form that is necessary to obtain the partial derivatives of the dependent variable with respect to one independent variable while holding the remaining independent variables constant. These are the only data known to the authors where measurements were obtained in this necessary manner. For the present report, polynomials were

used to fit the data to obtain the desired derivatives of Nu_o with respect to the independent variables. The degree of the polynomial was chosen to give the "*best fit*" to the data. In general, this method gives:

$$V = f(x,y,z) \tag{21}$$

where the function was assumed to be:

$$V(x,y,z) = a_0 + a_1x + a_2x^2 + \ldots a_nx^n \tag{22}$$

and:

$$a_m = f(y,z) \qquad m = 0,1,2,\ldots n \tag{23}$$

Using polynomials, the values for the a's can be expressed as:

$$a_m = b_o + b_1y + b_2y^2 + \ldots b_ny^n \tag{24}$$

where

$$b_m = f(z); \qquad m = 0,1,2,\ldots\ldots n \tag{25}$$

In a similar manner:

$$b_m = c_0 + c_1z + c_2z^2 + \ldots c_nz^n \tag{26}$$

From equation (22), the derivatives becomes:

$$\frac{\partial \log V}{\partial \log x} = \frac{a_1x + 2a_2x^2 + \ldots na_nx^n}{a_0 + a_1x + a_2x^2 + \ldots a_nx^n}. \tag{27}$$

The Sensitivities

After the partial deviates were determined, the sensitivities were obtained using equations (17) - (20). In general:

$$S_u : S_\rho : S_{T_o} = f(M, \rho, \tau_w) \tag{28}$$

For these calculations it was assumed that $\varepsilon = 0$. Plots of the sensitivities will not be presented since it will be shown subsequently that the ratios S_u / S_{T_o} and S_u / S_{T_o} are the important parameters. At some values of the Mach number, $S_u = 0$ and the wire, at these conditions, is not sensitive to changes in velocity.

The Mean Square Equation

In the past hot wire data, using a CCA, were obtained from mean square values. Following Kovasznay, squaring equation (16), dividing by $S_{T_o}^2$, and taking the mean gives:

$$\overline{\phi^2} = q^2\overline{\left(\frac{u'}{u}\right)^2} + s^2\overline{\left(\frac{\rho'}{\rho}\right)^2} + \overline{\left(\frac{T_o'}{T_o}\right)^2} + 2qs\frac{\overline{u'\rho'}}{u\rho} - 2q\frac{\overline{u'T_o'}}{uT_o} - 2s\frac{\overline{\rho'T_o'}}{\rho T_o} \tag{29}$$

This is a single equation in six unknowns, $\left(i.e., \frac{\tilde{u}}{u}, \frac{\tilde{\rho}}{\rho}, \frac{\tilde{T}_o}{T_o}, \frac{\overline{u'\rho'}}{u\rho}, \frac{\overline{u'T_o'}}{uT_o}, \frac{\overline{\rho'T_o'}}{\rho T_o}\right)$. Since $\overline{\phi^2}$, q and s are functions of the overheat of the wire, one can, in principal, operate a single wire at six overheats and solve a system of six equations for the fluctuations and their correlations. The unsuccessful attempts that were made in the past to obtain solutions in this manner were thought to be due to the mean flow calibrations not being accurate enough or the sensitivities not being sufficiently different to permit accurate solutions[4]. Demetriades[8] stated that no solutions to equation (29) are possible unless the independent variable occurs to at least the fifth power. It is shown in the Appendix that if s is assumed to be a function of q, solutions to equation (29) are possible if, after substituting the functional relationship for s into the equation, the resulting equation has six terms. This result requires that values for s have very restrictive, non-linear variations with respect to q as the overheat of the wire is changed. Table I presents conditions where solutions to equation (29) exist based on s being a simple, finite, power series of q.

Figure 2 is presented to show to what extent $q \neq s$ for $\tau_w = 2.192$. From the figure it can be seen that s is, in general, greater than q and the difference can be large since q can often approach zero at the higher values of M. At the higher values of M the sign of q can change and negative values are not presented in the figure.

For Spangenberg's data, which is considered herein, the Mach number ranged from 0.05 to 0.95. The equation given by Morkovin for the Knudsen number is:

$$Kn = \frac{7.75x10^{-9}}{\rho d} \tag{30}$$

where ρ is in gm/cm^3 and d is in cm. Using this equation, the value for the Knudsen number for these data ranged from 0.017 to 0.051. Reference 12 suggest that continuum flow occurs for $Kn < 0.001$ and slip flow occurs for $0.001 \le Kn \le 2$. Other references suggest that continuum flow occur for $Kn < 0.01$. These quoted boundaries are not sharply defined, but if it is assumed that slip flow occurs for $Kn > 0.01$, all of Spangenberg's data considered herein is in the slip flow regime. This result is in agreement with the data presented in figure 2 where $S_u/S_\tau \neq S_\rho/S_\tau$, however, a few data points do approach $S_u/S_\tau = S_\rho/S_\tau$.

Solution to Mean Square Equation

Solutions to equation (29) can be obtained by using the method of least squares. Applying this method results in the following matrix equation:

$$\begin{vmatrix} \Sigma q^4 & \Sigma q^2 s^2 & \Sigma q^2 & \Sigma s q^3 & \Sigma q^3 & \Sigma q^2 s \\ & \Sigma s^4 & \Sigma s^2 & \Sigma q s^3 & \Sigma q s^2 & \Sigma s^3 \\ & & n & \Sigma q s & \Sigma q & \Sigma s \\ & & & \Sigma q^2 s^2 & \Sigma q^2 s & \Sigma q s^2 \\ & & & & \Sigma q^2 & \Sigma s q \\ & & & & & \Sigma s^2 \end{vmatrix} \begin{vmatrix} \overline{(u'/u)^2} \\ \overline{(\rho/\rho)^2} \\ \overline{(T_o'/T_o)^2} \\ 2\overline{\frac{u'\rho}{u\rho}} \\ -2\overline{\frac{T_o' u'}{T_o u}} \\ -2\overline{\frac{\rho' T_o'}{\rho T_o}} \end{vmatrix} = \begin{vmatrix} \Sigma q^2 \overline{\phi'^2} \\ \Sigma s^2 \overline{\phi'^2} \\ \Sigma \overline{\phi'^2} \\ \Sigma q s \overline{\phi'^2} \\ \Sigma q \overline{\phi'^2} \\ \Sigma s \overline{\phi'^2} \end{vmatrix} \qquad (31)$$

In equation (31) q, s and $\overline{\phi'^2}$ are functions of the overheat parameter, τ_w. Solutions to equation (31) can be obtained as follows. Obtain a set of values for q, s and $\overline{\phi'^2}$ for a suitable number of values for τ_w, say 10 or 12. Fit suitable curves to q and $\overline{\phi'^2}$ vs τ_w. Also obtain curve fits for $s = f(q)$ that satisfies the requirements noted in the Appendix to determine if a solution to equation (31) is possible. The "*best curve fit*" to these data using the acceptable coefficients can be used to relate s to q and ultimately s and τ_w. Using the equations obtained for q, s and $\overline{\phi'^2}$ vs τ_w, compute a set of values, say 20, to be used in equation (31) to obtain the fluctuations and their correlations.

An additional datum point can be obtained for s and q by using the limiting values for these variables. These equations are:

$$q = -\frac{\dfrac{\partial \log \eta}{\partial \log M}}{\alpha\left(\dfrac{1}{2\alpha}\dfrac{\partial \log \eta}{\partial \log M} - 1\right)}; \quad \tau_w = 0 \qquad (32)$$

$$s = -\frac{\dfrac{\partial \log \eta}{\partial \log \rho}}{\left(\dfrac{1}{2\alpha}\dfrac{\partial \log \eta}{\partial \log M} - 1\right)}; \quad \tau_w = 0 \qquad (33)$$

An indication of the accuracy and suitability of these results can be obtained by computing the condition number[13] for the 6x6 matrix in equation (31). The smaller the condition number the more accuracy can be expected from the calculated results.

No fluctuating voltages were presented by Spangenberg, therefore, no fluctuating quantities could be calculated. His data were used to obtain relationships between q and s, to calculate the elements of the matrix in equation (31), and to obtain the condition numbers for these matrices. This procedure serves to illustrate that solutions to equation (31) are possible and give some indication of the accuracy of possible solutions.

Examples of the variation of s with q obtained from Spangenberg's data is presented in figure 3. The case where the Nusselt number was assumed to be a cubic relationship with respect to τ_w most often resulted in a hairpin like variation of s with q. This type of variation does not appear reasonable, therefore, a curve is also presented in the figure where Nu_o was assumed to be given by a second degree equation. This assumption resulted in what appears to be a more reasonable variation of s with q. It must be again noted that the behavior obtained with the cubic curve fit might be due to the limited amount of data available.

There were several sets of data where Nu_o could be fitted with a cubic equation with respect to τ_w, without the derivative of Nu_o increasing at the higher values of τ_w. Examples of s vs q for these cases are presented in figure 4. The powers of q presented in Table I were fitted to the $s-q$ data, and the powers that gave the "*best curve fits*" to the data are presented in the Table II. Most of the curves fitted

to the data appear to be good based on the R^2 values except for the case $M = 0.60$. Curves fitted to the data using the values of the powers presented in Table II are given in figure 4. The equations with these powers were used to relate s to q and in turn to τ_w. Twenty values for q were selected, the values for s computed, and the elements for the 6x6 matrix in equation (31) calculated. Using the elements of the matrix, the condition numbers for the cases presented in figure 4 were determined and these results are presented in the Table II. These large numbers indicate that the 6x6 matrix in equation (31) is very ill conditioned. It is not known if these results are general or limited to the cases investigated which has a limited number of overheats. There are techniques that can be used to improve solutions for equations having ill conditioned matrices[14]. It is not known if these techniques can be used to assure suitable solutions to the hot wire equation. There are cases where suitable solutions can be obtained to sets of equations where the matrix results in large condition numbers[15]. It must be demonstrated that satisfactory results can be obtained for the present equation. Thus, the necessary condition for a solution to the mean square equation has been established; it remains to be demonstrated that sufficient conditions can be established for suitable solutions.

There is an additional problem that could have an adverse effect on solutions to equation (29). Equations (32) and (33) show that s and q, in general, cannot be zero at the same time. This means that conditions required to obtain the total temperature fluctuations do not lie on the curve defined by $s = f(q)$. Therefore, the total temperature fluctuations must be obtained by extrapolation to the condition where $q = s = 0$. It must be noted that this condition is not determined by the accuracy of the mean flow calibration data but by the relationships used to obtain equation (29). This problem is not limited to the subsonic compressible flow case, but could also exist in supersonic flow if $d\log\eta/d\log Re \neq 0$. In supersonic flow the extrapolation is in two dimensional space, whereas in subsonic flow the extrapolation must be in three dimensional space (see Fluctuation and Mode diagram section). Extrapolation, in three dimensional space, of a nonlinear function could result in highly inaccurate solutions. At the present time it is not known whether other relationship could be used to obtain values for s and q such that this problem can be rectified. Possible remedy might be found in the techniques presented in reference 11.

Fluctuation and Mode Diagrams

Fluctuation Diagrams

It is recognized that, in general, if solutions to equation (29) can be obtained using the method of least squares then the fluctuations and their correlations can be obtained without considering the fluctuation diagram. However, the fluctuation diagram can often be used to advantage in determining the dominant mode in a flow[16].

Before considering the fluctuation diagram for subsonic compressible flows, consider the case for supersonic flow where the velocity and density sensitivities are equal. Under these conditions equation (16) becomes:

$$\frac{e'}{E} = -S_m\frac{m'}{m} + S_{T_o}\frac{T_o'}{T_o} \tag{34}$$

Dividing the above equation by S_{T_o}, squaring, and taking the mean gives:

$$\overline{\phi^2} = r^2\overline{\left(\frac{m'}{m}\right)^2} - 2rR_{mT_o}\left(\frac{\tilde{m}}{m}\right)\left(\frac{\tilde{T}_o}{T_o}\right) + \overline{\left(\frac{T_o'}{T_o}\right)^2} \tag{35}$$

This is a single equation with three unknowns $\left(i.e., \frac{\tilde{m}}{m}, \frac{\tilde{T}_o}{T_o}, \frac{\overline{m'T_o'}}{mT_o}\right)$. In principle, a single wire can be operated at three overheats and a system of three equations solved for the fluctuations and their correlation. Kovasznay[6] noted that this technique would probably result in inaccurate answers. He suggested that the wire be operated at several overheats and a graphical technique be used to obtain the fluctuations. Equation (35) is an equation of a hyperbola where the asymptote gives the mass flow fluctuation and the intercept of the curve with the $\tilde{\phi}$-axis gives the total temperature fluctuation. Note that the method of least squares can also be used to obtain solutions to equation (35). An example of a general fluctuation diagram for supersonic flow is presented in figure 5.

Kovasznay[6] demonstrated that fluctuations in compressible flow are composed of three basic fluctuations which are vorticity, entropy, and sound. He denoted these three basic fluctuations as modes. Vorticity is a velocity fluctuation that is usually described as turbulence and has no pressure or static temperature fluctuation. Entropy consists of static temperature fluctuation or temperature spottiness.

The sound field consists of isentropic fluctuations associated with pressure fluctuations and include density, velocity, and temperature fluctuations. If fluctuations are considered to be composed of a single mode then the fluctuation diagram was noted as a mode diagram.

If it is assumed that the velocity and density sensitivities are sufficiently different and sufficiently non-linear so that solutions to equation (29) are possible, what are the characteristics of the fluctuation diagrams in subsonic compressible flow? In equation (29), $\overline{\phi'^2}$ is a function of q and s, therefore, the fluctuation diagram exists on a three-dimensional surface, a hyperboloid, rather than a plane as in the case when $S_u = S_\rho$. The locus of points of the fluctuation diagram on the surface of the hyperboloid will depend on the relative changes in q and s as the overheat of the wire is changed. However, the important information exists in the $\tilde{\phi}-q$ and $\tilde{\phi}-s$ planes. For example when $s=0$, equation (29) reduces to an equation for a hyperbola in the $\tilde{\phi}-q$ plane where the asymptote gives the velocity fluctuations. If $q=0$, again equation (29) reduces to an equation for a hyperbola in the $\tilde{\phi}-s$ plane and the asymptote represents the density fluctuations. When q and s are zero, the intercept on the $\tilde{\phi}$-axis gives the fluctuations for the total temperature. In planes parallel to the $q-s$ plane, the locus of points of the fluctuation diagram is governed by the velocity and density fluctuations and their correlation. The cross product term, qs, requires a rotation of the axis before the characteristics of this locus can be identified.

Although the fluctuation diagram exists on the surface of a hyperboloid, the fluctuations can be determined from the intersection of the hyperboloid with the $\tilde{\phi}-q$ and $\tilde{\phi}-s$ planes. Because of this, the fluctuation and mode diagrams will be defined as the traces of these intersections in the noted planes. A general schematic representation of the fluctuation diagram for equation (29) is presented in figure 6.

Mode Diagrams

First, assume that the only fluctuations are vorticity. Then:

$$\frac{u'}{u}=\left(\frac{u'}{u}\right)_\omega;\quad \frac{\rho'}{\rho}=0;\quad \frac{T_o'}{T_o}=\beta\left(\frac{u'}{u}\right)_\omega;\quad \frac{m'}{m}=\left(\frac{u'}{u}\right)_\omega \tag{36}$$

Next, assume that the only fluctuations are entropy. This results in:

$$\frac{u'}{u}=0;\quad \frac{\rho'}{\rho}=-\left(\frac{T_o'}{T_o}\right)_\sigma;\quad \frac{T_o'}{T_o}=\alpha\left(\frac{T_o'}{T_o}\right)_\sigma;\quad \frac{m'}{m}=-\left(\frac{T_o'}{T_o}\right)_\sigma \tag{37}$$

Finally, assume that the only fluctuations are far-field sound. Then:

$$\frac{u'}{u}=\frac{1}{\gamma M}\left(\frac{p'}{p}\right)_{sf}\cos\theta;\quad \frac{\rho'}{\rho}=\frac{1}{\gamma}\left(\frac{p'}{p}\right)_{sf};\quad \frac{T_\infty'}{T_\infty}=\frac{(\gamma-1)}{\gamma}\left(\frac{p'}{p}\right)_{sf} \tag{38}$$

$$\frac{T_o'}{T_o}=\alpha\frac{(\gamma-1)}{\gamma}\left(\frac{p'}{p}\right)_{sf}+\beta\left(\frac{u'}{u}\right)_{sf};\quad \frac{m'}{m}=(M+\cos\theta)\frac{1}{\gamma M}\left(\frac{p'}{p}\right)_{sf} \tag{39}$$

A schematic of the mode diagrams for supersonic flow is presented in figure 7 for vorticity, entropy, and far-field sound. In all cases the mode diagrams are degenerate hyperbolas. This figure is presented in order to compare the mode diagram in supersonic flows with those in subsonic flows.

If it is assumed that in subsonic flow the fluctuations are only due to vorticity, equation (29) gives:

$$\overline{\phi'^2}=(q-\beta)^2\overline{\left(\frac{u'}{u}\right)_\omega^2} \tag{40}$$

Results obtained using this equation for the case where $(u'/u)_\omega = 0.01$ are presented in figure 8. The mode diagram for vorticity is identical to the one for supersonic flows except that S_m is replaced by S_u and the important part of the mode diagram lies in the $\tilde{\phi}-q$ plane since $\tilde{\rho}/\rho=0$. Equation (40) shows that when $\tilde{\phi}=0$, then $q=\beta$. Also, when $q=0$ then:

$$\tilde{\phi}=\beta\left(\frac{\tilde{u}}{u}\right)_\omega \tag{41}$$

which represents the total temperature fluctuation due to vorticity.

Next assume that the fluctuations are all entropy. Then equation (29) becomes:

$$\overline{\phi'^2}=(s+\alpha)^2\overline{\left(\frac{T_o'}{T_o}\right)_\sigma^2} \tag{42}$$

This equation is identical to the one for supersonic flow except that S_u is replaced by S_ρ and the mode diagram lies in the $\tilde{\phi}-s$ plane.

An example of the mode diagram for entropy when $\left(\tilde{T}_\infty/T_\infty\right)_\sigma = 0.01$ is presented in figure 9. Here again, only the $\tilde{\phi}-s$ plane is presented since $\tilde{u}/u = 0$. When $\tilde{\phi}=0$ then $s=-\alpha$, and when $s=0$ then:

$$\tilde{\phi} = \alpha\left(\frac{\tilde{T}_\infty}{T_\infty}\right)_\sigma \tag{43}$$

which represent the total temperature fluctuation due to entropy fluctuations.

Now assume that all the fluctuations are far-field sound (i.e., $\lambda/L \ll 1$). The equation for this case is:

$$\overline{\phi'^2} = \frac{1}{\gamma^2 M^2}\left(\frac{p'}{p}\right)^2_{sf}\left\{(\beta-q)\cos\theta+\left[\alpha(\gamma-1)-s\right]M\right\}^2 \tag{44}$$

Equation (44) represents a three-dimensional surface in the $\tilde{\phi}$, q, s coordinate system and the mode diagram, in general, lies on this surface. The intersections of the surface with the $\tilde{\phi}-q$ and $\tilde{\phi}-s$ planes are defined, herein, as the mode diagrams. When $s=0$ the above equation represents the mode diagram in the $\tilde{\phi}-q$ plane and when $q=0$ the mode diagram is in the $\tilde{\phi}-s$ plane. An example of the sound mode is presented in figure 10, where the $\tilde{\phi}-s$ plane has been rotated into the plane of the paper. The sound mode is the only mode that has non-zero values in the two planes, $\tilde{\phi}-q$ and $\tilde{\phi}-s$, since sound has both velocity and density fluctuations. All of the mode diagrams described above are degenerate hyperbolas in the $\tilde{\phi}-q$ and $\tilde{\phi}-s$ planes.

Concluding Remarks

From the present study of hot-wire anemometry for a constant-current anemometer applicable to subsonic compressible and subsonic slip flows, the following concluding remarks can be made:

- Based on Spangenberg's data, there appears to be a wide range of M and Kn available where a solution to the mean square equation for constant current hot-wire anemometry in subsonic flow might be possible based on the fact that $S_u \neq S_\rho$.
- It was shown that the mean square equation for CCA has possible solutions provided that the functional relationship which adequately relates s to q when substituted into the equation results in only six terms. Again Spangenberg's data were used to show that this condition can often be satisfied.
- The application of the method of least squares to the mean square equation resulted in a 6x6 matrix that was ill-conditioned for the data used. Methods to circumvent this problem, if it is general, must be found before reliable solution can be obtained.
- If a solution exists, the fluctuation diagram was shown to exists on a three dimensional surface - a hyperboloid.
- The intersection of the hyperboloid with two of the co-ordinate planes are hyperbolas, where in one plane, $\left(q-\tilde{\phi}\right)$, the asymptote gives the velocity fluctuation and in the other plane, $\left(s-\tilde{\phi}\right)$, the asymptote gives the density fluctuation. The intersection of the hyperboloid with the $\tilde{\phi}$ axis gives the total temperature fluctuation.
- The mode diagrams for vorticity, entropy, and sound are degenerate hyperbolas in two of the co-ordinate planes.

Acknowledgment

The second author acknowledge the support of this research by National Aeronautics and Space Administration under contracts NAG1-1552 and NAS1-18585.

References

1. Stainback, P.C., and Nagabushana, K.A., "***Invited Paper**: Review of Hot-wire Anemometry and the Range of their Applicability,*" FED-Vol. 167, pp. 93-134, Third International Symposium on Thermal Anemometry - ASME Fluids Engineering Division Summer Meeting, Washington, DC, USA, June 20-24, 1993.

2. Laufer, J., 1961, "*Aerodynamic Noise in Supersonic Wind Tunnels,*" Journal of the Aerospace Sciences, pp. 685-692.

3. Wagner, R.D., and Weinstein, L.M., 1974, "*Hot-Wire Anemometry in Hypersonic Helium Flow,*" NASA-TN-D-7465.

4. Morkovin, M.V., 1956, "*Fluctuations and Hot-Wire Anemometry in Compressible Flows,*" AGARDograph 24.

5. Kovasznay, L.S.G., 1950, "*The Hot-Wire Anemometer in Supersonic Flows,*" Journal of the Aeronautical Sciences, Vol. 17, No. 9, pp. 565-584.

6. Kovasznay, L.S.G., 1953, "*Turbulence in Supersonic Flow,*" Journal of the Aeronautical Sciences, Vol. 20, No. 10, pp. 657-674.

7. Jones, G.S., and Stainback, P.C., 1988, "*A New Look at Wind Tunnel Flow Quality for Transonic Flows,*" SAE 881452 Aerospace Technology Conference and Exposition, Anaheim, California.

8. Demetriades, A., 1978, "*Probes for Multivariant Flow Characteristics,*" Proceedings of the Dynamic Flow Conference on Dynamic Measurements in Unsteady Flows, IMST, Marseilles, France, pp. 13-44.

9. Spangenberg, W.G., 1955, "*Heat Loss Characteristics of Hot-Wire Anemometers at Various Densities in Transonic and Supersonic Flows,*" NACA-TN-3381.

10. Baldwin, L.V., 1958, "*Slip-Flow Heat Transfer From Cylinders in Subsonic Airstreams,*" NACA-TN-4369.

11. Nagabushana, K.A., and Stainback, P.C., 1994, "*A Rational Technique for Calibrating Hot-Wire Probes in Subsonic to Supersonic Speeds,*" AIAA-94-2536, AIAA 19th Aerospace Ground Test Conference, Colorado Springs, Colorado.

12. Stadler, J.R., Goodwin, G., and Creager, M.O., 1951, "*A Comparison of Theory and Experiment for High-Speed Free-Molecule Flow,*" NACA Rep. 1032 (Supersedes NACA-TN-2244).

13. Strang, G., 1976, "*Linear Algebra and its Application,*" Academic Press.

14. Ojalvo, I.U., 1991, "*Improved Solution for Ill-Conditioned Algebraic Equations by Epsilon Decomposition,*" AIAA Journal, Vol. 29, No. 12, pp. 2274-2277.

15. Haftka, R.T., 1990, "*Stiffness-Matrix Condition Number and Shape Sensitivity Errors,*" AIAA Journal, Vol. 28, No. 7, pp. 1322-1324.

16. Zinov'ev, V.N., and Lebiga, V.A., 1988, "*Measurements of Fluctuations For High Subsonic Velocities Using a Hot-Wire Anemometer,*" Plenum Publishing Corp. Novosibirsk, Translated from Zhurnal Prikladoni Mekhanikii Teckhnicheskoi Fiziki, No. 3, pp. 80-84.

Appendix

A Note on the Mean Square Equation for CCA

The necessary condition required to assure a solution to the hot-wire equation for the constant current anemometer can be developed as follows. The equation in terms of mean square values is:

$$\overline{\phi'^2} = q^2\overline{\left(\frac{u'}{u}\right)^2} + s^2\overline{\left(\frac{\rho'}{\rho}\right)^2} + \overline{\left(\frac{T_o'}{T_o}\right)^2} + 2qs\frac{\overline{u'\rho'}}{u\rho} - 2q\frac{\overline{u'T_o'}}{uT_o} - 2s\frac{\overline{\rho'T_o'}}{\rho T_o} \qquad (A-1)$$

where

$$q = \frac{S_u}{S_{\tau_w}} \text{ and } s = \frac{S_\rho}{S_{\tau_w}} \qquad (A\text{-}2)$$

In equation (A-1) the quantities $\overline{\phi'^2}$, q, and s are functions of τ_w. Therefore s can be considered to be function of q. Assume that solutions are sought using the method of least squares and $s = f(q)$; substitute this functional relationship into equation (A-1):

$$\overline{\phi'^2} = q^2\overline{\left(\frac{u'}{u}\right)^2} + [f(q)]^2\overline{\left(\frac{\rho'}{\rho}\right)^2} + \overline{\left(\frac{T_o'}{T_o}\right)^2} + 2qf(q)\frac{\overline{u'\rho'}}{u\rho} - 2q\frac{\overline{u'T_o'}}{uT_o} - 2f(q)\frac{\overline{\rho'T_o'}}{\rho T_o} \qquad (A-3)$$

Any functional relationship which adequately relates q and s and results in equation (A-3) having six terms will satisfy equation (A-1) and result in a solution. This can be illustrated by assuming the following equation for s:

$$s = a + bq^f + cq^g + dq^h \qquad (A\text{-}4)$$

Substituting equation (A-4) into (A-1) and collecting terms gives:

$$\overline{\phi^2} = \left(\frac{\overline{u'}}{u}\right)^2 q^2 + \left[2a\frac{\overline{u'\rho'}}{u\rho} - 2\frac{\overline{u'T_o'}}{uT_o}\right]q + \left[2ab\left(\frac{\overline{\rho'}}{\rho}\right)^2 - 2b\frac{\overline{\rho'T_o'}}{\rho T_o}\right]q^f + \left[2ac\left(\frac{\overline{\rho'}}{\rho}\right)^2 - 2c\frac{\overline{\rho'T_o'}}{\rho T_o}\right]q^g +$$

$$\left[2ad\left(\frac{\overline{\rho'}}{\rho}\right)^2 - 2d\frac{\overline{\rho'T_o'}}{\rho T_o}\right]q^h + \left[b^2\left(\frac{\overline{\rho'}}{\rho}\right)^2\right]q^{2f} + \left[c^2\left(\frac{\overline{\rho'}}{\rho}\right)^2\right]q^{2g} + \left[d^2\left(\frac{\overline{\rho'}}{\rho}\right)^2\right]q^{2h} + \qquad (A-5)$$

$$\left[2bc\left(\frac{\overline{\rho'}}{\rho}\right)^2\right]q^{f+g} + \left[2bd\left(\frac{\overline{\rho'}}{\rho}\right)^2\right]q^{f+h} + \left[2cd\left(\frac{\overline{\rho'}}{\rho}\right)^2\right]q^{h+g} +$$

$$\left[2b\frac{\overline{u'\rho'}}{u\rho}\right]q^{f+1} + \left[2c\frac{\overline{u'\rho'}}{u\rho}\right]q^{g+1} + \left[2d\frac{\overline{u'\rho'}}{u\rho}\right]q^{h+1} + \left[a^2\left(\frac{\overline{\rho'}}{\rho}\right)^2 + \left(\frac{\overline{T_o'}}{T_o}\right)^2 - 2a\frac{\overline{\rho'T_o'}}{\rho T_o}\right]$$

A solution to this equation is possible for any values of f, g, and h provided that the resultant equation, after the substitution of values for f, g, and h into the equation, has 6 terms. Some examples of values for f, g, and h which results in an equation which has six terms are presented in Table I. However, when equation (32) is considered, the non-integer values for f cannot be used to determine s in the vicinity of $\tau_w = 0$. This is due to the limiting value of q being negative. This results in the values of f being restricted to the values presented in the first two rows of Table I. The major problem in obtaining a solution to equation (A-1) is evaluating the powers of q in equation (A-4) which will give the best fit to the mean flow calibration data relating s to q. This can be done by using standard statistical techniques.

Table I

Possible Solutions to Mean Square Equation for CCA:

$$\overline{\phi^2} = q^2\left(\frac{\overline{u'}}{u}\right)^2 + [f(q)]^2\left(\frac{\overline{\rho'}}{\rho}\right)^2 + \left(\frac{\overline{T_o'}}{T_o}\right)^2 + 2qf(q)\frac{\overline{u'\rho'}}{u\rho} - 2q\frac{\overline{u'T_o'}}{uT_o} - 2f(q)\frac{\overline{\rho'T_o'}}{\rho T_o}$$

$$s = f(q) = a + bq^f + cq^g + dq^h$$

f	g	h	Terms in q	
f	1	0	$q^{2f};q^{f+1};q^f;q^2;q^1;q^0$	f = 3,4,5,... f = −2,−3,−4,...
f	0	0	$q^{2f};q^{f+1};q^f;q^2;q^1;q^0$	f = 3,4,5,... f = −2,−3,−4,...
f	1	0	$q^{2f};q^{f+1};q^f;q^2;q^1;q^0$	f = non-integer values $1 < f$
f	0	0	$q^{2f};q^{f+1};q^f;q^2;q^1;q^0$	f = non-integer values $1 < f$
f	1	0	$q^{2f};q^{f+1};q^f;q^2;q^1;q^0$	$0 < f < 1$ $f \neq 0.5$
f	0	0	$q^{2f};q^{f+1};q^f;q^2;q^1;q^0$	$0 < f < 1$ $f \neq 0.5$

TABLE II

Possible Solutions To Mean Square Equation For CCA Based On Spangenberg's Data:

M	ρ	f	g	h	R^2	Condition Number
0.05	0.0012	3.0	1	0	0.9936	1.97×10^7
0.10	0.0012	3.3	1	0	0.9966	2.92×10^8
0.20	0.0012	3.0	1	0	0.9933	1.92×10^8
0.40	0.0012	3.0	1	0	0.9997	1.09×10^7
0.60	0.0012	3.0	1	0	0.9718	6.54×10^8

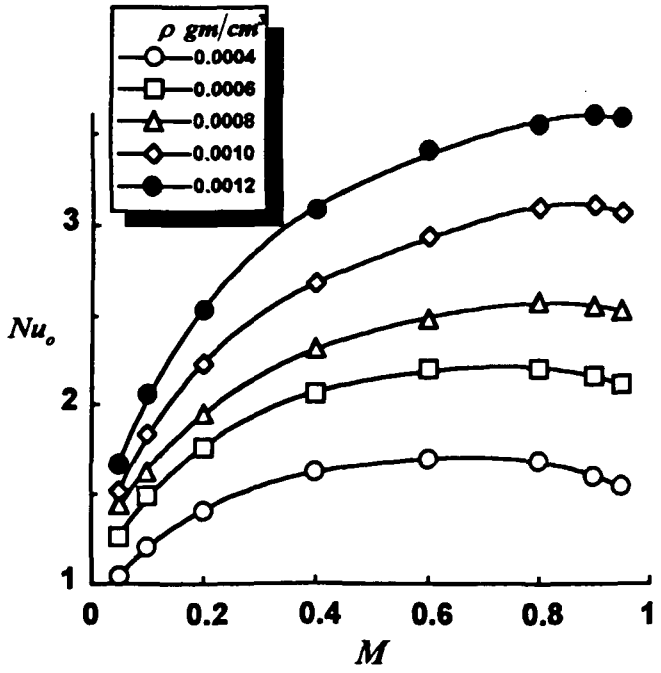

(a) Nu_o vs. M for $\tau_w = 1.696$

Figure 1. Examples of Spangenberg's Data (Ref. 9).

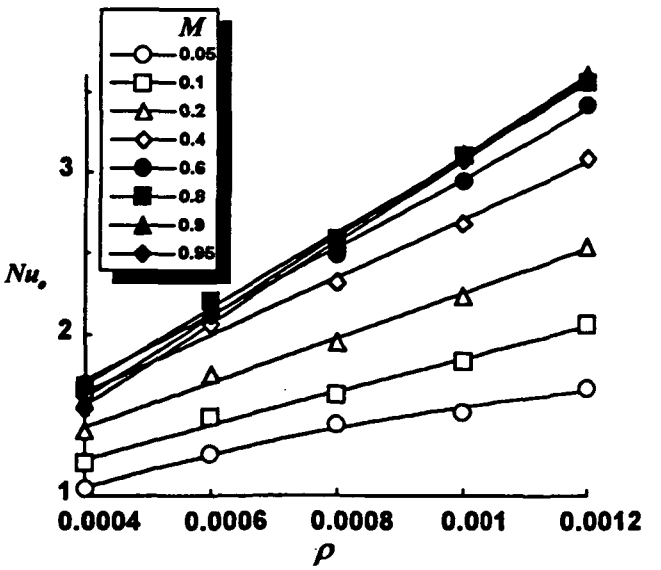

(b) Nu_o vs. ρ for $\tau_w = 1.696$

Figure 1. Continued.

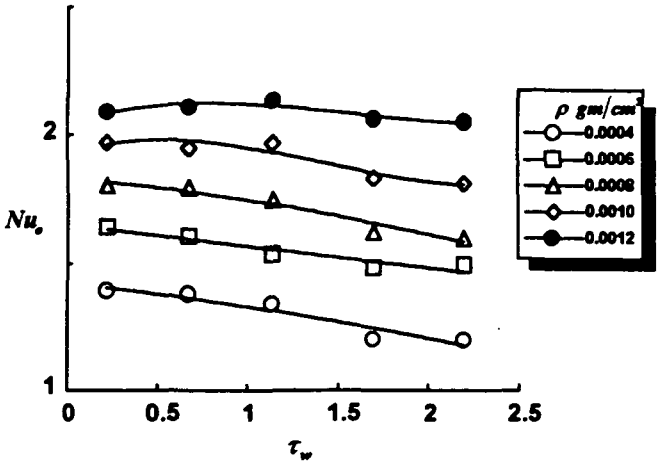

(c) Nu_o vs. τ_w for $M = 0.1$

Figure 1. Concluded.

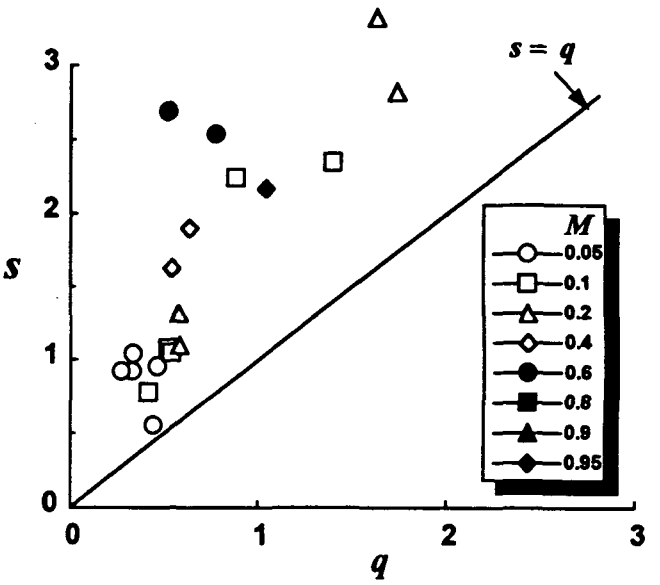

Figure 2. Density sensitivity ratio, s vs. velocity sensitivity ratio, q for $\tau_w = 2.192$; (Spangenberg's Data; Ref. 9).

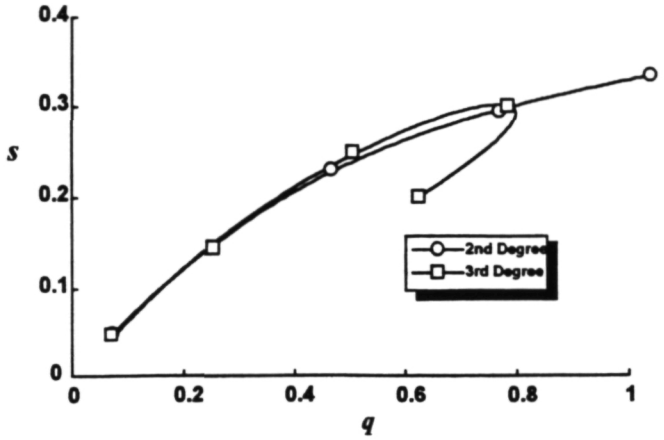

Figure 3. Example of s vs. q for $M = 0.05$ and $\rho = 0.0004\ gm/cm^3$ for variable τ_w; (Spangenberg's Data; Ref. 9).

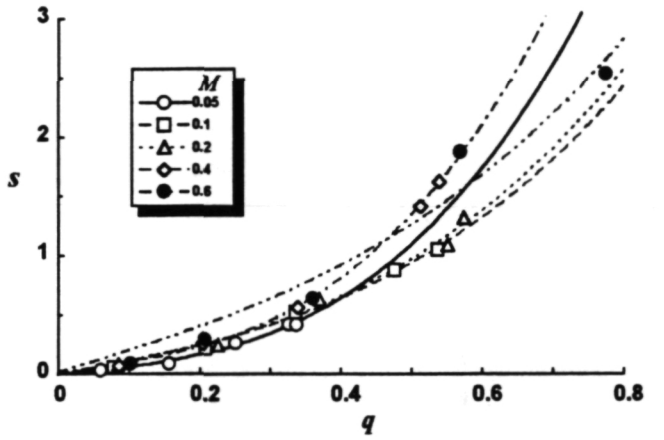

Figure 4. s vs. q for various Mach numbers and $\rho = 0.0012\ gm/cm^3$ for variable τ_w; (Spangenberg's Data; Ref. 9).

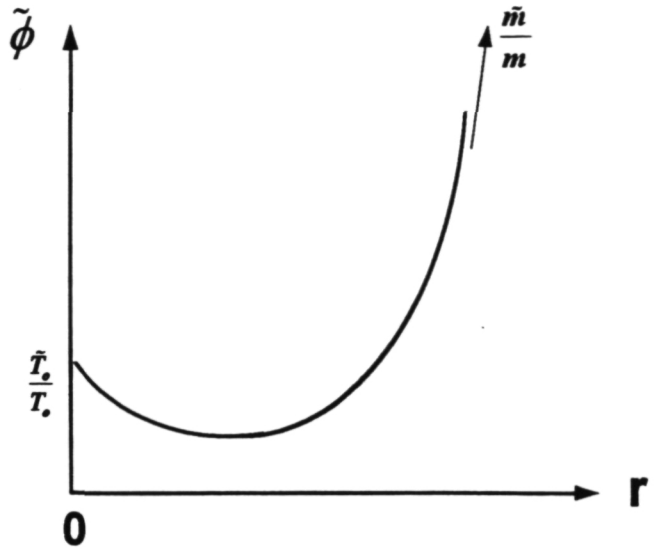

Figure 5. Fluctuation diagram for supersonic flow; $S_u = S_\rho$.

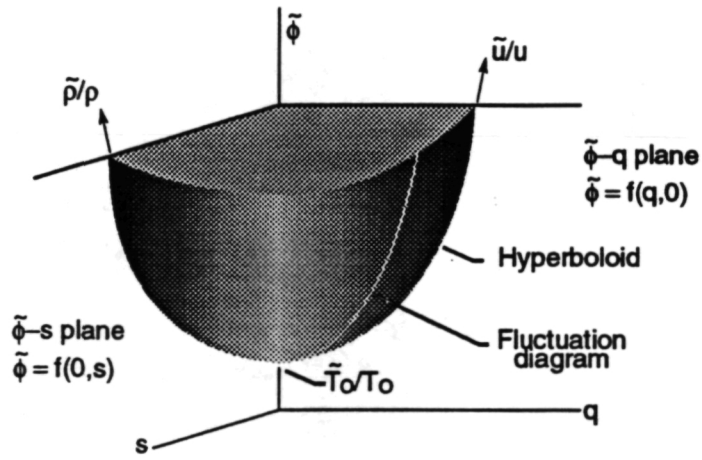

Figure 6. General fluctuation diagram for subsonic compressible flow; $S_u \neq S_\rho$.

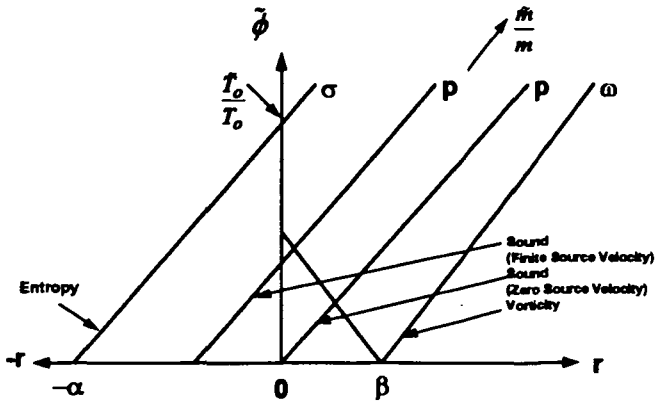

Figure 7. Vorticity-Entropy-Far-field sound modes for supersonic flow; $S_u = S_\rho$.

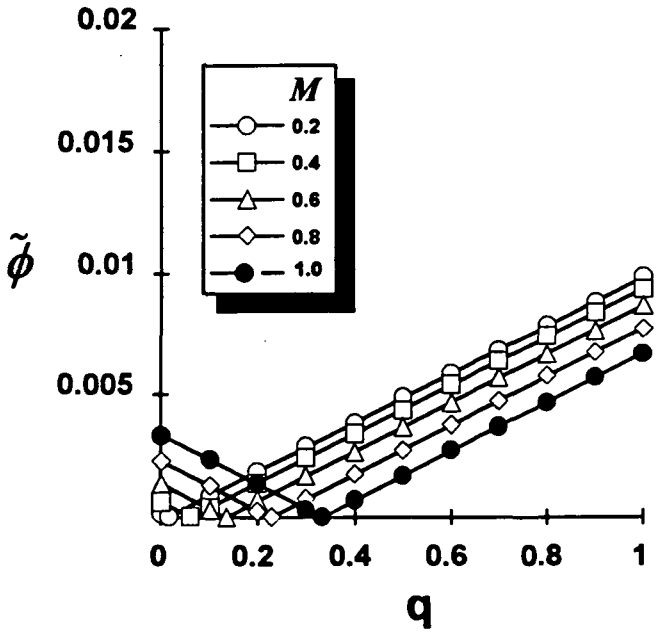

Figure 8. Vorticity mode for various Mach numbers; $S_u \neq S_\rho; \left(\frac{\tilde{u}}{u}\right)_\sigma = 0.01$

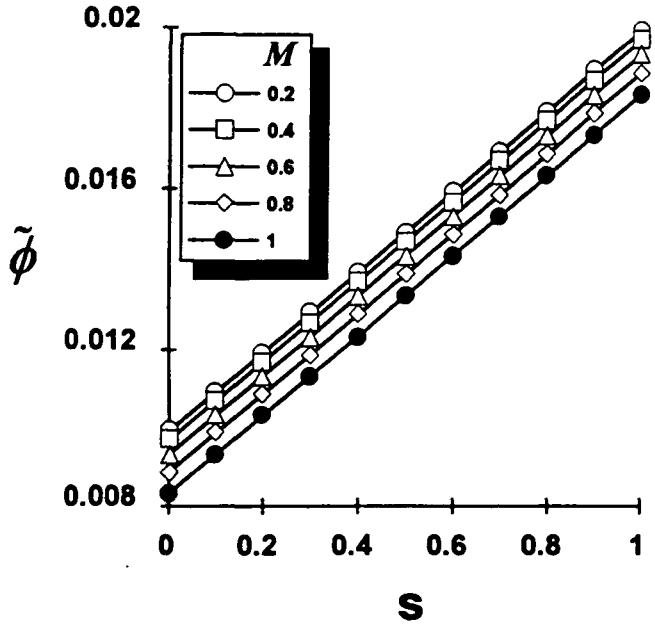

Figure 9. Entropy mode for various Mach numbers; $S_u \neq S_\rho; \left(\frac{\tilde{T}_\infty}{T_\infty}\right)_\sigma = 0.01$

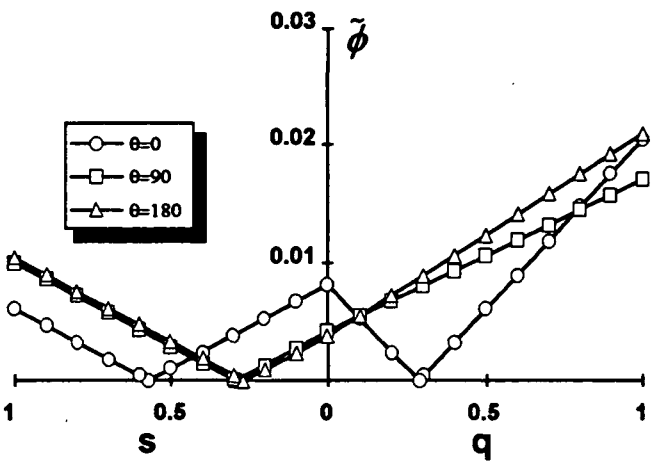

Figure 10. Far-field sound mode; $S_u \neq S_\rho; M = 0.5; \left(\frac{\tilde{P}}{P}\right)_{ff} = 0.01$

NLS

ADDENDUM AND ERRATA

AIAA 94-2535
HOT-WIRE ANEMOMETRY IN SUBSONIC SLIP AND TRANSONIC FLOW REGIMES

P.C. Stainback
and
K.A. Nagabushana

ADDENDUM

The present analysis of constant current anemometry in subsonic slip and transonic flows using the least square technique appeared to show that, based on Spangenberg's data, measured fluctuations would probably have substantial errors based on the large condition numbers calculated for the 6x6 sensitivity matrix. This was true even though the necessary conditions required for a solution to the mean square equation appeared to be satisfied. Because of this, additional studies of the problem were undertaken in attempts to determine the possible reason for the large condition numbers and to search for possible methods for reducing their magnitudes.

From an analytical point of view, consider equation (29). One serious problem which could affect the ability to obtain accurate solutions to this equation can be noted by considering the variation of the sensitivity ratios, q and s, with respect to changes in the overheat of the heated wire and their limiting values which are give in equations (32) and (33).

In subsonic slip and transonic flows, the values of s are, in general, larger than those for q. Both of these quantities approach small limiting values as the overheat of the wire approaches zero. However, except for very low densities, the limiting values for s are smaller in magnitude than those for q as the overheat approaches zero. Because of this, there is a range of overheats in the vicinity of zero where q and s are approximately equal and the locus of points for q and s in the $q-s$ plane crosses the $q=s$ line. Because of this, the mean square equation reduces from the case of a single equation with six unknowns to a single equation with three unknowns. In other words as the overheat is reduced, the mean square equation becomes degenerate from a three dimensional problem to a two dimensional one and this could result in an inability of the equation to give accurate results. Therefore, the present method would probably result in answers having large errors and accurate results cannot be expected unless some other suitable technique can be found to solve the mean square equation. Note that this problem in the limit is due to the heat transfer equation used and not due to any errors in the mean flow data. Is the heat transfer equation used adequate? If it is not, can another technique be found to circumvent the problem of obtaining accurate answers to the mean square equation?

After the wire is calibrated and the sensitivities obtained and the RMS and mean voltage measured across the wire, the search for a possible solution to the mean square equation becomes one of geometry. The trace of the values for q and s in the $q-s$ plane and the corresponding values of ϕ must be used to define the hyperboloid from which the fluctuations and their correlations can be accurately determined since the fluctuation diagram lies in its surface. In general, q and s exist in only one quadrant of the $q-s$ plane as the overheat of the wire is changed, and the hyperboloid must be determined from this limited amount of data. Table II shows that attempts to do this resulted in matrices with large condition numbers indicating that any answers obtained would be subject to large errors. These errors might be reduced if additional information could be obtained.

Is there a reasonable method that can be developed to supply additional information to help define more accurately the proper hyperboloid thereby producing more accurate solutions to the

AIAA 94-2535, 18th AIAA 19th Ground Test Conference
Colorado Springs, Colorado, July 20-23, 1994

mean square equation? If the functional relationship between q and s are valid in one quadrant, values for q and s can be obtained in a second quadrant by extending values from the equation into the second quadrant. This technique reduces the condition numbers of the matrix by about two orders of magnitude. There are, however, no corresponding values for ϕ in this second quadrant. A method to circumvent this problem is to assume ϕ is a function of q in the first quadrant then extend this relationship into the second quadrant. Using this technique the condition numbers of the sensitivity matrix were reduced to the values presented in Table II. These condition numbers indicate that significant improvements in possible solutions can be obtained, however, the condition numbers are still rather large. Because of the symmetry of the hyperboloid, the above technique might be acceptable. However, it should be noted that the coordinates of the hyperboloid is not symmetric with respect to the q , s , ϕ coordinate axes.

Based on the present paper and the Addendum, it appears that the possibility exist for obtaining solutions to the mean square equation for CCA in the subsonic slip and transonic flows. The accuracy of the results are , however, subject to question. In any case, the possibility of a solution suggest that data, including fluctuation measurements, should be obtained in an attempt to further investigate the problem.

ERRATA

In general, the values for q and s are negative and equation (16) is written so that the terms in equation (29) are all positive. For the present report the negative values for q and s were transformed to positive values. However, most of the equations were presented in the non-transformed coordinate system. This fact was not noted in the report and could lead to some confusion. Equations (31) - (33) are written in the non-transformed system.

Page 11 of the Appendix

However, when equation (32) is considered, the non-integer values for f cannot be used to determine s in the vicinity of τ_w equal zero. This is due to the limiting value of q being negative.

The above should read: However, non-integer values cannot be used since the fluctuation diagram exist on the surface of a hyperboloid and this surface must be defined in all quadrants.

The value 3.3 in Table II should be 3.0.

The notations for the coordinate axes in figure 3 should be interchanged.

New Table II

M	ρ gm/cm^3	f	g	h	R^2	$q_{min} \le q \le q_{max}$ Condition Number	$-q_{max} \le q \le q_{max}$ Condition Number
0.05	0.0012	3.0	1	0	0.9936	1.97×10^7	1.34×10^5
0.10	0.0012	3.0	1	0	0.9966	2.92×10^8	3.23×10^6
0.20	0.0012	3.0	1	0	0.9933	1.92×10^8	2.12×10^6
0.40	0.0012	3.0	1	0	0.9997	1.09×10^7	1.73×10^5
0.60	0.0012	3.0	1	0	0.9718	6.54×10^8	9.51×10^7

Submitted to Journal of Fluids Engineering, Transactions of The ASME
Also Invited Pape FED-Vol. 167, Thermal Anemometry, ASME 1993

N15

Review of Hot-Wire Anemometry Techniques and the Range of their Applicability for Various Flows

P.C. Stainback†
Distingushied Research Associate
NASA Langley Research Center
Hampton, VA 23681

and

K.A. Nagabushana
Research Engineer
VIGYAN Inc.
Hampton, VA 23666

ABSTRACT

A review of hot-wire anemometry was made to present examples of past work done in the field and to describe some of the recent and important developments in this extensive and ever expanding field. The review considered the flow regimes and flow fields in which measurements were made, including both mean flow and fluctuating measurements. Examples of hot-wire measurements made in the various flow regimes and flow fields are presented. Comments are made concerning the constant current and constant temperature anemometers generally in use and the recently developed constant voltage anemometer. Examples of hot-wire data obtained to substantiate theoretical results are presented. Some results are presented to compare hot-wire data with results obtained using other techniques. The review was limited to wires mounted normal to the flow in non-mixing gases.

NOMENCLATURE

$a_1 - a_4$	constants in equation (47)
a	speed of sound
A,B	constants in equation (24)
$A_1 - A_3$	constants in equation (18)
$b_1 - b_3$	order of q in equation (47)
$B_1 - B_5$	constants in equation (19)
$A'(T_o)$	Lk_f
A'_w	overheat parameter, $\frac{1}{2}(\partial \log R_w / \partial \log I)_h$
$B'(T_o)$	$2L\sqrt{\pi k_f c_p r_w}$
c_p	specific heat at constant pressure
c_v	specific heat at constant volume
c_w	specific heat of wire
d	wire diameter of mesh
$d(\ )/dt$	rate of change of quantity ( ) with respect to time
d_c	diameter of cylinder
d_j	diameter of jet
d_w	diameter of wire
e'	instantaneous voltage across the wire
E	mean voltage across the wire
E_{out}	anemometer output voltage
E'	finite-circuit parameter, $(1-\varepsilon)/(1+2A'_w\varepsilon)$
f	frequency
F	dimensionless frequency
F_{11}	true one-dimensional spectral density
F_M	measured one-dimensional spectral density
F_{trf}	turbulence reduction factor

† Formerly Senior Research Engineer, Analytical Services & Materials, Inc., Hampton, VA 23666

Gr	Grashof Number
h	coefficient of heat transfer
h_w	height above wire shock generator to probe
$h_{w,s}$	height above shock generator, immediate postshock value
I	current
k	thermal conductivity of air evaluated at subscript temperature
k_1	wave number in the flow direction
Kn	Knudsen number
L	characteristic length
m	mean mass flow
m_t	$\partial \log \mu_t / \partial \log T_o$
M	Mach number
M_m	mesh size
n	exponent for mass flow in equations (16) & (17)
n_t	$\partial \log k_t / \partial \log T_o$
Nu	Nusselt number evaluated at subscript temperature
p	mean static pressure
p_o	mean total pressure
P	electrical power to the hot-wire
Pr	Prandtl number
q	sensitivity ratio, S_u/S_{T_o}
q_∞	dynamic pressure
Q	forced convective heat transfer
r	sensitivity ratio, S_m/S_{T_o}
r_d	radial distance in cylinderical polar co-ordinate
r_p	distance of virtual source of jet from origin
r_w	radius of wire
r'	$r_p - r_d$
R	resistance
Re	Reynolds number based on viscosity evaluated at subscript temperature and wire diameter
R_{mT_o}	mass flow - total temperature correlation coefficient, $\overline{m' T_o'}/\tilde{m}\tilde{T}_o$
R_{uT_o}	velocity - total temperature correlation coefficient, $\overline{u' T_o'}/\tilde{u}\tilde{T}_o$
$R_{\rho T_o}$	density - total temperature correlation coefficient, $\overline{\rho' T_o'}/\tilde{\rho}\tilde{T}_o$
$R_{u\rho}$	velocity - density correlation coefficient, $\overline{u'\rho'}/\tilde{u}\tilde{\rho}$
R_{xx}	normalized auto-correlation function
s	sensitivity ratio, S_ρ/S_{T_o}
S	sensitivity of hot-wire to the subscript variable
t	time
T	temperature
T_f	$(T_w + T_o)/2$
u,v,w	velocity in x , y and z directions respectively
u_τ	frictional velocity
x	distance in the flow direction
x_o	virtual origin of the wake
x_w	distance along the length of wire
y	distance normal to the flow direction
α	$\left(1+\frac{\gamma-1}{2}M^2\right)^{-1}$
α_1	linear temperature - resistance coefficient of wire
β	$\alpha(\gamma-1)M^2$
β_1	second degree temperature - resistance coefficient of wire
δ	boundary layer thickness
δ^*	displacement thickness for Blasius flow
ε	finite circuit factor, $-(\partial \log I_w / \partial \log R_w)_t$
η_y	transformed co-ordinate distance normal to body
η	recovery temperature ratio, T_{adw}/T_o
θ	temperature parameter, T_w/T_o
θ_1	angle between plane sound wave and axis of probe
λ	mean free path
μ	absolute viscosity
γ	specific heat ratio, c_p/c_v
ρ	density
τ	time lag
τ_w	temperature loading parameter, $(T_w - T_{adw})/T_o$
τ_{ww}	temperature parameter, $(T_w - T_{adw})/T_{adw}$
τ_{wall}	shear stress at the wall
ϕ'	normalized fluctuation voltage ratio, $\left(e'/E\right)/S_{T_o}$

Subscript

adw	adiabatic wall condition
adw,c	adiabatic wall temperature, continuum flow condition
adw,f	adiabatic wall temperature, free molecular flow condition
B	due to buoyancy effect
C	constant current anemometer
e	edge condition

eff	effective velocity
f	film condition
h	M and Re_f are constant as Q varied
o	total condition
ref	reference condition
s	electrical system untouched as M and Re_f varied
s	sound source
sc	settling chamber
t	evaluated at total temperature
T	constant temperate anemometer
w	wire condition
∞	free stream or static condition

Superscript

'	instantaneous
~	RMS
—	mean

INTRODUCTION

Comte-Bellot[1] noted that the precise origin of hot-wire anemometry cannot be accurately determined. One of the earlier studies of heat transfer from a heated wire was made by Boussinesq[2] in 1905. The results obtained by Boussinesq was extended by King[3] and he attempted to experimentally verify his theoretical results. These earlier investigations of hot-wire anemometry considered only the mean heat transfer characteristics from heated wires. The first quantitative measurements of fluctuations in subsonic incompressible flows were made in 1929 by Dryden and Kuethe[4] using constant current anemometry where the frequency response of the wire was extended by the use of a compensating amplifier. In 1934 Ziegler[5] developed a constant temperature anemometer for measuring fluctuations by using a feedback amplifier to maintain a constant wire temperature up to a given frequency.

In the 1950's, Kovasznay[6,7] extended hot-wire anemometry to compressible flows where it was found experimentally that in supersonic flow the heated wire was sensitive only to mass flow and total temperature. Kovasznay developed a graphical technique to obtain these fluctuations, which is mostly used in supersonic flow. In subsonic compressible flows the heat transfer from a wire is a function of velocity, density, total temperature, and wire temperature. Because of this complexity, these flow regimes were largely bypassed until the 1970's and 1980's when attempts were made to develop methods applicable[8] for these flows. In recent years there were several new and promising developments in hot-wire anemometry that can be attributed to advances in electronics, data acquisition/reduction methods and new developments in basic anemometry techniques.

Previous reviews, survey reports, and conference proceedings on hot-wire anemometry are included in references 1,9-20. Several books[21-24] have been published on hot-wire anemometry and chapters[25-30] have been included in books where the general subject matter was related to anemometry.

This review considers the development of hot-wire anemometry from the earliest consideration of heat transfer from heated wires to the present. Although mean flow measurements are considered, the major portion of the review addresses the measurement of fluctuation quantities. Examples of some of the more important studies are addressed for wires mounted normal to the flow in non-mixing gases. The present review attempts to bring the development of hot-wire anemometry up to date and note some of the important, recent developments in this extensive and ever expanding field.

FLOW REGIMES AND FLOW FIELDS

Based on the applicable heat transfer laws and suitable approximations, hot-wire anemometry can be conveniently divided into the following flow regimes:

1. Subsonic incompressible flow
2. Subsonic compressible, transonic, and low supersonic flows
3. High supersonic and hypersonic flows

Within each of these major flow regimes are the following sub-regimes:

1. Continuum flow
2. Slip flow

3. Free molecular flow

In subsonic incompressible flow the heat transfer from a wire is a function of mass flow, total temperature and wire temperature. Since density variations are assumed to be zero, the mass flow variations reduce to velocity changes only. The non-dimensional heat transfer parameter, the Nusselt number, is usually assumed to be a function of Reynolds and Prandtl numbers and under most flow conditions the Prandtl number is constant. Evidence exist which indicate that Nu_f is also a function of a temperature parameter[6]. In subsonic compressible, transonic and low supersonic flows the effects of compressibility influence the heat transfer from a wire. For these conditions the heat transfer from the wire is a $f(u,\rho,T_o,T_w)$ and $Nu_f = f(Re_f,M,\theta)$. In high supersonic and hypersonic flows a strong shock occurs ahead of the wire and the heat transfer from the wire is influenced by subsonic flow downstream of the shock. Because of this, it was found experimentally that $Nu_f = f(Re_f,\theta)$ only, and the heat transfer from the wire is again a function of mass flow, total temperature, and wire temperature.

In continuum flow the mean free path of the particles is very much less than the diameter of the wire and conventional heat transfer theories are applicable. Where the diameter of the wire approaches a few mean free paths between the particles, the flow does not behave as a continuum, but exhibits some effects of the finite spacing between the particles. These effects have been studied[31,32] by assuming a finite velocity and a temperature jump at the surface of a body. This gas rarefaction regime was noted as slip flow. In free molecular flow the fluid is assumed to be composed of individual particles and the distance between the particles is sufficiently large that their impact with and reflection from a body is assumed to occur without interaction between the particles. Free molecular flow is theoretically studied[33] using the concepts of kinetic theory[34].

Figure 1 presents a plot of Mach number vs. Reynolds number for lines of constant Knudsen number where d_w = 0.00015 inch and for flow conditions where $1.5 \le p_o$, psia ≤ 150. Baldwin's results[35] indicated that the continuum flow regime existed for $Kn < 0.001$ and slip flow conditions existed for $0.001 \le Kn \le 2.0$. Other references suggest that slip flow conditions were attained only for $Kn > 0.01$. Even using the larger value of Kn for the slip flow boundary, (i.e., $Kn > 0.01$) operating a 0.00015 inch wire at low Mach numbers and at atmospheric conditions is near the slip flow boundary. If the total pressure is decreased or the wire diameter reduced, the value of Kn would be shifted farther into the slip flow regime. Free molecular flow conditions are generally assumed to exist for $Kn > 2.0$. Figure 1 can be used to delineate approximate values for M and Re_f for the various sub-regimes.

Various applications of hot-wire anemometry and the approximate level of velocity functuations are:

Types of Flows	Approximate[29] $\tilde{u}/u$
1. Freestream of wind tunnels[36,37]	0.05%
2. Down stream of screens and grids[25,38]	0.20 - 2.00 %
3. Boundary layers[39-42]	3.0 - 20.0 %
4. Wakes[43,44]	2.0 - 5.0 %
5. Jets[45-47]	Over 20.0 %
6. Flow downstream of shocks[48]	
7. Flight in Atmosphere[49]	
8. Rotating Machinery[50,51]	
9. Miscellaneous[52-56]	

TYPES OF ANEMOMETERS

The two types of anemometers primarily used are the constant current anemometer (CCA) and the constant temperature anemometer (CTA). A constant voltage anemometer (CVA) is presently under development[57]. Even though these three anemometers are described as maintaining a given variable "*constant*", none of these strictly accomplish this. The degree of non-constancy for the CCA is determined by the finite impedance of its circuit[58]. The constancy of the mean wire temperature for a CTA at high frequencies is limited by the rate at which the feedback amplifier can detect and respond to rapid fluctuations in the flow. The CVA maintains the voltage across the wire and leads constant rather than across the wire[57]. The non-constancy effects in the CCA and the CVA can be

accounted for by calibration of the CCA[58] and by knowing the lead resistance in the CVA.

The heat balance for an electrically heated wire, neglecting conduction and radiation is:

Heat Stored = Electrical Power In - Aerodynamic Heat Transfer Out

$$\frac{dc_w}{dt} T_w = P - Q \qquad (1)$$

$$\frac{dc_w}{dt} T_w = I^2 R_w - \pi L d_w h (T_w - T_{aw}) \qquad (2)$$

If the heat storage term is properly compensated, then equation (2) becomes:

$$I^2 R_w = \pi L d_w h (T_w - T_{aw}) \qquad (3)$$

The measurement of fluctuations in a flow requires a sensor, in this case a wire, with a time response up to a sufficiently high frequency. The time constant of even small wires are limited and the amplitude response of these wires at higher frequencies decreases with frequency. Therefore, some type of compensation must be made for the wire output. There are two methods for accomplishing this. Earlier approaches utilized a constant current anemometer with a compensating amplifier that had an increase in gain as the frequency increased[4]. An example of the roll off in the frequency of the wire, the gain of the amplifier and the resulting signal is shown schematically in figure 2. In principle, the output from the wire can be compensated to infinite frequencies. However, as the frequency increases, the noise output from the compensating amplifier will equal and ultimately exceed the wire output, which limits the gain that can be obtained. A schematic diagram of a CCA is presented in figure 3.

The constant temperature anemometer uses a feedback amplifier to maintain the average wire temperature and wire resistance constant {i.e., $dT_w/dt = 0$ in equation (2)}, within the capability of the amplifier. The practical upper frequency limit for a CTA is the frequency at which the feedback amplifier becomes unstable. A schematic diagram of a CTA is presented in figure 4. A third anemometer, presently under development[57], is the constant voltage anemometer. This anemometer is based on the alterations of an operational amplifier circuit and does not have a bridge circuit. A schematic diagram of a CVA is presented in figure 5.

The upper frequency response of a CCA is generally accepted to be higher than that of a CTA. There is some evidence that the frequency response of the CVA might equal or exceed that of the CCA. The fluctuation diagram technique described by Kovasznay is usually used with a CCA to obtain data at supersonic speeds. This technique depends on the sensitivity of the wire being a function of wire temperature or overheat and the frequency response of the wire being assessable to compensation to almost zero overheat. This technique has limited application for a CTA, since at low overheats, the frequency response of the anemometer approaches the frequency response of the wire[25].

An example of the difference between the fluctuation diagrams obtained[59] using a CTA and a CCA is presented in figure 6. The intersection of the diagram with the vertical axis at $S_{\rho u}/S_{T_t} = 0$ represents the total temperature fluctuation and the data show that the CTA cannot be used to measure these fluctuations. The reason for this is illustrated in figure 7a where the total temperature spectra at low overheats for the two anemometers are presented. In these cases the spectrum obtained with the CTA was attenuated at a frequency that was about two orders of magnitude less than for the CCA. At high overheats the two mass flow spectra were more nearly equivalent (figure 7b). However, in reference 60 the output of a laser was modulated and used to heat a wire to check the frequency response of a CTA. It was shown that the frequency response was essentially unchanged down to an overheat of 0.07.

The CTA can be used to make measurements in supersonic flows by using two wires. For these flows the CTA is operated with two wires having different but high overheats, digitizing the voltages and using two equations to obtain m', T_o' and $m'T_o'$ as a function of time[61]. Then statistical techniques are used to obtain quantities of interest. In general, the CTA is more suitable for measuring higher levels of fluctuations than a CCA[25]. It remains to be determined how the CVA will compare with the CCA and CTA. At present it appears that the CVA has a higher signal to noise

ratio than either CCA or CTA. Additional advantages and disadvantages of the CCA versus the CTA are described in references 1, 29, 57, 62 and 63.

At low speeds a linearizer is often used to convert the non-linear relationship between wire voltage and velocity to a linear relationship. There are two types of linearizers in use; the logarithmic and the polynomial. A linearizer makes it possible to directly relate the measured voltage to the velocity. However, the linearization process does not result in better measured quantities[25].

LIMITATIONS OF HOT-WIRE ANEMOMETRY

Most of the data obtained using hot-wire anemometry is limited to small perturbations. There are cases, however, where this linearization of the anemometry equation is not accurate and non-linear effects can influence both the mean[47] and fluctuating[25] voltages. Since high level fluctuations can influence the mean voltage measured across the heated wire, it is important to calibrate probes in flows with low levels of fluctuations.

Because of the mass associated with the wire supports, there can be a significant amount of heat loss from the wire due to conduction to the relatively cold supports. This heat loss results in a spanwise temperature distribution along the wire that, in turn, causes a variation of heat transfer from the wire[12,21,64] along its length. In order to compare the heat transfer results from one wire or probe with another, the heat transfer rates must be corrected for these losses. However, computation of fluctuation quantities requires that the uncorrected values of the heat transfer rates be used. An example of the temperature distribution along a wire and its mean temperature[21] is shown in figure 8. The finite length of the wire and its attendant temperature and heat transfer distribution influences the level of the spectra (especially at higher frequencies), correlations, and phase relationships between sensors[25,65].

The spacial resolution of a wire is limited by the length of the wire and the size of the smallest scale of fluctuations in the flow. If the length of the wire is larger than the smallest scale, the resultant magnitude of the spectra will be attenuated at the higher frequencies. The length of the wire with respect to the size of turbulence can have an effect on the measurements of fluctuation intensity, space and time correlations, and the turbulence scales and micro scales[66-68]. Additional spacial resolution problems encountered near walls was discussed in references 69 and 70. Proximity to walls of wind tunnels or to surfaces of models can introduce errors in measurements due to increased heat transfer from the wire due to conduction to the relatively cold walls[21,25]. An example of the effect of wire length on normalized spectra is presented in figure 9. The spacial resolution of multi-wire probes is further limited by the distance between the wires. The hot-wire probe intrusion into the flow can cause severe disturbance in certain flows. Examples are flows with large gradient such as boundary layers and vortices. Because of the above, hot-wire anemometry has limited resolution in space, time, and amplitude[29].

A severe problem is encountered in hypersonic flows when the gas is air. At higher Mach numbers the total temperature must be high enough to prevent liquefaction of air in the test section. There is a maximum recommended operating temperature for each wire material. These two facts places severe limitations on the maximum overheat at which wires can be operated. For example, the maximum recommended operating temperature for Platinum-10% Rhodium wire is 1842°R. For a M = 8 wind tunnel, the total temperature required can be as high as 1360°R. Using a recovery temperature ratio of 0.96, the maximum values for τ_w is 0.394 and θ_{max} = 1.354. If gas rarefaction effects are experienced and η is greater than one, then the problem is even more severe. For η = 1.1 the maximum value for τ_w under the above conditions is 0.254. The above values for τ_w are based on the average temperature for the wire. For small L/d_w wires the limitation on τ_w would be smaller due to higher temperatures at the mid-portion of the wire. The total temperature at low pressures where η could be larger need not be as high as those at higher pressures, however, the constraint of constant total temperature during the calibration process limits the amount that T_o can be reduced. (Also see ref. 71-76).

PROBE PRE-CALIBRATION PROCEDURE

Once a probe is constructed, the following procedure should ensure accurate and reliable measurements. First, the probe should be operated at the maximum q_∞ and T_w that will be used during the proposed test. This is done to pre-stress and pre-heat the wire to ensure that no additional strain will be imposed on the wire during the test that could alter its resistance. For supersonic and high q_∞ subsonic flows, the wires should also be checked for strain gaging, that is, stresses generated in the wire due to its vibration. Note, for testing in flows having high values of q_∞, the wires should have slack to reduce the stress in the wires and to help eliminate strain gaging. If strain gaging is significant the wire should be replaced. During this pre-testing many wires might fail due to faulty wires or manufacturing techniques, but it is better that the wires fail in pre-testing rather than during an actual test.

A temperature-resistance relationship for wires is usually requires to compute the heat transfer rate from the heated wires. It is generally recommended that the following equation, which is a second degree equation in ΔT, be used:

$$\frac{R}{R_{ref}} = 1 + \alpha_1 (T_w - T_{ref}) + \beta_1 (T_w - T_{ref})^2 \qquad (4)$$

After the wires have been pre-stressed and pre-heated, they should be placed in an "*oven*" and the wires calibrated to determine the values for α_1 and β_1. Once this calibration has been completed, the probes can be placed in a facility for mean flow calibration over the appropriate ranges of velocity, density, total temperature and wire temperature.

STATISTICAL QUANTITIES

Data obtained using hot-wire anemometry are typically reduced to statistical quantities. Over the past few years the analysis of random data has been developed to a very high degree[77-79]. This plus the rapid developments in electronics (i.e., the A/D converters and high speed computers), have made it possible to obtain almost any statistical quantity of interest within the error constraints of the heated wire. Much of this is due to the fact that the digital processing of data can be used to obtain many quantities that are difficult or impossible to obtain using analog data reduction techniques.

Many types of single point and multi-point statistical quantities can be obtained using hot-wire anemometry[80-83]. It is routine to measure mean flow and RMS values, histograms and the higher order moments of skewness and kurtosis, auto correlation, and one dimensional spectra. Measurements of multi-point statistical quantities include cross correlations, two-point histograms and higher order two-point moments, cross spectra, and coherence functions. Attempts were made to measure higher moments up to eighth order[81].

These measurements can be used in various ways to evaluate many characteristics of the flow such as scales, decay rate, energy content etc[25]. The coherence function is a useful statistical quantity that can be used to evaluate various properties of a flow[84]. It can often be used to determine the predominant sound propagating angle and to determine the dominant mode present in a fluctuating flow field[85,86].

A few examples of statistical quantities that were measured using hot-wire anemometry are presented in figures 10-13. Integral and micro time and length scales of a flow can be determined from autocorrelation functions such as the one presented in figure 10. The higher moments of skewness and kurtosis (figure 11a-b) can be used to determine if the fluctuations are Gaussian. For a Gaussian distribution the value of the skewness parameter is zero and for the kurtosis the value is 3. Figure 11 shows that both of these moments indicate that the mass flow and total temperature fluctuations are Gaussian over most of the thickness of the boundary layer. The value of third order auto-correlation function, such as the one shown in figure 12, can be used to support turbulent flow theories. An example of space-time correlations measured in a turbulent boundary[59,87] is presented in figure 13. The peak of these correlations at $t \neq 0$ indicate the presence of convection. The calculation of the convection velocity, obtained by dividing the separation distance by the time at which the individual curves peaks, indicates that there was no significant variation of the convective velocity over the spacings

used. An example of normalized spectra measured downstream of a grid[88] is presented in figure 14 and show the increased attenuation of high frequency disturbances with increased distance downstream from the grid. (Also see ref. 89-92).

GENERAL HEAT TRANSFER RELATIONSHIPS

The heat transfer from a wire under the limits of the present report (i.e., the wires mounted normal to flow in non-mixing gases) is [29]:

$$Q = f(u,\mu,\rho,c_p,T_w,T_{adw}) \tag{5}$$

if the fluid properties of μ, c_p, and k are based on T_o, then the above equation becomes:

$$Q = f(u,\rho,T_w,T_o) \tag{6}$$

Since $T_{adw} = \eta T_o$ and $\eta = f(Kn,M) = f(u,\rho,T_o)$. For incompressible continuum flows equation (6) reduces to:

$$Q = f(m,T_o,T_w) \tag{7}$$

Unless noted, the total temperature will be used throughout this report to evaluate μ_t, c_p, and k_t where as ρ will be based on T_∞.

For a wire with a given L/d_w the Nusselt number can be expressed[25] in terms of other dimensionless parameters as:

$$Nu_t = f\left(Re_t, Pr, Gr, \frac{T_w - T_{adw}}{T_o}, \frac{u^2}{c_p(T_w - T_{adw})}\right) \tag{8}$$

and can be written as follows to show the effects of compressibility:

$$Nu_t = f\left(Re_t, Pr, Gr, M_\infty, \frac{T_w - T_{adw}}{T_o}\right) \tag{9}$$

For relatively constant temperatures, Pr = constant and if $Gr < Re^3$, buoyancy effects will be small and Gr can be neglected. These approximations lead to:

$$Nu_t = f(Re_t, M_\infty, \tau_w) \tag{10}$$

MEAN FLOW MEASUREMENTS

SUBSONIC INCOMPRESSIBLE - CONTINUUM FLOW

Theoretical Considerations

The functional relationship between the power to the wire or the heat transfer from the wire and the mean flow variables are required to determine the so called "*static*" calibration of the wire from which the sensitivities to the various flow variables can be obtained in order to calculate the fluctuations. Because of this the mean flow results and probe mean flow calibration procedure are considered together.

The first attempt to obtain a theoretical solution for the heat transfer from a heated wire mounted normal to the flow was carried out by Boussinesq[2]. The equation that he obtained is:

$$Q = L\left(2\sqrt{\pi k_t c_p \rho u r_w}\right)(T_w - T_{adw}) \tag{11}$$

Equation (11) can be expressed in terms of non-dimensional quantities as follows:

$$Nu_t = \sqrt{\frac{2}{\pi}}\sqrt{PrRe_t} \tag{12}$$

King re-analyzed the problem of heat transfer from a heated wire and obtained the following relationship:

$$Q = L\left(k_t + 2\sqrt{\pi k_t c_p \rho u r_w}\right)(T_w - T_{adw}) \tag{13}$$

or in terms of non-dimensional quantities:

$$Nu_t = \frac{1}{\pi} + \sqrt{\frac{2}{\pi}}\sqrt{PrRe_t} \tag{14}$$

From equation (11) and (13) it can be seen that the only difference between Boussinesq's and King's results is the inclusion of the additional term k_t in King's result that attempts to account for the effects of natural convection. At "*high*" values of Reynolds number the two results are essentially equal.

Using equation (3), equation (13) can be expressed as:

$$P = \left[A'(T_o) + B'(T_o)\sqrt{m}\right]\left[T_w - T_{adw}\right] \qquad (15)$$

where $A'(T_o)$ and $B'(T_o)$ are based on King's results. However, the quantities A' and B' are usually determined for a given wire by direct mean flow calibration. Often the exponent for the mass flow term is determined from a curve fit to the data. The values for the exponent can range[25] from 0.45 to 0.50.

For a CTA, equation (15) can be generalized to:

$$\frac{E^2}{(R_w - R_{adw})} = A_T(T_o) + B_T(T_o)(m)^n \qquad (16)$$

where $A_T(T_o) = \dfrac{R_w A'(T_o)}{\alpha_1 R_{wf}}$ and $B_T(T_o) = \dfrac{R_w B'(T_o)}{\alpha_1 R_{wf}}$.

For a CCA:

$$\frac{I^2 R_w}{(R_w - R_{adw})} = A_C(T_o) + B_C(T_o)(m)^n \qquad (17)$$

where $A_C(T_o) = A'(T_o)/\alpha_1 R_{wf}$ and $B_C(T_o) = B'(T_o)/\alpha_1 R_{wf}$. Therefore, if wires operated with a CTA or a CCA are calibrated over a range of m and T_o, equations (16) and (17) indicate that the calibration curves will be straight lines if the left hand side of the equation is plotted as a function of $(m)^n$. In general, the slopes, B, and intercepts, A, will be functions of the total temperature. If the total temperature is constant, A and B will be constants and if the density is constant, the mass flow term will reduce to velocity. An example of voltage versus velocity for a wire operated with a CTA is presented in figure 15 for various values of total temperature. (Also see ref. 93-97).

Hot-wires have also been calibrated in the form of $u = f(E)$ rather than the more conventional form of $E = f(u)$. The constant T_o and ρ version of King's law for a CTA is $E^2 = A + B\sqrt{u}$ and when expressed as $u = f(E)$ gives:

$$u = A_1 - A_2 E^2 + A_3 E^4 \qquad (18)$$

In this equation George et. al.,[98] noted that $A_1 - A_3$ are functions of T_o. They proposed the following equation for the calibration of wires that is independent of T_o for a limited range:

$$Re_t = B_1 + B_2 Nu^{\frac{1}{2}} + B_3 Nu + B_4 Nu^{\frac{1}{3}} + B_5 Nu^2 \qquad (19)$$

where μ is evaluated at T_o and k evaluated at T_f.

Examples of Data

A summary of heat transfer data from cylinders in terms of Nu_t vs. Re_t taken in the subsonic continuum flow regime was presented in reference 21. The results from these experiments are compared with the theoretical results of Boussinesq and King in figure 16. This figure shows that there is a relatively good agreement between the measured results and King's theory over a wide range of Reynolds numbers. There is a substantial difference between Boussinesq's theory and King's theory and the measured results for Reynolds numbers less than about 100.

A large amount of heat transfer data was also presented by McAdam[99] in terms Nu_f vs. Re_f and he recommended the following equation:

$$Nu_f = 0.32 + 0.43(Re_f)^{0.52} \qquad (20)$$

In comparision, King's equation with $Pr = 0.70$ is:

$$Nu_t = 0.3183 + 0.6676(Re_t)^{0.50} \qquad (21)$$

For Reynolds number equal to zero the two equations give essentially the same value for the Nusselt number. At higher values of Reynolds number King's equation is about 40 percent higher than the values of Nusselt number presented by McAdam. A film temperature is often used as the temperature at which k, ρ and μ are evaluated when correlating Nu versus Re. However, ρ is sometimes evaluated at the free stream static temperatures. The use of the film temperature for evaluating fluid properties has been questioned in reference 100. However, in this reference the density in the Reynolds number was evaluated at T_f, where as, in reference 99 this apparently was not the case.

Bradshaw[27] notes that there is a difference of opinion throughout the hot-wire anemometry community about the usefulness of a universal correlation based on variables evaluated at a film temperature. These correlations provide a useful guide for plotting results and comparing mean flow results obtained by different investigators. However, if good accuracy is to be obtained for the fluctuations, individual calibration of probes is required.

Often attempts are made to measure mean velocities using hot-wire anemometry. It can be shown using equation (13) that the voltage across a wire is a $f(u,\rho,T_o,T_w)$. Therefore, to measure the mean velocity, the other variables must be held constant or a method must be used to correct the data for any variation in variables other than velocity[65,71,101]. Because of this, the hot-wire anemometer is not a very good mean flow measuring device, even if one utilizes some of the corrections that have been developed. However, for limited variations in the independent variables, corrected velocity measurements were reported in reference 101.

Very Low Velocities

At very low velocities the heated wire can cause a relatively significant vertical movement of a fluid due to buoyancy effects on the lower density fluid adjacent to the wire. This results in a change in the effective velocity around the wire. Efforts were made to calibrate and use hot-wire anemometry at very low velocities[102-107] where natural convection effects were present. The influences of natural convection are parameterized by the Grashof number. Experimental evidence[108] indicated that if $Gr < Re^3$ then free convection effects were negligible. An example of the effect of low velocities on the Nusselt number is presented in figure 17.

King also provided an equation suitable for low speed flows:

$$P = \frac{2\pi L k_f (T_w - T_{adw})}{\log(b/r_w)} \tag{22}$$

where $b = k_f e^{1-\gamma}/c_p \rho u$ and γ = Euler's Constant = 0.57721. In terms of non-dimensional quantities, equation (22) becomes:

$$Nu_f = \frac{2}{\log\left[2e^{1-\gamma}/(Pr\,Re_f)\right]} \tag{23}$$

Equation (22) is valid for $ud_w < 0.0187$ where u is in cm/sec and d_w is in cm. Equation (13) is valid for $ud_w > 0.0187$.

For velocities as low as 1.0 cm/sec, Haw and Foss[102] attempted to correlate their data using King's equation in the form:

$$E^2 = A + Bu^n \tag{24}$$

A deviation of their data from a fitted curve was observed at $u \approx 30$ cm/sec. The diameter of the wire used in their experiment[102] was not noted. However, if one assumes a value of 0.00015 inch or 0.00020 inch, the limits for the application of equations (13) and (22) indicate velocities of 49 cm/sec or 37 cm/sec, which are not too different from 30 cm/sec. The use of equation (22) would not improve the correlation presented in reference 102 since it can be shown that as $u \to 0$ in equation (22) $E_w \to 0$. The data of reference 102 indicates that at $u = 0$ the intercept of the curve is greater than the value indicated by the intercept in equation (24). Correlations obtained using the results of a theory based on Oseen[108] flow would not improve the correlation since this approach gives results that are similar to those obtained using equation (22). For a heated wire tested in horizontal wind tunnels, u_{eff} cannot reach zero since the effective velocity is:

$$u_{eff}^2 = u^2 + u_B^2 \tag{25}$$

and for a heated wire $u_B \neq 0$.

SUBSONIC SLIP FLOW AND TRANSONIC FLOW

Theoretical Considerations

These two flow regimes will be treated together since the experimental results are similar. Kovasznay[6] extended hot-wire anemometry results to compressible flows and showed that there was a significant difference between the heat transfer in compressible and incompressible flows. Several experimenters obtained heat transfer measurements at low speeds and found an

apparent compressibility or Mach number effect[35,64,109] at Mach numbers as low as 0.1. Spangenberg[110] conducted extensive tests over a wide range of variables and determined that the apparent compressible flow effects at Mach number as low as 0.05 was really due to gas rarefaction (e.g., slip flow).

In this flow regime the heat transfer from the heated wire is generally given as:

$$Q = P = \pi L k_f (T_w - \eta T_o) Nu_f \qquad (26)$$

In transonic flow and subsonic slip flows the Nusselt number is no longer only a function of Reynolds number and Kings' law is no longer applicable. The most common functional relationship for the Nusselt number in these flow regimes is[58]:

$$Nu_f = f(M, Re_f, \theta) \qquad (27)$$

since it was found that Nu_f is also a function of a temperature parameter. Another functional relationship that was used to analyze gas rarefaction effects is[35]:

$$Nu_f = f(M, Kn, \tau_w) \qquad (28)$$

In subsonic compressible flows the recovery temperature of the wire can change and functional relationships for η are:

$$\eta = f(M, Re_f) \quad \text{or} \quad \eta = f(M, Kn) \qquad (29)$$

	Dependent Variable	Independent Variable	Reference
①	Nu_f	Re_f, M_∞, θ	Morkovin[58]
②	Nu_f	Kn, M_∞, τ_w	Baldwin[35]
③	Nu_f	Re_f, M_∞, τ_w	
④	Nu_f	Kn, M_∞, θ	
⑤	η	Re_f, M_∞	Morkovin[58]
⑥	η	Kn, M_∞	Vrebalovich[111]

Table I. Functional Relationships for Nu_f and η.

Morkovin chose $Nu_f = f(M_\infty, Re_f, \theta)$ and $\eta = f(M_\infty, Re_f)$ for the development of his equations. In order to emphasize the gas rarefaction effects, Baldwin chose $Nu_f = f(M_\infty, Kn, \tau_w)$ and $\eta = f(M_\infty, Kn)$. Independent variables that might be used to relate Nu_f and η to the dependent variables are presented in Table 1. Although Morkovin and Baldwin chose the variables of ① and ②, one could just as well have chosen the variables noted in ③ or ④. It will be shown later that the variables in ④ might be the most efficient group to use.

Examples of Data

Baldwin[35] and Spangenberg[110] investigated the heat transfer from wires over a wide range of Re_f, M, and T_w in the slip flow and transonic flow regimes. Their results, presented in figures 18a-b, shows that $Nu_f = f(Re_f, M)$ for Mach numbers ranging from 0.05 to 0.90 and Reynolds numbers ranging from 1 to about 100. The effects of wire overheat on the values of Nu_f were also determined by Baldwin and Spangenberg and examples of these effects are shown in figure 19. The values of Nu_f can increase or decrease with increased overheat depending on the Mach number and Knudsen number.

Results from theoretical calculations made for the effects of slip flow on heat transfer from wires were reported in reference 31. An example of these results is presented in figure 20. The levels of the calculated Nusselt number do not agree with measured results, however, the trends of the theoretical results agree with the experimental trends shown in figure 18.

SUPERSONIC CONTINUUM FLOW

General results for compressible flow shows that $Nu_f = f(M, Re_f, \theta)$. However, it was experimentally[21,112] determined that $Nu_f \neq f(M)$ for Mach numbers greater than about 1.4. Typical heat transfer data for supersonic flow is presented in figure 21 to illustrate the approximate invariance of Nu_f with M. At higher Mach number and relatively low total pressures, there is a high probability that much of the data presented for supersonic and hypersonic flows are in the slip flow regime.

FREE MOLECULAR FLOW

Standler, Goodwin and Creager[33] computed the heat transfer from wires for free molecular flow and an example of their results along with measurements are presented in figure 22. A combination of continuum flow, slip flow and free molecular flow results[10] are shown in figure 23. From this figure it can be seen that for continuum flow at large Reynolds number $Nu_f \approx Re_f^{1/2}$. For free molecular flow $Nu_f \approx Re_f$ and slip flow results smoothly connect the two regimes. Therefore, for slip flows, Nu_f varies with exponent of Reynolds number which range from ½ to 1.

RECOVERY TEMPERATURE RATIO

The recovery temperature ratio must be known to compute the heat transfer from heated wires. In general, the recovery temperature ratio is a function of Mach and Reynolds numbers or Mach and Knudsen numbers. However, for Mach number greater than about 1.4 the recovery temperature ratio is not a function of Mach number for continuum flow. A "*universal*" curve presented by Vrebalovich[111] (figure 24) correlated the temperature recovery ratio with Knudsen number for all Mach numbers. Using the results presented in figure 24, the temperature recovery ratio for continuum flow and free molecular flow, curves of η vs. M and Kn can be calculated. An example of these calculations is presented in figure 25.

FLUCTUATION MEASUREMENTS

SUBSONIC INCOMPRESSIBLE FLOW

Theoretical Considerations

a. Constant Temperature Anemometer

For a constant temperature anemometer, King's[3] equation can be expressed as:

$$\frac{E^2}{R_w} = L\left[k_f + \sqrt{2\pi k_f c_p \rho u d_w}\right]\left[T_w - \eta T_o\right] \qquad (30)$$

where R_w and T_w are constants.

If one assumes that the changes in k_f, c_p and η can be neglected, the change in E will be a function of ρu and T_o as given by the following equation for small perturbations:

$$\frac{e'}{E} = S_m \frac{m'}{m} + S_{T_o} \frac{T_o'}{T_o} \qquad (31)$$

where

$$S_m = \frac{1}{4}\frac{\sqrt{2\pi}\sqrt{Re_f Pr}}{\left[1+\sqrt{2\pi}\sqrt{Re_f Pr}\right]} \text{ and } S_{T_o} = -\frac{1}{2}\frac{\eta}{\tau_w} \qquad (32)$$

From the above equation it can be seen that $S_m \to 0$ as $Re_f \to 0$ and $S_m \to ¼$ as $Re_f \to \infty$. For the temperature sensitivity, $S_{T_o} \to -\infty$ as $\tau_w \to 0$ and $S_{T_o} \to 0$ as $\tau_w \to \infty$. Equation (31) shows that $E = f(m, T_o)$ where $S_m = \partial \log E / \partial \log m$ and $S_{T_o} = \partial \log E / \partial \log T_o$.

Since equation (31) shows that $E = f(m, T_o)$, the fluctuation of mass flow and total temperature can be measured using a CTA[113-115]. This can best be done by using two wires operated at different, but high overheats, digitizing the data, and solving two equations for m', T_o' and $m'T_o'$ as functions of time.

If the total temperature and the Mach number varies significantly, then k_f and c_p must be differentiated with respect to T_o and η differentiated with respect to Mach number. Under these conditions it would be more appropriate to use the equation obtained by Rose and McDaid[8] with the assumption that $Nu_f \neq f(M)$.

Instead of using King's equation, consider equation (15) for measuring mass flow and total temperature fluctuation. For a CTA equation (15) becomes:

$$d\log E = \frac{B'(T_o)(m)^n}{2n\left[A'(T_o)+B'(T_o)(m)^n\right]} d\log m + \frac{1}{2}\left\{\frac{A'(T_o)\frac{\partial \log A'(T_o)}{\partial \log T_o}}{\left[A'(T_o)+B'(T_o)(m)^n\right]} + \frac{(m)^n B'(T_o)\frac{\partial \log B'(T_o)}{\partial \log T_o}}{\left[A'(T_o)+B'(T_o)(m)^n\right]} - \frac{\eta}{\tau_w}\right\} d\log T_o \qquad (33)$$

b. Constant Current Anemometer

For the CCA anemometer, Kings' equation becomes:

$$EI = L\left[k_t + \sqrt{2\pi k_t c_p \rho u d_w}\right]\left[T_w - \eta T_o\right] \tag{34}$$

Again assume that k_t, c_p and η are constant, the change in E is given by the following equation:

$$\frac{e'}{E} = S_m \frac{m'}{m} + S_{T_o} \frac{T_o'}{T_o} \tag{35}$$

where

$$S_m = \frac{k_t \tau_w (1-\varepsilon)}{2\left[(1-2\varepsilon)k_t \tau_w - \theta\right]} \frac{\sqrt{2\pi}\sqrt{Re_t Pr}}{\left[1+\sqrt{2\pi}\sqrt{Re_t Pr}\right]} \quad \text{and} \quad S_{T_o} = \frac{-k_t \eta (1-\varepsilon)}{\left[(1-2\varepsilon)k_t \tau_w - \theta\right]} \tag{36}$$

If $d\log I = 0$ then

$$S_m = \frac{k_t \tau_w}{2\left[k_t \tau_w - \theta\right]} \frac{\sqrt{2\pi}\sqrt{Re_t Pr}}{\left[1+\sqrt{2\pi}\sqrt{Re_t Pr}\right]} \text{ and } S_{T_o} = \frac{-k_t \eta}{\left[k_t \tau_w - \theta\right]} \tag{37}$$

Equation (36) and (37) shows that $S_m = f(\tau_w)$. If $Re_t \to 0$ then $S_m \to 0$, but if $Re_t \to \infty$ then $S_m \approx \frac{k_t \tau_w}{2\left[k_t \tau_w - \theta\right]}$. On the other hand, if $\tau_w \to 0$ then $S_m \to 0$ and if $\tau_w \to \infty$ then $S_m \to \frac{1}{2}\frac{\sqrt{2\pi}\sqrt{Re_t Pr}}{\left[1+\sqrt{2\pi}\sqrt{Re_t Pr}\right]}$.

If $\tau_w \to 0$ then $S_{T_o} \to \frac{k_t \eta}{\theta}$ and if $\tau_w \to \infty$ then $S_{T_o} \to 0$.

Again, it is possible to measure both $\tilde{m}$, $\tilde{T}_o$ and R_{mT_o} using a CCA[113] and the fluctuation diagram developed by Kovasznay[6]. An example of fluctuation diagrams for two discrete frequencies measured with a CCA is presented in figure 26. Again if the total temperature and the Mach number varies significantly, then it would be more appropriate to use Morkovin's equation with the assumption that $Nu_t \neq f(M)$.

Similarly, to measure mass flow and total temperature fluctuation,equation (15) for CCA becomes:

$$d\log E = \left\{\frac{k_t \tau_w (1-\varepsilon)}{\left[(1-\varepsilon)k_t \tau_w - \theta\right]} \frac{B'(T_o)(m)^n}{\left[A'(T_o)+B'(T_o)(m)^n\right]}\right\} d\log m +$$

$$\frac{k_t \tau_w (1-\varepsilon)}{\left[(1-\varepsilon)k_t \tau_w - \theta\right]}\left\{\frac{A'(T_o)\frac{\partial \log A'(T_o)}{\partial \log T_o}}{\left[A'(T_o)+B'(T_o)(m)^n\right]} + \frac{(m)^n B'(T_o)\frac{\partial \log B'(T_o)}{\partial \log T_o}}{\left[A'(T_o)+B'(T_o)(m)^n\right]} - \frac{\eta}{\tau_w}\right\} d\log T_o \tag{38}$$

Mass flow fluctuations measured in subsonic flows can be very misleading where there is a significant amount of far-field sound. The mean square value of mass flow fluctuation is:

$$\overline{\left(\frac{m'}{m}\right)^2} = \overline{\left(\frac{u'}{u}\right)^2} + 2R_{u\rho}\left(\frac{\tilde{u}}{u}\right)\left(\frac{\tilde{\rho}}{\rho}\right) + \overline{\left(\frac{\rho'}{\rho}\right)^2} \tag{39}$$

The magnitude of the mass flow fluctuation depends on $\tilde{u}$, $\tilde{\rho}$, and $R_{u\rho}$ where $-1 \le R_{u\rho} \le 1$. As an example, assume $R_{u\rho} = 1$, indicating downstream moving sound, and $\tilde{u}/u = \tilde{\rho}/\rho$. Under these assumption the mass flow fluctuation equals twice the velocity or density fluctuation. However, if $R_{u\rho} = -1$, indicating upstream moving sound, and $\tilde{u}/u = \tilde{\rho}/\rho$; the mass flow fluctuation are zero.

Examples of Data

Most of the measurements made using hot-wire anemometry were and still are being made in the subsonic, incompressible, continuum flow regime. An extensive amount of data was accumulated over the years in various flow fields[25].

a. Freestream

Some of the first fluctuation measurements made using hot-wire anemometers were obtained in the freestream of wind tunnels to help evaluate the effects of turbulence on the transition of laminar boundary layers[116]. The purpose of this effort was an attempt to extend wind tunnel transition data to flight conditions in order that the on-set of transition might be predicted on full scale aircraft. Measurements in the freestream are also required to study the effect of freestream disturbances on laminar boundary layer receptivity. An example of measurements made in the freestream is presented in figure 27 for the Low Turbulence Pressure Tunnel located at the NASA Langley Research Center[37]. The filled symbols represent data taken in the facility during 1940[117] and the curves represent measurements made in 1980. The agreement between the two sets of data is very good when it is noted that the data taken in 1940 was obtained at

$p_o = 4$ atmospheres and the low datum point at $Re_t = 5 \times 10^5$ is for $M \approx 0.02$.

Fluctuation measurements were also made in various location within wind tunnel circuits, predominantly in the settling chamber. Anemometry was used to evaluate the efficiency of contractions in reducing vorticity levels in the test section of wind tunnels[118]. An example of the results obtained through a contraction is presented in figure 28. The absolute value of the velocity fluctuation in the direction of the flow was reduced through the contraction but the relative values were greatly reduced depending on the area ratio of the contraction. For example in figure 28 the velocity fluctuation downstream of the contraction are ratioed to the mean flow in the large section of the contraction where the local velocity is low. If these downstream velocity fluctuations were ratioed to the local mean velocity, these normalized fluctuations would be substantially smaller, i.e., $\tilde{u}/u_\infty = 2.6$ vs. $\tilde{u}/u = 0.16$.

b. Grids

It was found that screens or grids can effectively reduce vorticity fluctuations. Because of this attenuation, screens have been extensively investigated[25,38,119] using hot-wire anemometry to optimize their characteristics for use in wind tunnels to reduce the vorticity levels in the test section. An example of these measurements is presented in figure 29 where the turbulent reduction factor is given as a function of the $\Delta p/q_\infty$ across the screens[120]. Therefore, the use of screens in the settling chamber along with a contraction of adequate area ratio, can substantially reduce velocity fluctuations in the test section due to voriticity[121]. (Also see ref. 122-130).

c. Boundary Layers

Hot-wire measurements were made in turbulent boundary layers[42] to measure the Reynolds stresses and other fluctuation quantities to furnish data for the development of turbulent boundary layer theories. An example of measurements made in the boundary layer on a flat plate[131] is presented in figure 30a-b. Figure 30a shows the significant variation of the velocity fluctuation across the boundary layer while figure 30b shows an example of the local streamwise velocity fluctuation ratioed to the local velocity. Forming the ratio in this latter manner indicates that the velocity fluctuations can exceed 40 percent, a value that is too large for an accurate assumption of small perturbation.

Extensive measurements were made of turbulent flows in pipes[40,41] to compare theoretical and measured results. From these measurements many statistical quantities were obtained including Reynolds stresses; triple and quadruple correlations; energy spectra; rates of turbulent energy production, dissipation, and diffusion; and turbulent energy balance. An example of the streamwise velocity fluctuations across a pipe is presented in figure 31a-b.

Hot-wire anemometry has been extensively used to investigate the characteristic of various boundary layer flow manipulators such as Large Eddy Break-up devices (LEBUS)[132], Riblets[133] and roughness elements[134]. Laminar boundary layer transition due to T-S waves[135], cross flow[136] and Gortler vortices[137] was extensively studied using the hot-wire techniques. Also the effects of heat addition[138], sound[139] and vorticity[140] on boundary layer characteristics have been investigated.

The hot-wire anemometer with a single wire cannot determine the direction of flow. However, a technique using a multi-wire, "*ladder probe*" was developed[141] to study the separated boundary layer where a significant amount of reverse flow occurred. This technique was used to determine the location of the zero average velocity in a subsonic turbulent boundary layer. (Also see ref. 142-144).

d. Laminar Boundary Layer Receptivity

One of the major impediments to a through understanding of laminar boundary layer transition is the ability to predict the process by which freestream disturbances are assimilated into the boundary layer. These free stream disturbances can be either vorticity, entropy, sound or a combination of these fluctuations.

The effect of freestream fluctuations on the stability of the laminar boundary can be investigated by making measurements in the freestream and in the boundary layer to evaluate the receptivity of the boundary layer to fluctuations[145] in the freestream. An example of

fluctuations measured in a subsonic boundary layer on a flat plate for various frequency bands is presented in figure 32. Kendall[145] presented three types of measurements made in a laminar boundary layer due to velocity fluctuations from the free stream. The first type is illustrated by the x's and consisted of broadband velocity fluctuation where the peak level occurs towards the inner part of the boundary layer. This type of measurement is noted as the Klebanoff's mode and is represented by the solid line. The results obtained when the data were filtered at the Tollmein-Schlichting (T-S) frequency are represented by circles. Although the frequencies were identical to those of T-S waves they were not T-S waves since the convection velocity was equal to the free stream value. The maximum level of these fluctuations occurred at the outer part of the boundary layer. The third type of fluctuation is represented by the dotted line. These were true T-S waves which occurred in packets and had a convective velocity of 0.35 to 0.4 of the free stream velocity. These peak fluctuation levels occurred near the wall. (Also see ref. 146-156).

e. Jets

Hot-wire measurements were obtained in jets[45-47] to measure the Reynolds stresses associated with free shear layers and to help evaluate the RMS levels and frequencies associated with jet noise. An example of the velocity and temperature fluctuations measured[157] across a heated jet is presented in figure 33. The two types of fluctuations were normalized by the maximum and the local mean values, respectively. (Also see ref. 158-160).

f. Wakes

Various statistical quantities were measured downstream of a heated cylinder by Townsend[43] to obtain experimental results to help improve turbulent theories applicable to this type of flow. Some of the quantities obtained included turbulent intensities, sheer stress, velocity-temperature correlation, triple velocity correlation, diffusion rate and energy dissipation. Measurements were made from 500 to 950 diameter downstream of the cylinder where dynamical similarity was assumed to exist. An example of the mean curve fitted to the u-component of the velocity fluctuation is presented in figure 34 and shows good similarity. Uberoi and Freymuth[44] made extensive spectral measurements downstream of a cylinder and their data indicated that only the spectra of large-scale turbulence were dynamically similar.

SUBSONIC SLIP FLOW AND TRANSONIC FLOW

Theoretical Considerations

In compressible flows the heat transfer from a wire is usually described by the following equation:

$$Q = \pi L k_f (T_w - \eta T_o) Nu_f \tag{40}$$

Differentiating the above equation for the case where $Q = P$ gives:

$$d\log P - \frac{\theta}{\tau_w} d\log \tau_w = d\log Nu_f - \frac{\eta}{\tau_w} d\log \eta - \frac{\eta}{\tau_w} d\log T_o + d\log k_f \tag{41}$$

The terms on the right hand side of the above equation depend only on the functional forms assumed for Nu_f and η (Table I) and the chosen independent variables (Table II). Ultimately these terms depend on the variation of Nu_f and η with the flow variables along with the aerodynamic and thermodynamic properties of the flow. The final form for the left hand side of the equation depends on the type of anemometer used.

It was shown in reference 161 that, for a wire mounted normal to the flow, $E = f(u,\rho,T_o,T_w)$. Morkovin[58] and Baldwin[35] related Nu_f and η to the non-dimensional variables noted in Table I. However, recent results presented by Barre et.al.,[162] suggested advantages from using the following variables: $E = f(m,M_\infty,T_o,T_w)$ and $E = f(p,m,T_o,T_w)$. In order to obtain the equation for the CCA, they transformed Morkovin's equations into their variables. This transformation is not necessary, since once the variables are chosen, the equations can be derived directly using a method similar to the one described by Anders[161].

The equations obtained using the variables of ❷ from table II gives the same results as those of ❶, Morkovin[58], namely $E = f(m,T_o)$ under the condition where $Nu_f \neq f(M_\infty)$ and $S_w = S_\rho$. Using the variables in ❶, Barre et.al.,[162] applied the resultant equations to measurements made in a turbulent boundary layer under the assumption

that $\tilde{p} = 0$ without assuming that $S_u = S_\rho$. They also extended the equation to the case of supersonic flow in the test section of wind tunnels by assuming that all the fluctuations were sound, again not assuming $S_u = S_\rho$.

Once the independent variables are chosen, it is not necessary to derive the equations using Nu_t and η. The "*primitive*" variables, u, ρ, T_o etc., greatly simplifies the manipulation of the calibration data and can be used to correlate E as a function of u, ρ, T_o etc., without evaluating Nu_t and η. This technique might have advantages in the calibration of wires and the ease of operation of calibration facilities.

The possible sets of variables based on the above discussion is presented in Table II.

	Dependent Variable	Independent Variable	Reference
❶	E, Nu_t, η	u, ρ, T_o	Baldwin[35], Morkovin[58]
❷	E, Nu_t, η	m, M_∞, T_o	Barr, Quine and Dussauge[162]
❸	E, Nu_t, η	p_∞, m, T_o	Barr, Quine and Dussauge[162]
❹	E	u, ρ, T_o	Rose and McDaid[8] Stainback and Johnson[85]
❺	E	m, M_∞, T_o	
❻	E	p_∞, m, T_o	

Table II. Various Independent Variables to Derive the Hot-Wire Anemometry Equations

Therefore, there are many forms for the hot-wire equations depending on the variables chosen and the anemometer used. One should choose the variables that are most convenient for the flow situation under investigation.

a. Constant Current Anemometer

Using the heat transfer equation (40) and the functional relationship from equation (27) and (29), the change in voltage across a wire can be related to the changes in u, ρ, and T_o. An example of a set of equations obtained for a constant current anemometer was given by Morkovin[58] as:

$$\frac{e'}{E} = -S_u\frac{u'}{u} - S_\rho\frac{\rho'}{\rho} + S_{T_o}\frac{T_o'}{T_o} \tag{42}$$

where

$$S_u = \frac{\partial \log E}{\partial \log u} = \frac{E'A_w'}{\tau_{ww}}\left[\tau_{ww}\left(\frac{\partial \log Nu_t}{\partial \log Re_t} + \frac{1}{a}\frac{\partial \log Nu_t}{\partial \log M}\right) - \left(\frac{1}{a}\frac{\partial \log \eta}{\partial \log M} + \frac{\partial \log \eta}{\partial \log Re_t}\right)\right] \tag{43}$$

$$S_\rho = \frac{\partial \log E}{\partial \log \rho} = \frac{E'A_w'}{\tau_{ww}}\left[\tau_{ww}\frac{\partial \log Nu_t}{\partial \log Re_t} - \frac{\partial \log \eta}{\partial \log Re_t}\right] \tag{44}$$

$$S_{T_o} = \frac{\partial \log E}{\partial \log T_o} = \frac{E'A_w'}{\tau_{ww}}\left[\begin{array}{l} k_t\tau_{ww}(1+\mathcal{A}_w) + \mathcal{A}_w\tau_{ww}\left(-1 - n_t + m_t\dfrac{\partial \log Nu_t}{\partial \log Re_t} + \dfrac{1}{2a}\dfrac{\partial \log Nu_t}{\partial \log M}\right) \\ \qquad -\mathcal{A}_w\left(\dfrac{1}{2a}\dfrac{\partial \log \eta}{\partial \log M} + m_t\dfrac{\partial \log \eta}{\partial \log Re_t}\right) \end{array}\right] \tag{45}$$

For a large range of Reynolds numbers and Mach numbers, S_u and S_ρ in equation (42) are unequal[35]. Following Kovasznay's technique for supersonic flow, dividing equation (42) by S_{T_o}, squaring and forming the mean gives:

$$\overline{\phi^2} = q^2\overline{\left(\frac{u'}{u}\right)^2} + s^2\overline{\left(\frac{\rho'}{\rho}\right)^2} + \overline{\left(\frac{T_o'}{T_o}\right)^2} + 2qsR_{u\rho}\frac{\tilde{u}\tilde{\rho}}{u\rho} - 2qR_{uT_o}\frac{\tilde{u}\tilde{T}_o}{uT_o} - 2sR_{\rho T_o}\frac{\tilde{\rho}\tilde{T}_o}{\rho T_o} \tag{46}$$

This is a general equation for a wire mounted normal to the flow in compressible flows where $S_u \neq S_\rho$. This is a single equation with six unknowns. In principal, this equation can be solved by operating a single wire at six overheats and solving six equations to obtain the three fluctuating quantities and their correlations. In the past, it was generally stated that the calibration of the wire cannot be made sufficiently accurate or the velocity and density sensitivities cannot be made sufficiently different to obtain a suitable solution using this technique. Demetriades[163] noted that the coefficient in equation (46) must occur to at least the fifth degree. This constraint, however, appears to be too restrictive. For example, assume that s is a function of q as follows:

$$s = a_1 + a_2q^{b_1} + a_3q^{b_2} + a_4q^{b_3} \tag{47}$$

It ca be shown that b_1, b_2 and b_3 can have any value provided that the substitution of the relationship for s into equation (46) results in an equation having at least six terms. An analysis of data obtained at transonic Mach number by Spangenberg indicates that s can be non-linearly related to q and suggest

b. Boundary Layer

Horstman and Rose[170] made measurements at transonic speeds where, for their flow condition, it was found that $S_u \approx S_\rho$. For this condition the transonic hot-wire problem degenerated to the supersonic flow problem where only $\tilde{m}/m$, $\tilde{T}_o/T_o$ and $R_{m T_o}$ could be measured. From their measurement of $\tilde{m}/m$, the velocity and density fluctuations were computed by assuming that $\tilde{T}_o/T_o$ and $\tilde{p}/p$ were zero. An example of these results is presented in figure 40. In this figure Horstman and Rose's hot-wire results, represented by the circles, are compared with the thin film results obtained by Mikulla[170].

c. Flight in Atmosphere

Any attempts to extrapolate the effect of wind tunnel disturbances on laminar boundary layer transition to flight conditions requires some knowledge of the disturbance levels in the atmosphere. Much of the fluctuation data obtained in the atmosphere was measured using sonic anemometers on towers[179]. There was a limited amount of data obtained in the atmosphere using hot-wire anemometry on flight vehicles[49,180]. Otten et. al.,[49] expanded the methods devised by Rose and McDaid by using a two wire probe. One wire was operated by a CCA at a low over heat to measure $\tilde{T}_o$. The other wire was operated with a CTA that was sensitive to $\tilde{m}$ and $\tilde{T}_o$. The results from these two wires were used to measure $\tilde{m}$ and $\tilde{T}_o$ in the atmosphere. An example of spectral data obtained in the atmosphere is presented in figure 41 and reveals the expected $-5/3$ slope, for $\tilde{m}$ and $\tilde{T}_o$.

d. Subsonic Slip Flow

For this regime $Nu_t = f(M_\infty, Re_t, \tau_w)$ and $S_u \neq S_\rho$. These results are identical to those in the transonic flow regime and attempts have been made to apply the three wire technique developed for transonic flows to subsonic slip flows. For tests in subsonic slip flows the three wires were of different diameters in addition to being operated at different overheats. Some very preliminary data obtained using this technique in the Langley LTPT tunnel is presented in figure 42a-b where comparison with results obtained using King's equation are made.

HIGH SUPERSONIC AND HYPERSONIC FLOW

Theoretical Consideration

a. Constant Current Anemometer

In the 1950's and 1960's hot-wire anemometry was extended into the high supersonic and hypersonic flow regime[6,7,181,182]. For high supersonic flows it was found experimentally that $S_u = S_\rho$ and equation (42) becomes:

$$\frac{e'}{E} = -S_m \frac{m'}{m} + S_{T_o} \frac{T_o'}{T_o} \tag{49}$$

Dividing equation (49) by the total temperature sensitivity, squaring, and then taking the mean results in the following equation:

$$\overline{\phi'^2} = r^2 \overline{\left(\frac{m'}{m}\right)^2} - 2r R_{m T_o} \left(\frac{\tilde{m}}{m}\right)\left(\frac{\tilde{T}_o}{T_o}\right) + \overline{\left(\frac{T_o'}{T_o}\right)^2} \tag{50}$$

This equation was derived by Kovasznay[6] and used to generate fluctuation diagrams for supersonic flows. This equation was also used in references 167 and 168 for subsonic compressible flows. The general form of equation (50) is a hyperbola where the intercept on the ϕ-axis represents the total temperature fluctuation and the asymptotes represent the mass flow fluctuation[7].

Kovasznay demonstrated that the basic linear perturbation in compressible flows consists of vorticity, entropy and sound. He termed these basic fluctuations as "*modes*". If the fluctuation diagram is assumed to consist of a single mode the diagrams were termed "*mode diagrams*". An example of a general fluctuation diagram and the various mode diagrams for supersonic flow are presented in figures 43 and 44.

b. Constant Temperature Anemometer

For this case equation (42) becomes:

$$\frac{e'}{E} = S_m \frac{m'}{m} + S_{T_o} \frac{T_o'}{T_o} \tag{51}$$

This is a single equation in two unknowns and a two wire probe can be used to obtain m', T_o' and $m'T_o'$ similar to the compressible subsonic flow case[61,183,184].

PRECEDING PAGE BLANK NOT FILMED

17,18

Examples of Data

a. Freestream

In order to evaluate the relative "*goodness*" of supersonic wind tunnels and to relate the levels of disturbances in the test section to laminar boundary layer transition on models, a large amount of hot-wire measurements were made in the test sections of supersonic and hypersonic wind tunnels. In 1961 Laufer[185] presented measurements made in the test section of the Jet Propulsion Laboratory 18 x 20 inch supersonic wind tunnel over a Mach number range from 1.6 to 5.0 using CCA. An example of the fluctuation diagrams obtained by Laufer is presented in figure 45. From these diagrams the mass flow and total temperature fluctuations were obtained. Examples of the mass flow fluctuations are presented in figure 46a. There was a significant increase of $\tilde{m}/m$ with Mach number ranging from 0.07% at $M = 1.6$ to about 1.0 to 1.35% at $M = 5.0$, depending on Reynolds number. All of the fluctuation diagrams were straight lines and Laufer demonstrated that these results indicated that the fluctuations were predominantly pressure fluctuations due to sound. Examples of the calculated pressure fluctuations are presented in figure 46b. Laufer concluded that the pressure fluctuations originated at the turbulent boundary on the wall of the tunnel and because of the finite value of the temperature fluctuations the sound source had a finite velocity. An example of the sound source velocities is presented in figure 47.

A large amount of hot-wire data was taken in the freestream of various facilities to measure disturbance levels in efforts to develop quiet supersonic wind tunnels. A review of this effort was reported in reference 186.

Measurements in the freestream of the Langley Research Center Mach 20 High Reynolds number Helium Tunnel were performed by Wagner and Weinstein[181]. All of their fluctuation diagrams were straight lines similar to the results obtained in supersonic flows. Examples of their measured mass flow and total temperature fluctuations are presented in figure 48. The mass flow fluctuations were substantially higher than the values measured by Laufer at $M = 5.0$. Pressure fluctuation measurements presented in figure 49 indicate that at low total pressures the boundary layer on the nozzle wall was probably transitional at the acoustic origin of the sound source. Relative sound source velocities are presented in figure 50. The source velocities for the Mach 20 tunnel at the higher pressures are significantly higher than those measured by Laufer at Mach numbers up to 5. (Also see ref. 187).

b. Boundary Layer

Measurements were made in supersonic and hypersonic turbulent boundary layers to extend the range of Reynolds stress measurements needed in the development of turbulent boundary layer theories. Barre et. al.,[162] conducted hot-wire tests in a supersonic boundary layer where transonic effects were accounted for by using a transformation of equation (42-45) from u, ρ, T_o to p, m, and T_o. Using the assumption that $E = f(p,m,T_o)$ and $\tilde{p}/p \approx 0$, reduced their equation to $E = f(m,T_o)$. Under these condition the fluctuation diagram developed by Kovasznay was used to obtain $\tilde{m}/m$, $\tilde{T}_o/T_o$ and R_{uT_o} without the assumption that $S_u = S_\rho$.

Examples of their results are presented in figures 51 and 52. Figure 51 shows that the quantity $\sqrt{\rho u'^2/\tau_w}$ is greatly underestimated if the assumption is made that $S_u = S_\rho$ when the velocity in the boundary is transonic and $S_u \neq S_\rho$. Figure 52 show the variation of R_{uT_o} with the local Mach number through the boundary layer. The expected value for R_{uT_o} is -0.85 and the data obtained for $S_u \neq S_\rho$ agrees well with this value. However, data evaluated where S_u was assumed to be equal to S_ρ were substantially higher at the lower transonic Mach numbers.

Fluctuations in a hypersonic boundary layer were made by Laderman and Demitrades[182] and reported in reference 188. An example of the mass flow and total temperature fluctuations measured across the boundary layer is presented in figure 53. The velocity, density, static temperature, and pressure fluctuations were calculated using the mass flow and total temperature fluctuations and various assumptions. An example of these measurements is presented in figures 54 and 55.

Additional measurements were made in hypersonic boundary layers by Laderman[189] and

on an ogive cylinder by Owen and Horstman[59] at $M \approx 7.0$. The measurements made by Owen and Horstman included not only data for $\tilde{m}$, $\tilde{T}_o$ and $R_{m\tau}$ but integral scales and microscales, probability density distributions, skewness, kurtosis and intermittancy distribution across the boundary layer. A summary paper by Owen[190] presents additional data which included space-time correlation, convective velocities, disturbance inclination angle, and turbulence life time distributions. (Also see ref. 87, 191-196).

c. Wake

An example of fluctuation diagrams measured in the wake behind a 15° half angle wedge at $M = 15.5$ is presented in figure 56. From these results Wagner and Weinstein concluded that the predominant fluctuation in this wake was entropy since the fluctuation diagrams were straight lines that intersected the r -axis at approximately $-\alpha$.

d. Downstream of Shock

In supersonic and hypersonic flows the disturbances measured in the freestream of the test section are not necessarily the disturbances that can affect the transition of the laminar boundary layer on a body. The passage of sound waves through shocks will result in a combination of vorticity, entropy, and sound downstream of the shock[197]. Because of this the fluctuation diagram will no longer be a straight line but a general hyperbola[48]. An example of this result is presented in figure 57. (Also see ref. 198-201).

CONFIRMATION OF THEORETICAL RESULTS

Hot-wire anemometry was used extensively to validate or confirm theoretical results. Some examples of these efforts are presented below.

Theoretical studies of the stability of laminar boundary layers to small disturbances were initially performed by Tollmein[202,203] and Schlichting[204]. These calculations indicated that disturbances of a given frequency could decrease, remain constant or be amplified depending on the frequency chosen and the Reynolds number. The first experimental verification of the theory was made by Schubauer and Skramstad[135]. An example of recent experimental and theoretical results for the determination of the neutral stability boundary[205] in a laminar boundary layer is presented in figure 58.

Hot-wire measurements were made downstream of "*grids*" to evaluate the theory for the decay of turbulence. Tests conducted by Kistler and Vrebalovich[206] to evaluate the "*linear*" decay law is presented in figure 59 and confirm this law for large values of the Reynolds number. At lower Reynolds number[25] the exponent can be closer to 1.20 - 1.25. Measurements of spectra for velocity fluctuations downstream of grids was also made and compared with theory. Two examples of these spectra are presented[206,207] in figure 60a-b. The spectra in figure 60a had an insignificant amount of energy in the expected inertial sub-range indicated by a slope of $-5/3$. This result was attributed to the low Reynolds number of the flow. The spectra presented in figure 60b was measured in a high Reynolds number flow and revealed a significant amount of energy in the inertial sub-range. Theoretical calculations were made for the temperature spectra in a heated jet and downstream of a heated grid. An example of the theory and measurements[207] is presented in figure 61. Attempts have been made to predict the influence of measured freestream fluctuations on laminar boundary transition. An example of this efforts[208] is presented in figures 62.

A considerable amount of data was obtained by Stetson et. al.,[209] in hypersonic flow to study the stability of laminar boundary layer. An example of these results are presented in figure 63 and indicates the existence of first and second mode instabilities in the laminar boundary layer. These results were in agreement with those obtained by Kendall[155] and Demetriades[210] and was in qualitative agreement with the theoretical results obtained by Mack[156].

OTHER APPLICATIONS

Hot-wire anemometry was used in shock tubes in an attempt to check the frequency response of probes and to trigger other events[52,211].

Theoretical results indicated that there would be "*temperature fronts or steps*" in cryogenic

wind tunnels due to the injection of liquid nitrogen into the circuit. Measurements were made using a hot-wire anemometer to determine the possible occurrences of these thermal steps[53].

A pulsed hot-wire was used to measure the velocities and flow angle in low speed flows[212]. A wire, which was operated by an anemometer, was place in the wake of a second wire which could be alternately heated. The time lag between heating the forward wire, this pulse being detected by the second wire and the distance between the wires was used to compute the velocity of the flow. In reference 213 a somewhat different technique was described that used two CCA's and a CTA to measure the velocity and flow angle.

Hot-wire anemometry was used to obtain the location of transition in a laminar boundary in addition to obtaining some information on the fluctuations in the laminar, transitional and turbulent boundary layers[214,215]. In some flows where the fluctuation levels are high, such as a jet, a moving hot-wire probe was found to improve the accuracy of the results[216]. This technique is usually noted as flying hot-wire anemometry. (Also see ref. 217-221).

Hot-wire anemometry was used[222] to measure the focal points of the laser beams for Laser Transit anemometry (LTA) . Using a traversing mechanism and a CTA, the distance between the two beams was determined by measuring the difference between the two maximum voltage outputs from the anemometer. It was noted that additional information could be obtained such as the mean value of the beam intensity intersected by the wire, laser beam power, beam separation, beam diameter, beam divergence, cross-sectional beam-intensity distribution and relative beam intensity.

CONDITIONAL SAMPLING

Organized motion or structures in a turbulent boundary layer has been extensively studied[20,223-225] using the concept of conditional sampling. The flow of a turbulent boundary layer over a concave surface was studied in reference 226 to search for organized motion in the boundary layer. The possible existence of organized motion is illustrated in figure 64 from measurements made with two hot-wire probes located 0.1δ apart. The conditional sampling technique was used to determine the characteristic shape of the mass flow signal during the passage of an organized motion. An example of these results are presented in figure 64. Figure 65 shows that the measured event at an upstream and a downstream station had the same general characteristic shape.

COMPARISON OF HOT-WIRE MEASUREMENTS WITH OTHER TECHNIQUES

In the past the hot-wire anemometer, with all its limitations, was the only instrument available that was capable of measuring fluctuations with adequate fidelity[12]. To some extent, this is no longer the case as other techniques such as LV, LIF, CARS, and Raman scattering are now available for measuring various mean flow and fluctuating quantities. In inviscid flow where the fluctuations can be low, the anemometer is presently the only reliable instrument available. Compared to other techniques the anemometer is still relatively simple to operate and relatively inexpensive. Because of its long history, the results obtained using anemometry is still often used as a standard for evaluating measurements obtained using other techniques. The extent to which the anemometer can maintain these advantages depends on the continued development of the other techniques.

Tests were conducted in turbulent boundary layers to compare hot-wire results with other techniques to validate hot-wire/laser velocimeter (LV)[227,228] and hot-wire/laser-induced fluorescence (LIF)[229] techniques. An example of velocity fluctuations obtained using hot-wire anemometer and a LV system is presented in figure 66 for streamwise velocity fluctuations. The agreement between the two sets of data is very good. Measured density and static temperature fluctuations measured with a hot-wire and a LIF system in a turbulent supersonic boundary layer is presented in figure 67. Again, except for two values for the density fluctuation obtained with the LIF system, the agreement between the two sets of data is very good. Various experiments were made using LIF and LIF/RAMAN techniques to measure $\tilde{T}_o/T_o$ and $\tilde{\rho}/\rho$ where results were compared with hot-wire

measurements[228]. An example[230] of these results is presented in figure 68. The only disagreement between the hot-wire and the other results was attributed to a shock that apparently did not cross the hot-wire probe.

CONCLUDING REMARKS

A review was made to illustrate the versatility of hot-wire anemometry in addition to noting some of its limitations. The review included examples of results obtained in the various flow regimes and various types of flow fields. Examples of data were presented for the subsonic incompressible flow regime that were used to evaluate the flow quality in the test section of wind tunnels, to obtain measurements in turbulent boundary layer, and to substantiate or validate various theories of turbulence.

Recently attempts to extend hot-wire anemometry into the transonic and subsonic slip flow regimes were presented for cases where $S_u = S_\rho$ and $S_u \neq S_\rho$. Examples of data obtained at high supersonic and hypersonic Mach numbers were presented. These results revealed that the fluctuation diagrams measured in the test section were a straight line, indicating that the disturbances in the test sections were due to sound mode.

Examples were also presented to illustrate measurements made to substantiate turbulent theories, to compare with other techniques, and to illustrate the concept of conditional sampling.

ACKNOWLEDGMENT

The authors acknowledge the support of this research by the National Aeronautics and Space Administration under contracts NAS1-19320 and NAS1-19672 respectively.

REFERENCES

1. Comte-Bellot, G., 1977, "*Hot-Wire and Hot-Film Anemometers*," Measurement of Unsteady Fluid Dynamic Phenomena, Hemisphere Publishing Co., pp. 123-162.

2. Boussinesq, J., 1905, "*An Equation for the Phenomena of Heat Convection and an Estimate of the Cooling Power of Fluids*," Journal de Mathematiques, Vol. 1, pp. 285-332, also Comptes Rendus, Vol. 133, pp. 257.

3. King, L.V., 1914, "*On the Convection of Heat from Small Cylinders in a Stream of Fluid*," Phil. Trans. of Roy. Soc. (London), Ser. A. Vol. 214, No. 14, pp. 373-432.

4. Dryden, H.L., and Kuethe, A.M., 1929, "*The Measurement of Fluctuations of Air Speed by the Hot-Wire Anemometer*," NACA-TR-320.

5. Ziegler, M., 1934, "*The Construction of a Hot-Wire Anemometer with Linear Scale and Negligible Lag*," Proc. K. Ned. Akad. Wet. 15, No. 1.

6. Kovasznay, L.S.G., 1950, "*The Hot-Wire Anemometer in Supersonic Flows*," Journal of the Aeronautical Sciences, Vol. 17, No. 9, pp. 565-584.

7. Kovasznay, L.S.G., 1953, "*Turbulence in Supersonic Flow*," Journal of the Aeronautical Sciences, Vol. 20, No. 10, pp. 657-674.

8. Rose, W.C., and McDaid, E.P., 1976, "*Turbulence Measurement in Transonic Flow*," Proceedings of the AIAA 9th Aerodynamic Testing Conference, Arlington, Texas.

9. Sandborn, V.A., 1974, "*A Review of Turbulence Measurements in Compressible Flow*," NASA-TMX-62337.

10. Baldwin, L.V., Sandborn, V.A., and Laurence, J.C., 1960, "*Heat Transfer from Transverse and Yawed Cylinders in Continuum, Slip, and Free Molecule Air Flows*," Journal of Heat Transfer, Transaction of ASME, C82, pp. 77-86.

11. Vagt, J.D., 1979, "*Hot-Wire Probes in Low Speed Flow*," Progress in Aerospace Sciences, Vol. 18, pp. 271-323.

12. Kovasznay, L.S.G., 1959, "*Turbulence Measurements*," Applied Mechanics Reviews, Vol. 12, No. 6, pp. 375-380.

13. Owen, F.K., and Foire, A.W., 1986, "*Principles and Practices of Hot-Wire Anemometers,*" Complere Inc., Palo Alto, CA.

14. Laufer, J., 1975, "*New Trends in Experimental Turbulent Research,*" Annual Review of Fluid Mechanics, Vol. 7, pp. 307-326.

15. Olivari, D., 1980, "*Hot Wire Techniques: Conditional Sampling and Intermittency,*" Von Karman Institute for Fluid Dynamics, Lecture Series - 3, Measurements and Predictions of Complex Turbulent Flows.

16. Ardonceau, P., 1980, "*Turbulence Measurements in Supersonic Flows,*" Von Karman Institute for Fluid Dynamics, Lecture Series - 3, Measurements and Predictions of Complex Turbulent Flows.

17. Proceedings of the Dynamic Flow Conference on Dynamic Measurements in Unsteady Flow, 1978, Editors: Kovasznay, L.S.G., Favre, A., Buchhave, P., Fulachier, L., and Hansen, B.W.H., IMST, Marseille, France, John Hopkins University Baltimore, MD, Sept. 11-14, 1978.

18. The Heuristics of Thermal Anemometry, 1990, ASME-FED Vol. 97, Editors: Stock, D.E., Sherif, S.A., and Smits, A.J., The 1990 Spring Meeting of the Fluids Engineering Division, University of Toronto, Toronto, Ontario, Canada, June 4-7.

19. Symposium on Thermal Anemometry, 1987, Editor: Stock, D.E., 1987, ASME-FED Vol. 53, The 1987 ASME Applied Mechanics, Bioengineering, and Fluids Engineering Conference, Cincinnati, Ohio, June 14-17.

20. Comte-Bellot, G., Charnay, G., and Sabot, J., 1981, "*Hot-Wire and Hot-Film Anemometry and Conditional Measurements: A Report on Euromech 132,*" Journal of Fluid Mechanics, Vol. 110, pp. 115-128.

21. Sandborn, V.A., 1972, "*Resistance Temperature Transducers,*" Metrology Press, Fort Collins, Colorado.

22. Perry, A.E., 1982, "*Hot-Wire Anemometry,*" Oxford: Clarendon Press.

23. Lomas, C.G., 1986, "*Fundamentals of Hot-Wire Anemometry,*" Cambridge University Press.

24. Goldstein, R.J., 1983, "*Fluid Mechanics Measurements,*" Hemisphere Publishing Corporation.

25. Hinze, J.O., 1975, "*Turbulence,*" McGraw-Hill Book Co., New York.

26. Smol'yakov, A.V., and Tkachenko, V.M., 1983, "*The Measurement of Turbulent Fluctuations : An Introduction of Hot-Wire Anemometry and Related Transducers,*" Springer-Verlag, New York.

27. Bradshaw, P., 1971, "*An Introduction to Turbulence and its Measurement,*" Pergamon Press, New York.

28. Blackwelder, R.F., 1981, "*Hot-Wire and Hot-Film Anemometers,*" Methods of Experimental Physics: Fluid Dynamics, Editor: Emrich, R.J., Vol. 18, Part A, Academic Press Inc., New York.

29. Corrsin, S., 1963, "*Turbulence: Experimental Methods,*" Handbook of Physics, 8/2, pp. 523-590.

30. Kovasznay, L.S.G., 1954, "*Methods to Distinguish Between Laminar and Turbulent Flow,*" Article F-1, Volume IX, Physical Measurements in Gas Dynamics and Combustion, Princeton University Press, pp. 213-285.

31. Sauer, F.M., and Drake, Jr., R.M., 1953, "*Forced Convection Heat Transfer from Horizontal Cylinders in a Rarefied Gas,*" Journal of the Aeronautical Sciences, Vol. 20, pp. 175-180, 209.

32. Weltmann, R.N., and Kuhns, P.W., 1960, "*Heat Transfer to Cylinders in Crossflow in Hypersonic Rarefied Gas Streams,*" NASA-TND-267.

33. Standler, J.R., Goodwin, G., and Creager, M.O., 1951, "*A Comparison of Theory and*

Experiment for High-Speed Free-Molecule Flow," NACA Rep. 1032 (Supersedes NACA-TN-2244).

34. Kennard, E.H., 1938, "*Kinetic Theory of Gases,*" McGraw-Hill Book Co., Inc.

35. Baldwin, L.V., 1958, "*Slip-Flow Heat Transfer From Cylinders in Subsonic Airstreams,*" NACA-TN-4369.

36. Dryden, H.L., and Kuethe, A.M., 1930, "*Effect of Turbulence in Wind Tunnel Measurements,*" NACA-TR-342.

37. Stainback, P.C., and Owen, F.K., 1984, "*Dynamic Flow Quality Measurements in the Langley Low Turbulence Pressure Tunnel,*" AIAA-84-0621.

38. Schubauer, G.B., Spangenberg, W.G., and Klebanoff, P.S., 1950, "*Aerodynamic Characteristics of Damping Screens,*" NACA-TN-2001.

39. Klebanoff, P.S., Tidstrom, K.D., and Sargent, 1962, "*The Three-Dimensional Nature of Boundary-Layer Instability,*" Journal of Fluid Mechanics, Vol. 12, pp. 1-37.

40. Laufer, J., 1954, "*The Structure of Turbulence in Fully Developed Pipe Flow,*" NACA Report 1174.

41. Sandborn, V.A., 1955, "*Experimental Evaluation of Momentum Terms in Turbulent Pipe Flow,*" NACA-TN-3266.

42. Sandborn, V.A., and Slogar, R.J., 1955, "*Longitudinal Turbulent Spectrum Survey of Boundary Layers in Adverse Pressure Gradients,*" NACA-TN-3453.

43. Townsend, A.A., 1949, "*The Fully Developed Turbulent Wake of a Circular Cylinder,*" Australian Journal of Scientific Research, Series A, Physical Sciences, Vol. 2, pp. 451-468.

44. Uberoi, M.S., and Freymuth, P., 1969, "*Spectra of Turbulence in Wakes Behind Circular Cylinders,*" The Physics of Fluids, Vol. 12, No. 7, pp. 1359-1363.

45. Miksad, R.W., Jones, F.L., Powers, E.J., Kim, Y.C., and Khadra, L., 1982, "*Experiments on the Role of Amplitude and Phase Modulations During Transition to Turbulence,*" Journal of Fluid Mechanics, Vol. 123, pp. 1-29.

46. Wygnanski, I., and Fiedler, H., 1969, "*Some Measurements in the Self-Preserving Jet,*" Journal of Fluid Mechanics, Vol. 38, Part 3, pp. 577-612.

47. Corrsin, S., 1943, "*Investigation of Flow in an Axially Symmetrical Heated Jet of Air,*" NACA-WR-W-94, (Issued as: NACA-ACR-3L23).

48. Weinstein, L.M., 1972, "*Oblique Shock-Sound Interaction at $M_\infty \equiv 20$ in Helium,*" AIAA Journal, Vol. 10, No. 12, pp. 1718-1720.

49. Otten, L.J., Pavel, A.L., Finley, W.E., and Rose, W.C., 1981, "*A Survey of Recent Atmospheric Turbulence Measurements from a Subsonic Aircraft,*" AIAA-81-0298.

50. Okiishi, T.H., and Schmidt, D.P., 1978, "*Measurement of the Periodic Variation of Turbomachine Flow Fields,*" Proceedings of the Dynamic Flow Conference, pp. 249-269.

51. Wilkinson, S.P., and Malik, M.R., 1985, "*Stability Experiments in the Flow over a Rotating Disk,*" AIAA Journal, Vol. 23, No. 4, pp. 588-595.

52. Darshan, S.D., 1953, "*Use of a Hot-Wire Anemometer as a Triggering and Timing Device for Wave Phenomena in a Shock Tube,*" Ph.D., Thesis, Part I and II, John Hopkins University.

53. Johnson, C.B., and Stainback, P.C., 1984, "*A Study of Dynamic Measurements Made in the Settling Chamber of the Langley 0.3-Meter Transonic Cryogenic Tunnel,*" AIAA-84-0596.

54. Kovasznay, L.S.G., 1978, "*Measurement in Intermittent and Periodic Flow,*" Proceedings of the Dynamic Flow Conference, pp. 133-159.

55. Blackwelder, R.F., 1978, "*Pattern Recognition of Coherent Eddies,*" Proceedings of the Dynamic Flow Conference, pp. 173-190.

56. Wagner, T.C., and Kent, J.C., 1987, "*Measurement of Intake Valve/Cylinder Boundary Flows Using a Multiple Orientation Hot-Wire Technique,*" Symposium on Thermal Anemometry, ASME-FED Vol. 53, pp. 79-85.

57. Mangalam, S.M., Sarma, G.R., Kuppa, S., and Kubendran, L.R., 1992, "*A New Approach to High-Speed Flow Measurements Using Constant Voltage Anemometry,*" AIAA-92-3957.

58. Morkovin, M.V., 1956, "*Fluctuations and Hot-Wire Anemometry in Compressible Flows,*" AGARDograph 24.

59. Owen, F.K., and Horstman, C.C., 1974, "*Turbulence Measurements in an Equilibrium Hypersonic Boundary Layer,*" AIAA-74-0093.

60. Bonnet, J.P., and Alziary de Roquefort, T., 1980, "*Determination and Optimization of Frequency Response of Constant Temperature Hot-Wire Anemometers in Supersonic Flows,*" Rev. Sci. Instrum. Vol. 51, No. 2, pp. 234-239.

61. Walker, D.A., Ng, W.F., and Walker, M.D., 1989, "*Experimental Comparison of Two Hot-Wire Techniques in Supersonic Flow,*" AIAA Journal, Vol. 27, No. 8, pp. 1074-1080.

62. Weinberg, B.C., and Laderman, S., 1969, "*Constant Current Anemometer Diagnostics of Flow Fields,*" Contract No. Nonr-839(38), Report of Aerospace Engineering and Applied Mechanics, Polytechnic Institute of Brooklyn.

63. Kidron, I., 1967, "*The Signal-to-Noise Ratio of Constant-Current and Constant-Temperature Hot-Wire Anemometers,*" IEEE Transaction on Instrumentation and Measurement, Vol 1M-16, No. 1, pp. 68-73.

64. Lowell, H.H., 1950, "*Design and Application of Hot-Wire Anemometers for Steady-State Measurements at Transonic and Supersonic Airspeeds,*" NACA-TN-2117.

65. Ram, V.V., 1992, "*On the Effects of Fluid Temperature on Hot-Wire Characteristics. Part 2: Foundations of a Rational Theory,*" Experiments in Fluids, Vol. 13, pp. 267-278.

66. Frenkiel, F.N., 1954, "*Effect of Wire Length in Turbulence Investigation with Hot-Wire Anemometer,*" The Aeronautical Quarterly, Vol. V, pp. 1-24.

67. Dreksen, R.W., and Azad, R.S., 1983, "*An Examination of Hot-Wire Length Corrections,*" The Physics of Fluids, Vol. 26, No. 7, pp. 1751-1754.

68. Larsen, S., and Hojstrop, J., 1982, "*Spatial and Temporal Resolution of a Thin-Wire Resistance Thermometer,*" Journal of Physics, Series E - Scientific Instruments, Vol. 15, pp. 471-477.

69. Westpal, R.V., 1990, "*Near-Wall Measurement Errors For Hot-Wire Probes with Finite Spatial Resolution,*" The Heuristics of Thermal Anemometry, ASME-FED Vol. 97, pp. 1-8.

70. Hebbar, K.S., 1980, "*Wall Proximity Correction for Hot-Wire Readings in Turbulent Flows,*" DISA Information No. 25, pp. 15-16.

71. Kanevce, G., and Oka, S., 1973, "*Correcting Hot-Wire Readings for Influence of Fluid Temperature Variation,*" DISA Information No. 15, pp. 21-24.

72. Martinez-Val, R., Jimenez, J., and Rebollo, M., 1982, "*Sensor Contamination Effects in Hot-Wire Anemometry in Air,*" DISA Information No. 27, pp. 12-14.

73. Paranthoen, P., Lecordier, J.C., and Petit, C., 1982, "*Influence of Dust Contamination on Frequency Response of Wire Resistance Thermometers,*" DISA Information No. 27, pp. 36-37.

74. Drubka, R.E., Tan-Atichat, J., and Nagib, H.M., 1977, "*Analysis of Temperature Compensating Circuits for Hot-Wires and Hot-Films,*" DISA Information No. 22, pp. 5-14.

75. Oka, S., and Kostic, Z., 1972, "*Influence of Wall Proximity on Hot-Wire Velocity*

Measurements," DISA Information No. 13, pp. 29-33.

76. Klatt, F., 1973, "*A Study of Systematic Errors in Measurements with the Constant-Temperature Anemometer in High-Turbulence Flow With and Without Hot-Wire Signal Linearization,*" DISA Information No. 14.

77. Hardin, J.C., 1986, "*Introduction to Time Series Analysis,*" NASA-RP-1145.

78. Bendat, J.S., and Piersol, A.G., 1985, "*Random Data,*" A Wiley Interscience Publication.

79. Bruun, H.H., 1978, "*Multi-Probes and Higher Moments,*" Proceedings of the Dynamic Flow Conference, pp. 943-961.

80. Frenkiel, F.N., and Klebanoff, P.S., 1967, "*Higher-Order Correlation in a Turbulent Fluid,*" The Physics of Fluids, Vol. 10, No. 3, pp. 507-520.

81. Van Atta, C.W., 1978, "*Multi Channel Measurements and High-Order Statistics,*" Proceedings of the Dynamic Flow Conference, pp. 919-941.

82. Frenkiel, F.N., and Klebanoff, P.S., 1967, "*Correlation Measurements in a Turbulent Flow Using High-Speed Computing Methods,*" The Physics of Fluids, Vol. 10, No. 8, pp. 507-520.

83. George, W.K, 1978, "*Processing of Random Signals* (with appendices by Beuther, P.D., and Lumley, J.L.,)," Proceedings of the Dynamic Flow Conference, pp. 757-800.

84. Bendat, J.S., and Piersol, A.G., 1980, "*Engineering Applications of Correlation and Spectral Analysis,*" A Wiley Interscience Publication.

85. Stainback, P.C., and Johnson, C.B., 1983, "*Preliminary Measurements of Velocity, Density and Total Temperature Fluctuations in Compressible Subsonic Flow,*" AIAA-83-0384.

86. Jones, G.S., Stainback, P.C., Harris, C.D., Brooks, C.W., and Clukey, S.J., 1989, "*Flow Quality Measurements for the Langley 8-Foot Transonic Pressure Tunnel LFC Experiment,*" AIAA-89-0150.

87. Owen, F.K., and Horstman, C.C., 1972, "*Hypersonic transitional Boundary Layers,*" AIAA Journal, Vol. 10, No. 6, pp. 769-775.

88. Sato, H., 1951, "*Experimental Study of the Spectrum of Isotropic Turbulence, I,*" Journal of Phys. Soc. Japan, Vol. 6, pp. 387-392. (Also, 1952, "*Experimental Study of the Spectrum of Isotropic Turbulence, II,*" Journal of Phys. Soc. Japan, Vol. 7, pp. 392-396).

89. Champagne, F.H., 1978, "*The Fine-Scale Structure of the Turbulent Velocity Field,*" Journal of Fluid Mechanics, Vol. 86, Part 1, pp. 67-108.

90. Uberoi, M.S., and Kovasznay, L.S.G., 1952, "*On Mapping and Measurement of Random Fields,*" Vol. X, No. 4, pp. 375-393.

91. Gagne, Y., Hopfinger, E.J., and Marechal, J., 1978, "*Measurements of Internal Intermittency and Dissipation Correlations in Fully Developed Turbulence,*" Proceedings of the Dynamics Flow Conference, pp. 271-277.

92. Schumann, U., and Patterson, G.S., 1978, "*Numerical Study of Pressure and Velocity Fluctuations in Nearly Isotropic Turbulence,*" Journal of Fluid Mechanics, Vol. 88, part 4, pp. 685-709.

93. Artt, D.W., and Brown, A., 1971, "*The Simultaneous Measurement of Velocity and Temperature,*" Journal of Physics E: Scientific Instruments, Vol. 4, pp. 72-74.

94. Davis, M.R., and Davies, P.O.A.L., 1972, "*Factors Influencing the Heat Transfer from Cylindrical Anemometer Probes,*" Journal of Heat and Mass Transfer, Vol. 15, pp. 1659-1677.

95. Cimbala, J.M., and Park, W.J., 1990, "*A Direct Hot-Wire Calibration Technique to Account for Ambient Temperature Drift in Incompressible Flow,*" Experiments in Fluids, Vol. 8, pp. 299-300.

96. Boman, U.R., 1992, "*Hot-Wire Calibration Over a Large Temperature Range,*" Experiments in Fluids, Vol. 12, pp. 427-428.

97. Fulachier, L., 1978, "*Hot-Wire Measurements in Low Speed Heated Flow,*" Proceedings of the Dynamic Flow Conference.

98. George, W.K., Beuther, P.D., and Shabbir, D., 1987, "*Polynomial Calibrations for Hot-Wires in Thermally-Varying Flows,*" Symposium on Thermal Anemometry, ASME-FED Vol. 53, pp. 1-6.

99. McAdam, W.H., 1954, "*Heat Transmission,*" McGraw-Hill Book Company Inc.

100. Kostka, M., and Ram, V.V., 1992, "*On the Effects of Fluid Temperature on Hot Wire Characteristics. Part 1: Results of Experiments,*" Experiments in Fluids, Vol. 13, pp. 115-162.

101. Crimbala, J.M., and Pork, W.J., 1990, "*A Direct Hot-Wire Calibration Technique to Account for Ambient Temperature Drift in Incompressible Flow,*" Experiments in Fluids, Vol. 8, pp. 299-300.

102. Haw, R.C., and Foss, J.F., 1990, "*A Facility for Low Speed Calibration,*" The Heuristics of Thermal Anemometry, ASME-FED-Vol. 97, pp. 29-33.

103. Haw, R.C., Ali, S.K., and Foss, J.F., 1987, "*Gravitationally Defined Velocities for a Low Speed Hot-Wire Calibration,*" Symposium on Thermal Anemometry, ASME-FED Vol. 53, pp. 7-14.

104. Collin, D.C., and Williams, M.J., 1959, "*Two Dimensional Convection From Heated Wires at Low Reynolds Numbers,*" Journal of Fluid Mechanics, Vol. 6, pp. 357-384.

105. Andrews, G.E., Bradley, D., and Hardy, G.F., 1972, "*Hot-Wire Anemometer Calibration for Measurements of Small Gas Velocities,*" Int. Journal of Heat and Mass Transfer, Vol. 15, pp. 1765-1786.

106. Bruun, H.H., 1971, "*Interpretation of a Hot-Wire Signal using a Universal Calibration Law,*" Journal of Physics, E, Vol. 4, pp. 225-231.

107. Zabat, M., Browand, F.K., and Plocher, D., "*In-Situ Swinging Arm Calibration for Hot-Film Anemometers,*" Experiments in Fluids, Vol. 12, pp. 223-228.

108. Cole, J.D., and Roshko, A., 1954, "*Heat Transfer from Wires at Reynolds Numbers in the Oseen Range,*" Proceedings Heat Transfer and Fluid Mechanics Institute, Stanford, California, pp. 13-24.

109. Laurence, J.C., and Landes, L.G., 1952, "*Auxiliary Equipment and Techniques for Adapting the Constant-Temperature Hot-Wire Anemometer to Specific Problems in Air-Flow Measurements,*" NACA-TN-2843.

110. Spangenberg, W.G., 1955, "*Heat Loss Characteristics of Hot-Wire Anemometers at Various Densities in Transonic and Supersonic Flows,*" NACA-TN-3381.

111. Vrebalovich, T., 1962, "*Heat Loss From Hot-Wires in Transonic Flow,*" Research Summary No. 36-14, Jet Propulsion Lab., Pasadena, California.

112. Laufer, J., and McClellan, R., 1956, "*Measurement of Heat Transfer from Fine Wires in Supersonic Flow,*" Journal of Fluid Mechanics, Vol. 1, pp. 276-289.

113. Corrsin, S., 1949, "*Extended Applications of the Hot-Wire Anemometer,*" NACA-TN-1864.

114. Fiedler, H., 1978, "*On Data Acquisition in Heated Turbulent Flows,*" Proceedings of the Dynamic Flow Conference, pp. 81-100.

115. Champagne, F.H., 1978, "*The Temperature Sensitivity of Hot-Wires,*" Proceedings of the Dynamic Flow Conference, pp. 101-114.

116. Millikan, C.B., and Klein, A.L., 1933, "*The Effect of Turbulence - An Investigation of Maximum Lift Coefficient and Turbulence in Wind Tunnels and in Flight,*" Aircraft Engineering, Vol. V, pp. 169-174.

117. von Doenhoff, A.E., and Abbott, F.T., 1947, "*The Langley Two-Dimensional Low-Turbulence Pressure Tunnel,*" NACA-TN-1283.

118. Uberoi, M.S., 1956, "*Effect of Wind-Tunnel Contraction on Free-Stream Turbulence,*" Journal of the Aeronautical Sciences, Vol. 23, No. 8, pp. 754-764.

119. Wigeland, R.A., Tan-atichat, J., and Nagib, H.M., 1981, "*Evaluation of a New Concept for Reducing Freestream Turbulence in Wind Tunnels,*" Journal of Aircraft, Vol. 18, No. 7, pp. 528-536, (also AIAA-80-0432R).

120. Scheiman, J., and Brooks, J.D., 1980, "*A Comparison of Experimental and Theoretical Turbulence Reduction from Screens, Honeycomb and Honeycomb-Screen Combinations,*" AIAA-80-0433.

121. Dryden, H.L., and Abbott, I.H., 1949, "*The Design of Low-Turbulence Wind Tunnels,*" NACA-R940.

122. Budwig, R., Tavoularic, S., and Corrsin, S., 1985, "*Temperature Fluctuations and Heat Flux in Grid-Generated Isotropic Turbulence with Streamwise and Transverse Mean-Temperature Gradients,*" Journal of Fluid Mechanics, Vol. 153, pp. 414-460.

123. Warhaft, Z., and Lumley, J.L., 1978, "*An Experimental Study of the Decay of Temperature Fluctuation in Grid-Generated Turbulence,*" Journal of Fluid Mechanics, Vol. 88, part 4, pp. 659-684.

124. Warhaft, Z., 1980, "*On Experimental Study of the Effect of Uniform Strain on Thermal Fluctuations in Grid-Generated Turbulence,*" Journal of Fluid Mechanics, Vol. 99, part 3, pp. 545-573.

125. Tucker, M., 1953, "*Combined Effect of Damping Screens and Stream Convergence on Turbulence,*" NACA-TN-2878.

126. Taylor, G.I., and Batchelor, G.K., 1949, "*The Effect of Wire Gauze on Sound Disturbances in a Uniform Stream,*" Quarterly Journal of Mech. and Applied Math, Vol. II, part I, pp. 1-29.

127. Tucker, H.J., and Ali, S.F., 1973, "*Decay of Anisotropic Turbulence,*" AIAA Journal, Vol. 11, No. 4, pp. 546-548.

128. Frenkiel, F.N., Klebanoff, P.S., and Huag, T.T., 1979, "*Grid Turbulence in Air and Water,*" The Physics of Fluids, Vol. 22, No. 9, pp. 1606-1617.

129. Tucker, H.J., and Reynolds, A.J., 1968, "*The Distortion of Turbulence by Irrotational Plane Strain,*" Journal of Fluid Mechanics, Vol. 32, part 4, pp. 657-673.

130. Durbin, P.A., 1982, "*Analysis of the Decay of Temperature Fluctuations in Isotropic Turbulence,*" Physics of Fluids, Vol. 25, No. 8, pp. 1328-1332.

131. Klebanoff, P.S., 1954, "*Characteristics of Turbulence in a Boundary Layer with Zero Pressure Gradient,*" NACA Report 1247 (Supersedes NACA-TN-3178).

132. Bardakhnov, S.P., Kozlov, V.V., and Larichkin, V.V., 1989, "*Influence of an Acoustic Field on the Flow Structure Behind a LEBU in a Turbulent Boundary Layer,*" Second IUTAM Symposium on Structure of Turbulence and Drag Reduction, Zurich, Switzerland, pp. 503-506.

133. Coustols, E., Gleyzes, C., Schmitt, V., and Berrue, P., 1988, "*Etude Experimentale de la Reduction du Frottement Turbulent au Moyen de Parois Rainurees,*" L'Aeronautique et L'Astronautique, No. 34, No. 129, pp. 34-46.

134. Azad. R.S., and Doell, B., 1989, "*Behaviour of Separation Bubble with Different Roughness Elements at the Leading Edge of a Flat Plate,*" Second IUTAM Symposium on Structure of Turbulence and Drag Reduction, Zurich, Switzerland, pp. 85-92.

135. Schubauer, G.B., and Skramstad, H.K., 1948, "*Laminar-Boundary-Layer Oscillations and Transition on a Flat Plate,*" NACA-TR-909.

136. Kohama, Y., Ohta, F., and Segawa, K., 1989, "*Development and Interaction of Instabilities in the Cross Flow Field,*" Laminar-turbulent transition; Proceedings of the IUTAM Symposium, Toulouse, France, pp. 431-440.

137. Ito, A., 1985, "*O-Kyoku Men ni Tomonau Tate Uzu Hokai no Kozo,*" Nihon Koku Uchu Gakkai-shi, Vol. 33, No. 374, pp. 58-65. (Journal of Japan Society for Aeronautical and Space Sciences).

138. Dovgal', A.V., Levchenko, V.Ya., and Timofeyev, V.A., 1989, "*LaminarizatsiyPogranichnovo Sloya Putem Loklizovannovo Nagrevaniya Poverkhnosti,*" Izvestiya Sibirskovo Otdeleniya Akademii Nauk SSSR, Seriya Tekhnicheskoy Nauk, ISS. 3, pp. 60-65.

139. Mechel, F., and Schilz, W., 1986, "*Studies of Acoustic Effects on a Flow Boundary Layer in Air,*" NASA-TM-77981.

140. Kendall, J.M., 1985, "*Experimental Study of Disturbances Produced in a Pre-Transitional Laminar Boundary Layer by Weak Freestream Turbulence,*" AIAA-85-1695.

141. Sokolov, M., and Giant, Z., 1992, "*The Ladder Probe: Reverse Flow Measurements with a Hot-Wire Rake,*" Experiments in Fluids, Vol. 12, pp. 307-318.

142. Rose, W.C., and Otten, L.J, 1983, "*High Reynolds-Number Shear-Stress Measurements,*" AIAA-83-0053.

143. Wyngaard, J.C., 1968, "*Measurement of Small-Scale Turbulence Structure with Hot-Wires,*" Journal of Scientific Instruments, (Journal of Physics E), Series 2, Vol. 1, pp. 1105-1108.

144. Davies, P.O.A.L., and Yule, A.J., 1974, "*Structure of Turbulence,*" I.S.V.R.

145. Kendall, J.M., 1990, "*Boundary Layer Receptivity to Freestream Turbulence,*" AIAA-90-1504.

146. Goldstein, M.E., 1983, "*The Evolution of Tollmien-Schlitching Waves Near a Leading Edge,*" Journal of Fluid Mechanics, Vol. 127, pp. 59-81.

147. Kerschen, E.J., 1989, "*Boundary Layer Receptivity,*" AIAA-89-1109.

148. Klebanoff, P.S., 1971, "*Effect of Freestream Turbulence on the Laminar Boundary Layer (Abstract),*" Bulletin of American Physical Society, Vol. 10, No. 11, pp. 1323.

149. Arnal, D., and Juillen, J., 1978, "*Contribution Experimentale a l'Etude de la Receptivite d'une Couche Limite Laminaire, a la Turbulence de l'Ecoulement General,*" ONERA Technical Report No. 1/5018-AYD.

150. Kosyrigin, V., Levchenko, Y., and Polyakov, N., 1988, "*The Laminar Boundary Layer in the Presence of a Moderately Turbulent Freestream,*" Preprint No. 16-88, USSR Academy of Sciences, Institute for Theoretical and Applied Mechanics, Novosibirsk.

151. Suder, K., O'Brien, J., and Reshotko, E., 1988, "*Experimental Study of Bypass Transition in a Boundary Layer,*" NASA-TM-100913.

152. Kendall, J.M., 1982, "*Study of the Effect of Freestream Turbulence Upon Disturbances in the Laminar Boundary Layer,*" Report AFWAL-TR-82-3002.

153. Kendall, J.M., 1984, "*Experiments on the Generation of Tollmien-Schlichting Waves in a Flat Plate Boundary Layer by Weak Freestream Turbulence,*" AIAA-84-0011.

154. Kendall, J.M., "*Hot-Wire and Shadowgraph Studies Relating to Boundary Layer Transition on a Slender Cone at Mach 4.5,*" (Private Communications).

155. Kendall, J.M., 1975, "*Wind Tunnel Experiments Relating to Supersonic and Hypersonic Boundary Layer Transition,*" AIAA Journal, Vol. 13, No. 3, pp. 290-299.

156. Mack, L.M., 1975, "*Linear Stability Theory and Problem of Supersonic Boundary Layer Transition,*" AIAA Journal, Vol. 13, No. 3, pp. 278-289.

157. Corrsin, S., and Uberoi, M.S., 1949, "*Further Experiments on the Flow and Heat Transfer in a Heated Turbulent Air Jet,*" NACA-TN-1865 (Issued as NACA Report 998, 1950).

158. Manjunath, A., Gowda, B.H.L., and Natarajan, R., 1992, "*Studies on the Mixing of Two Non-Axial Jets in a Confined Passage-Turbulence Characteristics,*" Experiments in Fluids, Vol. 13, pp. 147-154.

159. Laurence, J.C., 1955, "*Intensity, Scale, and Spectra of Turbulence in Mixing Region of Free Subsonic Jet,*" NACA-TN-3561.

160. Miksad, R.W., Jones, F.L., and Powers, E.J., 1983, "*Measurements of Nonlinear Interactions During Natural Transition of a Symmetric Wake,*" The Physics of Fluids, Vol. 26, No. 6, pp. 1402-1409.

161. Anders, J.B., Jr., 1974, "*Turbulence Measurements in Hypersonic Helium Flow,*" Report 1157, Gas Dynamics Laboratory, Princeton University, Princeton, New Jersey.

162. Barre, S., Quine, C., and Dussauge, J.P., 1992, "*Compressibility Effects on the Structure of Supersonic Mixing Layers: Experimental Results,*" Institut de Mécanique de Marseilles, Institut de Mécanique Statistique de la Turbulence, U.M. CNRS-Université Aix-Marseille II n° 380033, 12 avenue du Général Lecleerc, 13003, MARSEILLES, FRANCE.

163. Demetriades, A., 1978, "*Probes for Multivariant Flow Characteristics,*" Proceedings of the Dynamic Flow Conference on Dynamic Measurements in Unsteady Flows, IMST, Marseille, France, pp. 13-44.

164. Stainback, P.C., and Nagabushana, K.A., "*Reinvestigation of Hot-Wire Anemometry Applicable to Subsonic Compressible Flows Using Fluctuation Diagrams,*" (submitted to Journal of Fluids Engineering, Transactions of the ASME, Log No. 3538-DPT).

165. Stainback, P.C., Nagabushana, K.A., and Bushnell, D.M., 1992, "*Mode Diagrams for Hot Wire Anemometry in Subsonic Flows,*" International Conference on Methods of Aerophysical Research, organized by Institute of Theoretical and Applied Mechanics (ITAM) of the Siberian Division of the Russian Academy of Sciences, Novosibirsk, RUSSIA.

166. Stainback, P.C., and Nagabushana, K.A., 1991, "*Fluctuation Diagrams for Hot Wire Anemometry in Subsonic Compressible Flows,*" NASA-CR-189580.

167. Zinov'ev, V.N., and Lebiga, V.A., 1988, "*Measurements of Fluctuations For High Subsonic Velocities Using a Hot-Wire Anemometer,*" Plenum Publishing Corp. Novosibirsk, Translated from Zhurnal Prikladoni Mekhanikii Teckhnicheskoi Fiziki, No. 3, pp. 80-84.

168. Lebiga, V.A., and Zinoviev, V.N., 1989, "*Hot-Wire Measurements in Compressible Flow,*" ICIASF'89 Record, IEEE-89CH2762-3., The 13th International Congress on Instrumentation in Aerospace Simulation Facilities, DFVLR Research Center Göttingen.

169. Lebiga, V.A., and Zinovyev, V.N., 1991, "*Acoustic Measurements with a Hot-Wire Anemometer at High Subsonic Velocities,*" Dantec Information No. 10, 14-16.

170. Horstman, C.C., and Rose, W.C., 1977, "*Hot-Wire Anemometry in Transonic Flow,*" AIAA Journal, Vol. 15, No. 3, pp. 395-401.

171. Davies, P.O.A.L., and Fisher, M.J., 1964, "*Heat Transfer from Electrically Heated Cylinders,*" Proceedings of the Royal Society, Series A, Mathematical and Physical Sciences, Vol. 280, No. 1383, pp. 486-527.

172. Jones, G.S., Stainback, P.C., and Nagabushana, K.A., 1992, "*A Comparison of Calibration Techniques for Hot-Wires Operated in Transonic Slip Flows,*" AIAA-92-4007.

173. Stainback, P.C., Nagabushana, K.A., and Jones, G.S., 1993, "*A Status Report for Hot-Wire Anemometry Development at the Langley Research Center for Transonic and Subsonic Slip Flow Regimes,*" Third International Symposium on Thermal Anemometry - ASME

Fluids Engineering Division Summer Meeting, Washington, D.C.

174. Stainback, P.C., Nagabushana, K.A., Clukey, S.J., and Jones, G.S., 1991, "*Heat Transfer From Heater Cylinders in Subsonic Flows,*" First Joint ASME-JSME Fluids Engineering Conference, Portland, Oregon.

175. Stainback, P.C., and Nagabushana, K.A., 1992, "*Re-investigation of Hot-Wire Anemometry Applicable to Subsonic Compressible Flows Using Fluctuation Diagrams,*" to appear in JNASA-CR-4429.

176. Rong, B.S., Tan, D.K.M., and Smits, A.J., 1985, "*Calibration of the Constant Temperature Normal Hot-Wire Anemometer in Transonic Flow,*" Report MAE-1696.

177. Barre, S., Dupont, P., and Dussauge, J.P., 1992, "*Hot-Wire Measurements in Turbulent Transonic Flows,*" European Journal Mechanics B, Vol. 11, No. 4, pp. 439-454.

178. Winovich, W., and Stein, H.A., 1957, "*Measurements of the Nonlinear Variation with Temperature of Heat-Transfer Rate from Hot-Wires in Transonic and Supersonic Flow,*" NACA-TN-3965.

179. Kaimal, J.C., Wyngaard, J.C., Izumi, Y., and Cote, O.R., 1972, "*Spectral Characteristics of Surface-Layer Turbulence,*" Quarterly Journal of the Royal Meteorological Society, Vol. 98, No. 417, pp. 563-589.

180. MacCready, P.B., 1953, "*Atmospheric Turbulence Measurements,*" Journal of Meteor, Vol. 10, No. 5, pp. 325-337.

181. Wagner, R.D., and Weinstein, L.M., 1974, "*Hot-Wire Anemometry in Hypersonic Helium Flow,*" NASA-TN-D-7465.

182. Laderman, A.J., and Demetriades, A., 1973, "*Hot-Wire Measurements of Hypersonic Boundary-Layer Turbulence,*" The Physics of Fluids, Vol. 16, pp. 179-181.

183. Smits, A.J., 1990, "*An Introduction to Constant-Temperature Hot-Wire Anemometry in Supersonic Flows,*" The Heuristics of Thermal Anemometry, ASME-FED Vol. 97, pp. 35-40.

184. Smith, D.R., and Smits, A.J., 1993, "*The Simultaneous Measurement of Velocity and Temperature Fluctuations in the Boundary Layer of a Supersonic Flow,*" Experimental Thermal and Fluid Science, Vol. 6.

185. Laufer, J., 1961, "*Aerodynamic Noise in Supersonic Wind Tunnels,*" Journal of the Aerospace Sciences, Vol. 28, No. 9, pp. 685-692.

186. Wilkinson, S.P., Anders, S.G., Chen, F.-J., and Beckwith, I.E., 1992, "*Supersonic and Hypersonic Quiet Tunnel Technology at NASA Langley,*" AIAA-92-3908.

187. Vrebalovich, T., 1962, "*Application of Hot-Wire Techniques in Unsteady Compressible Flows,*" The ASME Hydraulic Division Conference, Symposium on Measurement in Unsteady Flow, pp. 61-70.

188. Laderman, A.J., and Demetriades, A., 1974, "*Mean and Fluctuating Flow Measurements in the Hypersonic Boundary Layer Over a Cooled Wall,*" Journal of Fluid Mechanics, Vol. 63, pp. 121-144.

189. Laderman, A.J., 1974, "*Hypersonic Viscous Flow over a Slender Cone, Part II: Turbulent Structures of the Boundary Layer,*" AIAA-74-0534.

190. Owen, F.K., 1988, "*Measurements of Hypersonic Flow Fields,*" AGARD-FDP-VKI Special Course, Aerothermodynamics of Hypersonic Velocities.

191. Owen, F.K., and Calarence, W., 1987, "*Turbulent Measurement in Hypersonic Flow,*" Paper No. 5, AGARD-CP-428, Fluid Dynamic Panal Symposium on Aerodynamic of Hypersonic Lifting Vehicles, Bristol, UK.

192. Smits, A.J., 1991, "*Turbulent Boundary-Layer in Supersonic Flow,*" Phil. Trans. R. Soc., Lond. A, Vol. 336, pp. 81-93.

193. Smits, A.J., Hayakawa, K., and Muck, K.C., 1983, "*Constant Temperature Hot-Wire Anemometer Practice in Supersonic Flows; Part 1: The Normal Wire,*" Experiments in Fluids, Vol. 1, pp. 83-92.

194. Dupont, P., and Debieve, J.F., 1992, "*A Hot-Wire Method for Measuring Turbulence in Transonic or Supersonic Heated Flows,*" Experiments in Fluids, Vol. 13, pp. 84-90. (Also Twelfth Symposium on Turbulence, Department of Chemical Engineering, Continuing Education, University of Missouri-Rolla), 1990.

195. Rose, W.C., 1973, "*The Behavior of a Compressible Turbulent Boundary Layer in a Shock-Wave-Induced Adverse Pressure Gradient,*" NASA TN D-7092, (Also Ph.D., Thesis, University of Washington 1972, CAT-7306-S).

196. Fisher, M.C., Maddalon, D.V., Weinstein, L.M., and Wagner, Jr., R.D., 1971, "*Boundary Layer Pitot and Hot-Wire Surveys at $M_\infty = 20$,*" AIAA Journal, Vol. 9, No. 5, pp. 826-834.

197. Moore, F.K., 1953, "*Unsteady Oblique Interaction of a Shock Wave with a Plane Disturbance,*" NACA-TN-2879, also NACA Rept. 1165.

198. D'iakov, S.P., 1958, "*The Interaction of Shock Waves with Small Perturbations. I,*" Soviet Physics Jetp, Vol. 6(33), No. 4, pp. 729-739.

199. D'iakov, S.P., 1958, "*The Interaction of Shock Waves with Small Perturbations. II,*" Soviet Physics JETP, Vol. 6(33), No. 4, pp. 740-747.

200. Dewey, Jr., C.F., 1961, "*Hot-Wire Measurements in Low Reynolds Number Hypersonic Flows,*" ARS Journal, The American Rocket Society, Vol. 31, No. 12, pp. 1709-1718.

201. Stetson, K.F., and Kimmel, R.L., 1992, "*On Hypersonic Boundary Layer Stability,*" AIAA-92-0737.

202. Tollmien, W., 1929, "*Über die Entstehung der Turbulenz,*" 1. Mitteilung, Nachr. Wiss. Göttingen, Math. Phys. Klasse, pp. 21-44, (also English translation "*The production of turbulence,*" NACA-TM-609, 1931).

203. Tollmien, W., 1936, "*General Instability Criterion of Laminar Velocity Distribution,*" NACA-TM-792.

204. Schlichting, H., 1987, "*Boundary Layer Theory,*" McGraw-Hill Book Company, Co.

205. Saric, W.S., and Nayfeh, A.H., 1977, "*Nonparallel Stability of Boundary Layer with Pressure Gradient and Suction,*" AGARD-CP-224.

206. Kistler, A.L., and Vrebalovich, T., 1966, "*Grid Turbulence at Large Reynolds Numbers,*" Journal of Fluid Mechanics, Vol. 26, No. 37, pp. 37-47.

207. Pao., Y.H., 1965, "*Structure of Turbulent Velocity and Scale Fields at Large Wave Number,*" The Physics of Fluids, Vol. 8, No. 6, pp. 1063-1075.

208. Mack, L.M., 1977, "*Transition Prediction and Linear Stability Theory,*" AGARD-CP-224.

209. Stetson, K.F., Thompson, E.R., Donaldson, J.C., and Sibr, L.G., 1983, "*Laminar Boundary Layer Stability Experiments on a Cone at Mach 8. Part 1: Sharp Cone,*" AIAA-83-1761.

210. Demetriades, A., 1971, "*Laminar Boundary Layer Stability Measurements at Mach 7 Including Wall Temperature Effects,*" AFOSR-TR-77-1311.

211. Billington, I.J., 1955, "*The Hot-Wire Anemometer and its use in Non-Steady Flow,*" University of Toronto, Ins. Aero. Phys., Tech. Note No. 5.

212. Toy, N., and Thoma, S.H., 1987, "*The Twin Pulsed Wire Anemometer - A New Instrument for Measurements in Complex Flows,*" Symposium on Thermal Anemometry, ASME-FED Vol. 53, pp. 65-72.

213. Blackwelder, R.F., and McLean, 1987, "*A Hot-Wire Probe for Velocity Measurement in Reverse*

Flows," Symposium on Thermal Anemometry, ASME-FED Vol. 53, pp. 73-78.

214. LaGraff, J.E., 1972, "*Observation of Hypersonic Boundary Layer Transition Using Hot-Wire Anemometry,*" AIAA Journal, Vol. 10, No. 6, pp. 762-769.

215. Sandborn, V.A., and Wisniewski, R.J., 1960, "*Hot-Wire Exploration of Transition on Cone in Supersonic Flow,*" Proceedings of Heat Transfer and Fluid Mechanics Institute Meeting, Stanford, Ohio, pp. 120-134.

216. Hussein, H.J., 1990, "*Measurements of Turbulent Flows with Flying Hot-Wire Anemometry,*" The Heuristics of Thermal Anemometry, ASME-FED Vol. 97, pp. 77-80.

217. Spangler, J.G., and Wells, Jr., C.S., 1968, "*Effects of Freestream Disturbances on Boundary Layer Transition,*" AIAA Journal, Vol. 6, No. 3, pp. 543-554.

218. Obremski, H.J., and Fejer, A.A., 1967, "*Transition in Oscillating Boundary Layer Flows,*" Journal of Fluid Mechanics, Vol. 29, part 1, pp. 93-111.

219. Mack, L.M., 1975, "*A Numerical Method for the Prediction of High-Speed Boundary-Layer Transition Using Linear Theory,*" NASA-SP-347, Part 1, pp. 101-123.

220. Reshotko, E., 1976, "*Boundary-Layer Stability and Transition,*" Annual Review of Fluid Mechanics, Vol. 8, pp. 311-349.

221. Laufer, J., and Vrebalovich, T., 1960, "*Stability and Transition of a Supersonic Laminar Boundary Layer on an Insulated Flat Plate,*" Journal of Fluid Mechanics, Vol. 9, part 2, pp. 257-299.

222. Takagi, S., 1992, "*Simple Method for Determining the Laser-Velocimeter Focal Point with the Aid of the Hot-Wire Anemometer,*" AIAA Journal, Vol. 30, No. 6, pp. 1664-1665.

223. Blackwelder, R.F., and Kaplan, R.E., 1976, "*On the Wall Structure of the Turbulent Boundary Layer,*" Journal of Fluid Mechanics, Vol. 26, pp. 89-112.

224. Moin, P., and Kim, J., 1985, "*The Structure of the Vorticity Field in Turbulent Channel Flow, Part I, Analysis of Instantaneous Fields and Statistical Correlations,*" Journal of Fluid Mechanics, Vol. 155, pp. 441-464 .

225. Perry, A.E., and Cheng, M.S., 1982, "*On the Mechanism of Wall Turbulence,*" Journal of Fluid Mechanics, Vol. 119, pp. 173-217.

226. Donovan, J.F., and Smits, A.J., 1987, "*A Preliminary Investigation of Large Scale Organized Motion in a Supersonic Turbulent Boundary Layer on a Curved Surface,*" AIAA-87-1285.

227. Rose, W.C., and Johnson, D.A., 1974, "*Study of Shock-Wave Turbulent Boundary Layer Interaction Using Laser Velocimeter and Hot-Wire Anemometer Techniques,*" AIAA-74-0095.

228. Polyakov, A.F., and Shindin, S.A., 1983, "*Some Aspects of Measuring the Structure of Non-Isothermal Turbulence by Simultaneous Application of DISA's LDA and Hot-Wire Anemometer,*" DISA Information No. 28, pp. 10-14.

229. Logan, P., McKenzie, R.L., and Bershader, D., 1988, "*Hot-Wire Accuracy in Supersonic Turbulence from Comparisons with Laser-Induced Fluorescence,*" AIAA Journal, Vol. 26, No. 3, pp. 316-322.

230. McKenzie, R.L., and Fletcher, D.G., 1992, "*Laser-Spectroscopic Measurement Techniques for Hypersonic, Turbulent Wind Tunnel Flows,*" NASA-TM-103928.

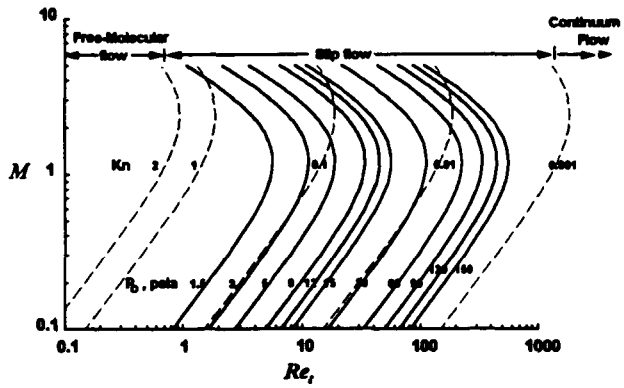

Figure 1. Mach number vs. Reynolds number for lines of Constant Total Pressure and Constant Knudsen Number; $d_w = 0.00015\ inch$; $T_o = 560°F$.

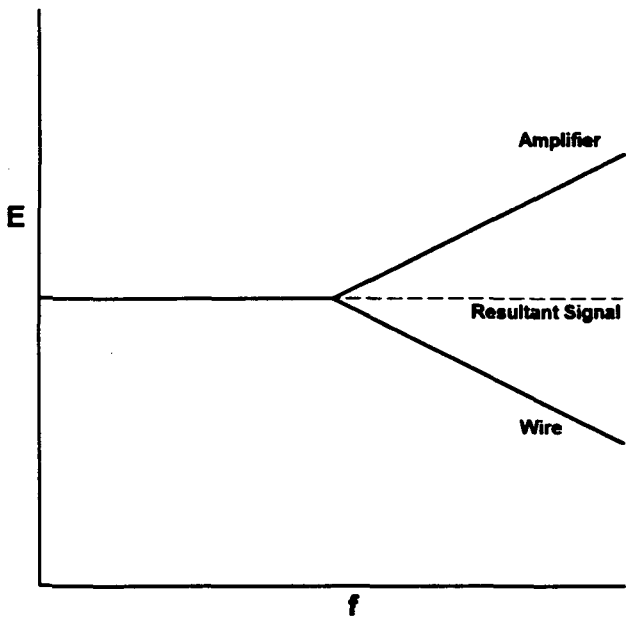

Figure 2. Frequency Compensation for CCA.

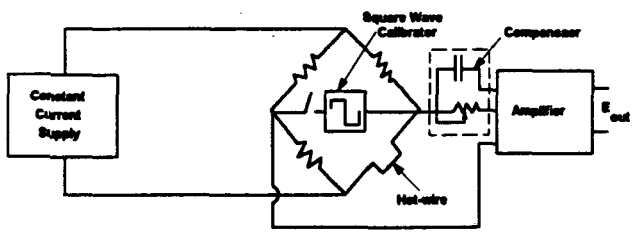

Figure 3. Schematic Representation of Constant Current Hot-Wire System; (ref. 62).

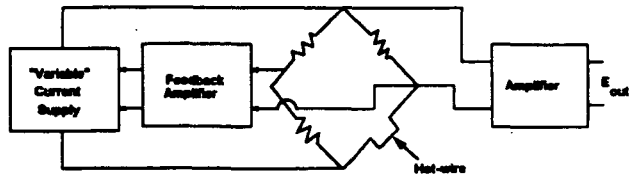

Figure 4. Schematic Representation of Constant Temperature Hot-Wire System; (ref. 62).

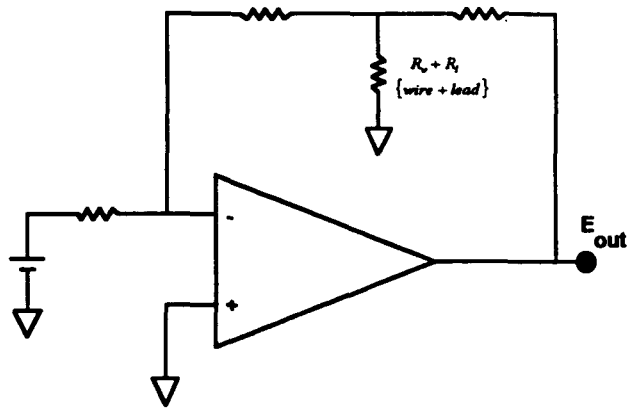

Figure 5. Schematic Representation of Constant Voltage Hot-Wire System; (ref. 57).

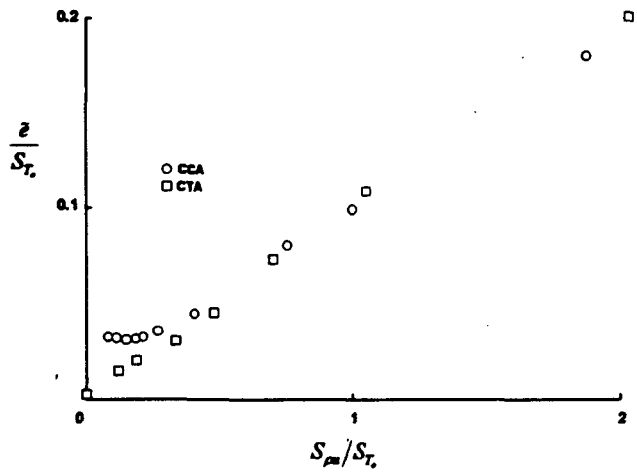

Figure 6. Modal Analysis that Compares the CTA and CCA Systems; $y/\delta = 0.23$; (ref. 59).

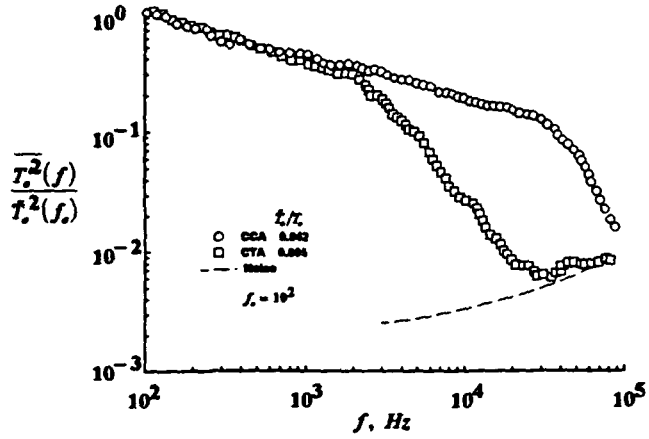

(a) Low Overheat;
Total Temperature Fluctuations

Figure 7. Normalized Power Spectra that Compare the Constant Temperature Anemometer (CTA) and Constant Current Anemometer (CCA) Systems; $y/\delta = 0.23$; (ref. 59).

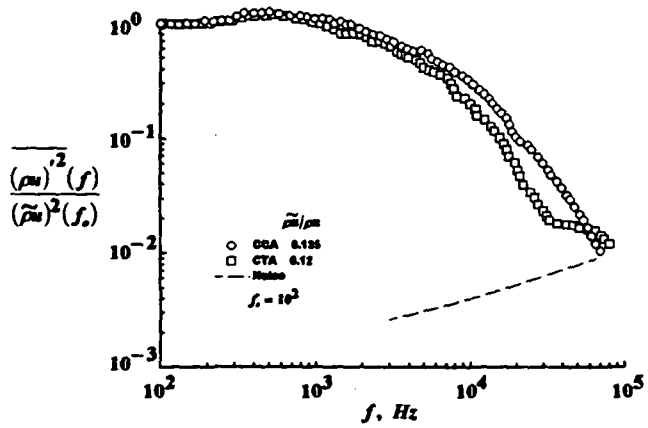

(b) High Overheat;
Mass-Flow Fluctuations

Figure 7. Concluded.

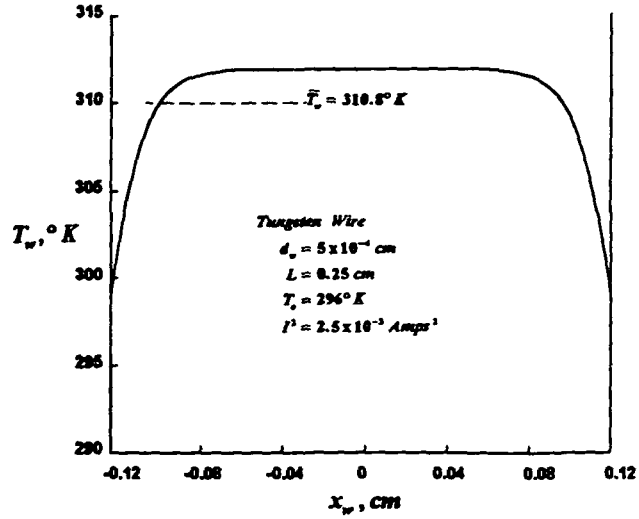

Figure 8. Typical Temperature Distribution Along a Convection Controlled Hot-Wire; (ref. 21).

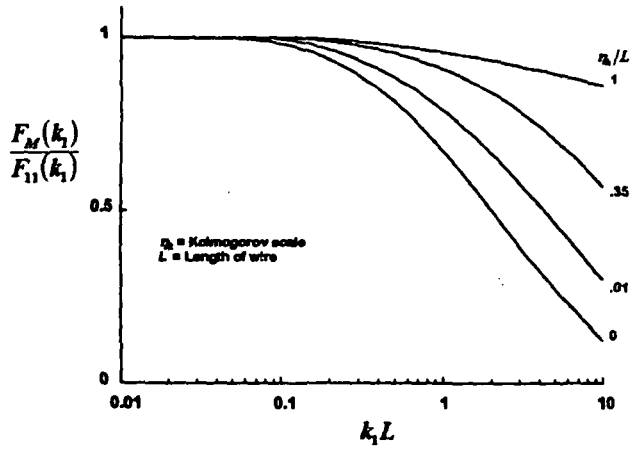

Figure 9. Hot-Wire Spectral Transfer Function; (ref. 143).

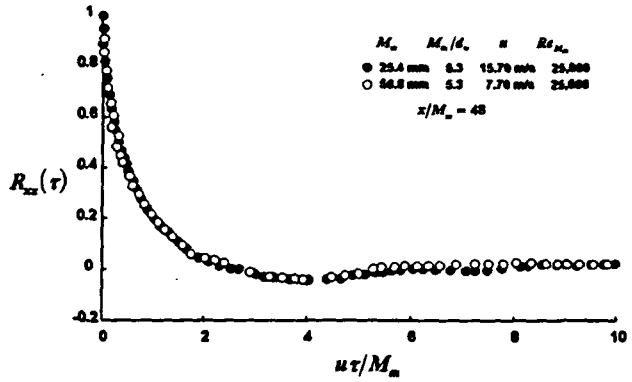

Figure 10. Auto-Correlation Coefficient $R_{uu}(\tau)$; (ref. 25).

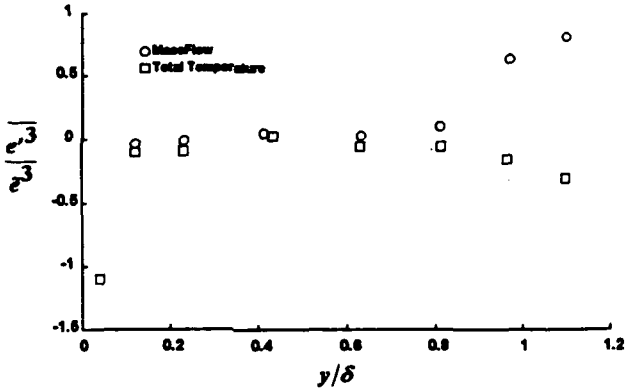

(a) Third Moment; Skewness

Figure 11. Distribution of the Mass-Flow and Total Temperature Fluctuations Across the Boundary Layer; (ref. 59).

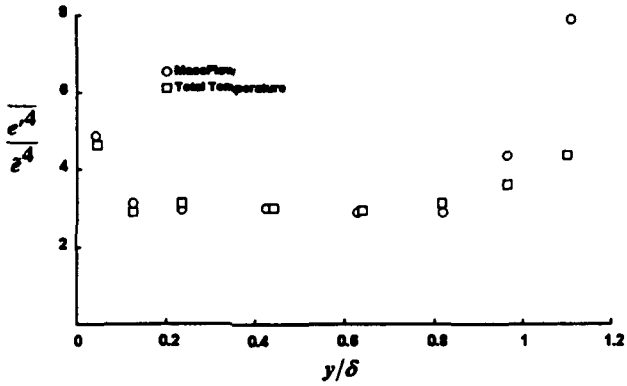

(b) Fourth Moment; Flatness

Figure 11. Concluded.

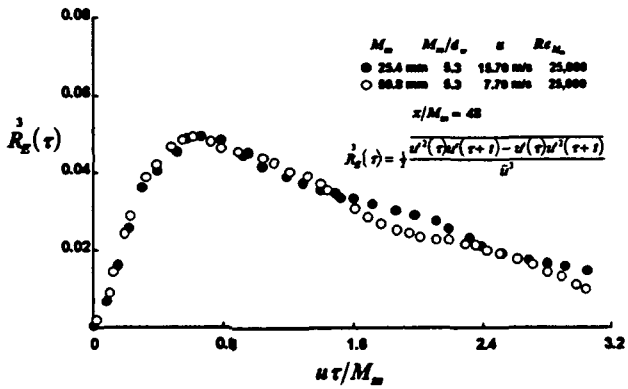

Figure 12. Composite Third-Order Auto-Correlation Coefficient $\overline{R}_g^3(\tau)u$; (ref. 25).

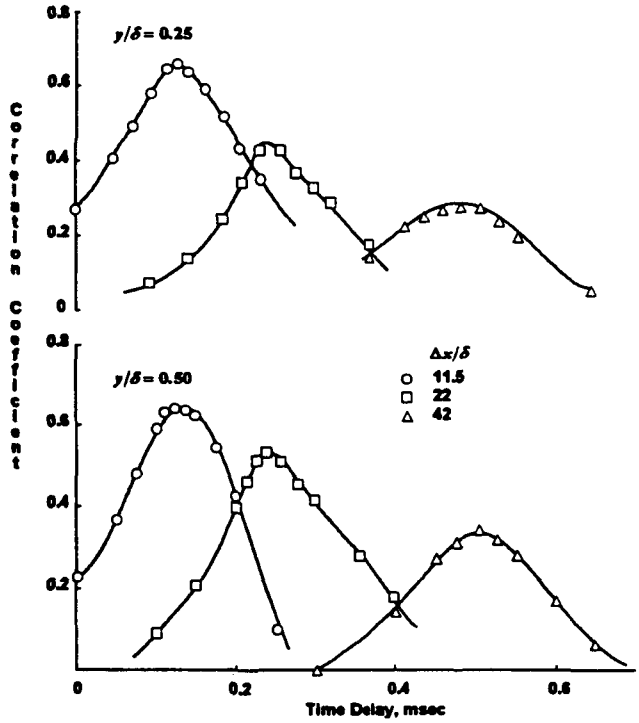

Figure 13. Examples of Filtered Space-Time Correlation Coefficient - 4 kHz; (ref. 87).

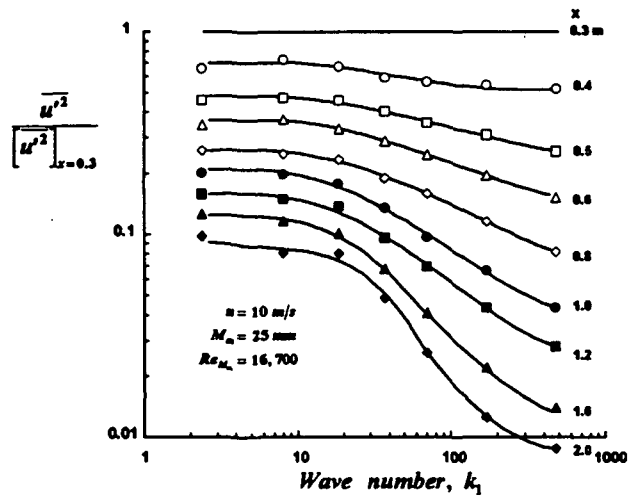

Figure 14. Decay of Energy of the Spectral Components; (ref. 88).

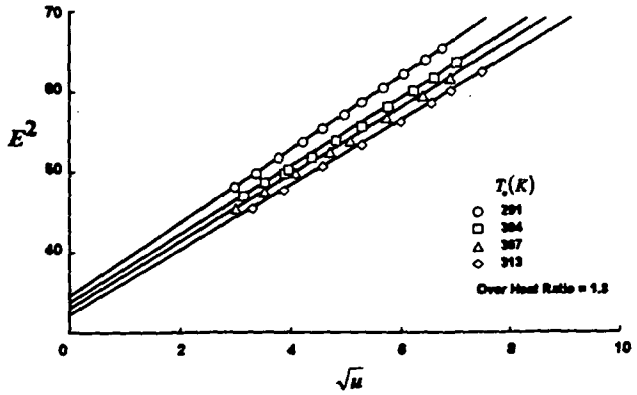

Figure 15. Voltage vs. Velocity for a Wire Operated with CTA; (ref. 93).

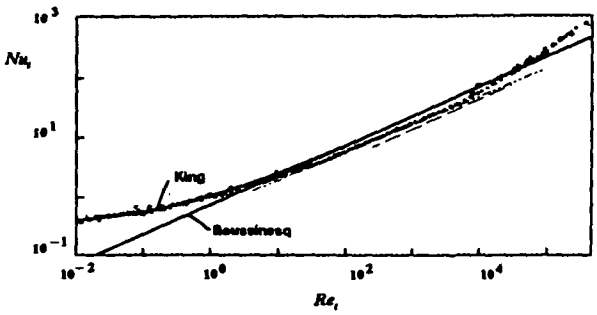

Figure 16. Summary of Heat Loss from Circular Cylinders Over a Wide Range of Reynolds Number in Continuum Flow; (ref. 21).

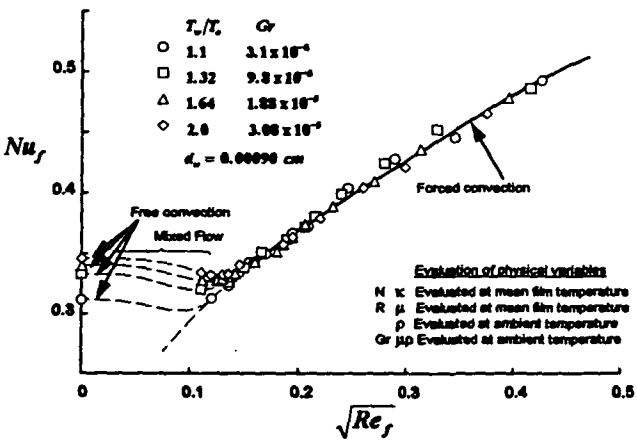

Figure 17. Interaction of Free and Forced Convection; (ref. 104).

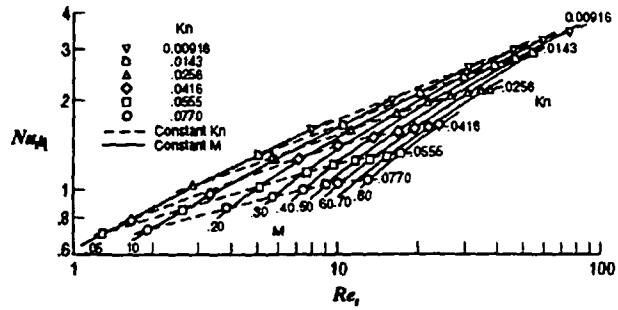

Figure 18a. Nusselt Number Correlation for Cylinders in Subsonic Slip Flow; $T_o = 80°F$; $T_w = 584°F$; (ref. 35).

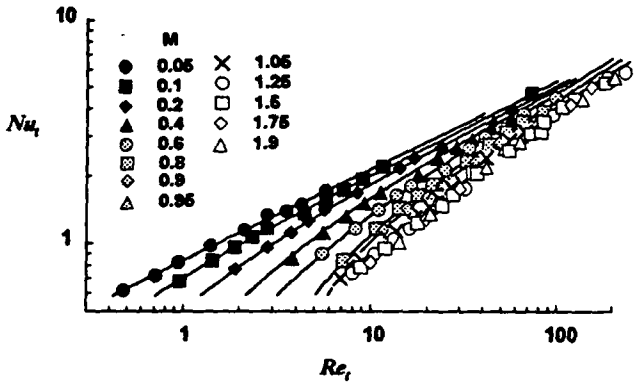

Figure 18b. Spangenberg's Reported Heat Loss Measurements from Electrically Heated Wires in Air; (ref. 171).

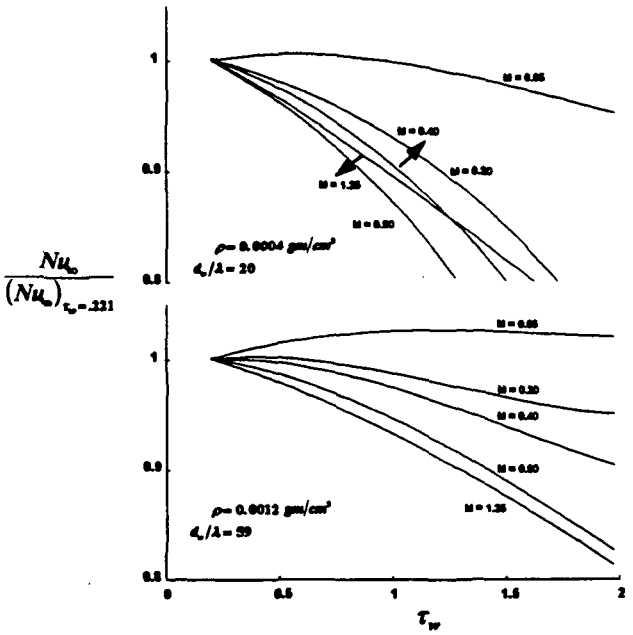

Figure 19. Normalized Nusselt Number Variation with Overheat for 0.00015 inch Diameter Platinum Wire Containing 10% Rhodium; (ref. 110).

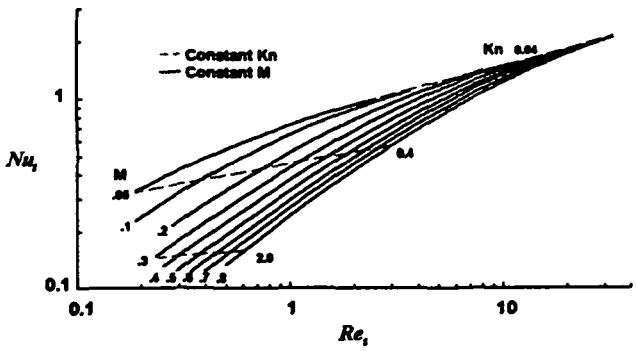

Figure 20. Predicted Nusselt Number Correlation from Approximate Slip-Flow Theory; (ref. 35).

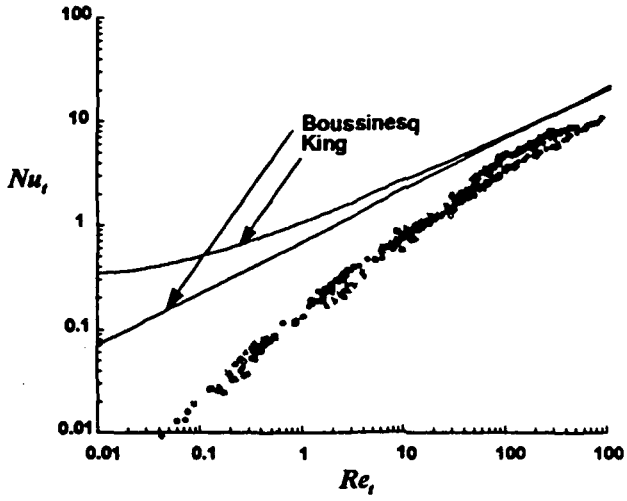

Figure 21. Summary of Supersonic Heat Transfer from Transverse Cylinders in Rarefied Air Flow; (ref. 21).

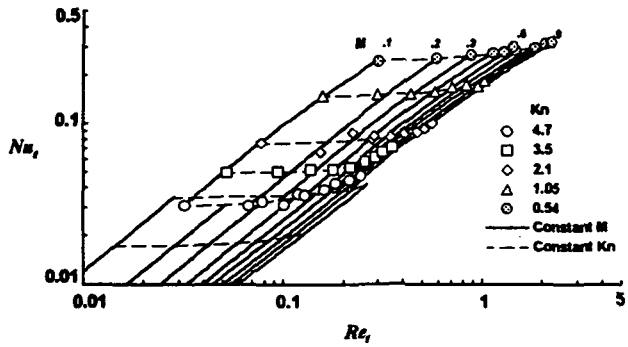

Figure 22. Comparison of Heat-Transfer Data with Free-Molecule-Flow Theory Using $\alpha = 0.57$; (ref. 33).

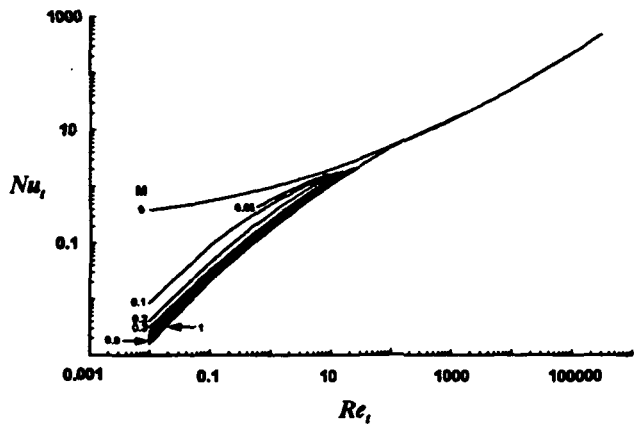

Figure 23. Correlation of Convective Heat Transfer from Transverse Cylinders; (ref. 10).

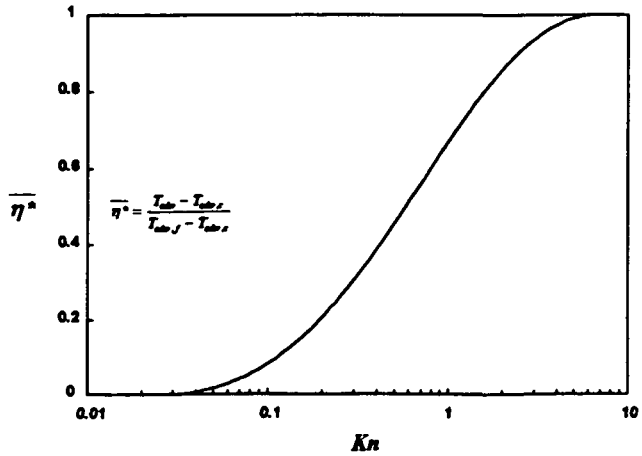

Figure 24. Normalized Recovery Temperature Ratio vs. Free Stream Knudsen Number; (ref. 21).

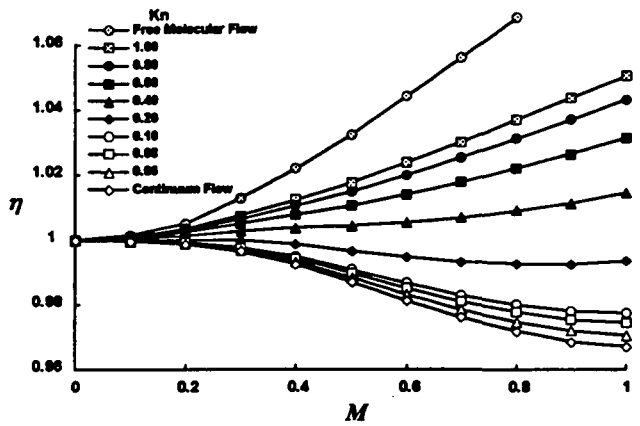

Figure 25. Recovery Temperature Ratio vs. Mach Number for Constant Values of Knudsen Number.

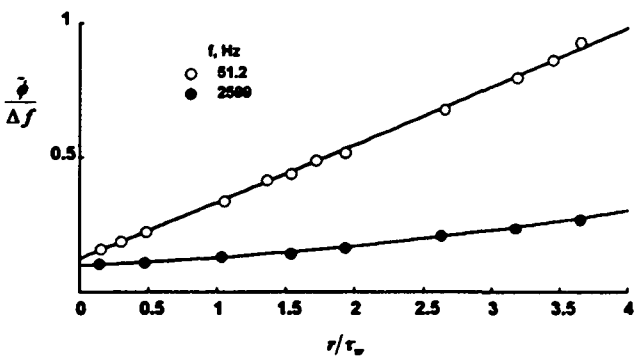

Figure 26. Fluctuation-Diagram of the Filtered Signals (Single-Wire); (ref. 97).

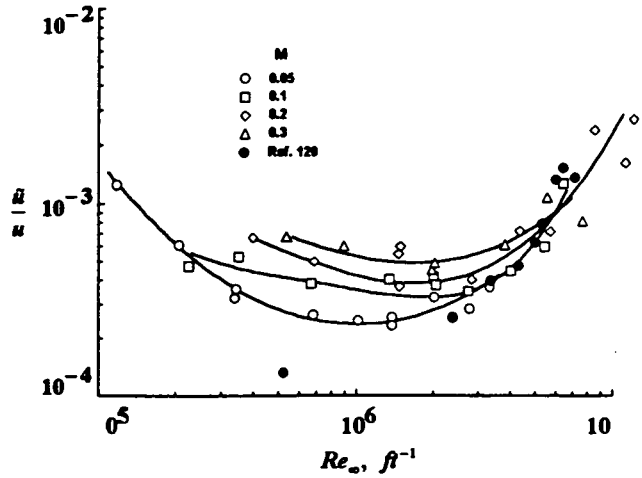

Figure 27. Velocity Fluctuations Measured in the Test Section of LaRC Low Turbulence Pressure Tunnel; (ref. 37).

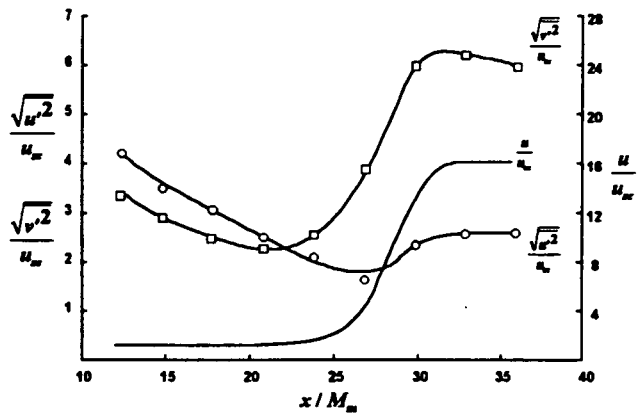

Figure 28. Effect of 16:1 Contraction on Turbulence Generated by 2-inch Square Mesh Grid; R_{M_∞} = 3710; (ref. 118).

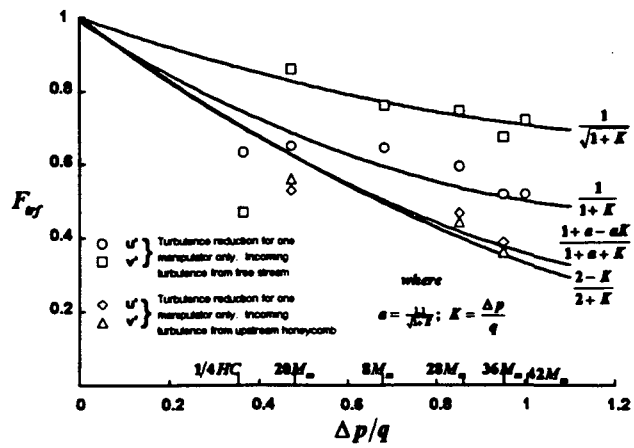

Figure 29. Measured Turbulence Reduction Factor for Various Screens and Combinations of Screens with Honeycomb Compared With Different Theories; (ref. 120).

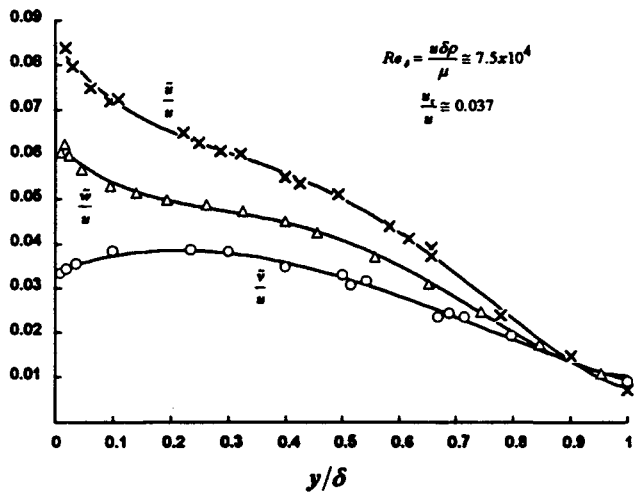

(a) Zero Pressure Gradient

Figure 30. Relative Turbulence Intensities in a Boundary Layer Along a Smooth Wall; (ref. 131).

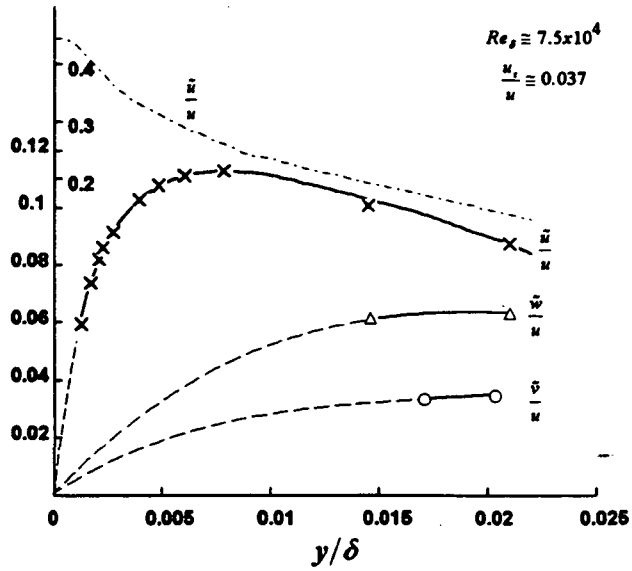

(b) Constant-Stress Layer

Figure 30. Concluded.

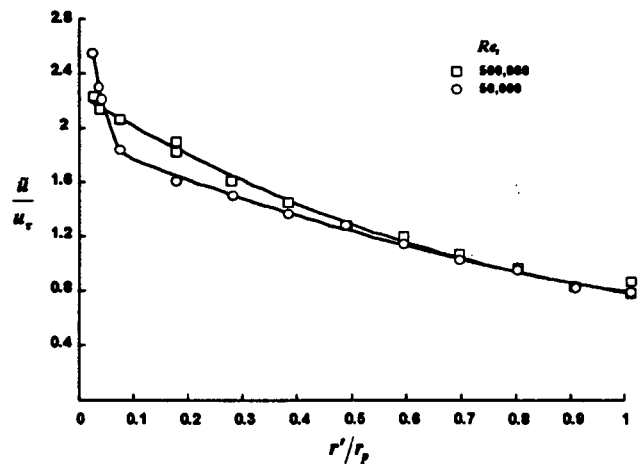

(a) Across the pipe

Figure 31. Distribution of velocity fluctuation in a pipe; (ref. 40).

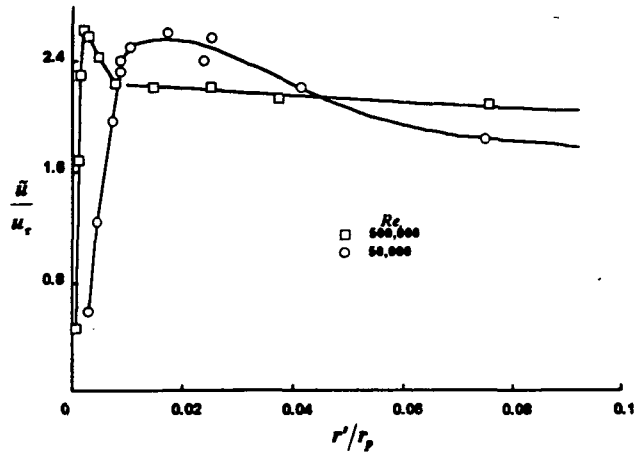

(b) Near the wall

Figure 31. Concluded.

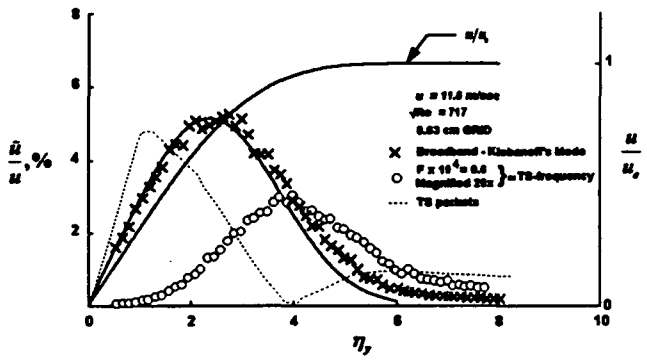

Figure 32. Types of Fluctuation Simultaneously Present in Boundary Layer; (ref. 145).

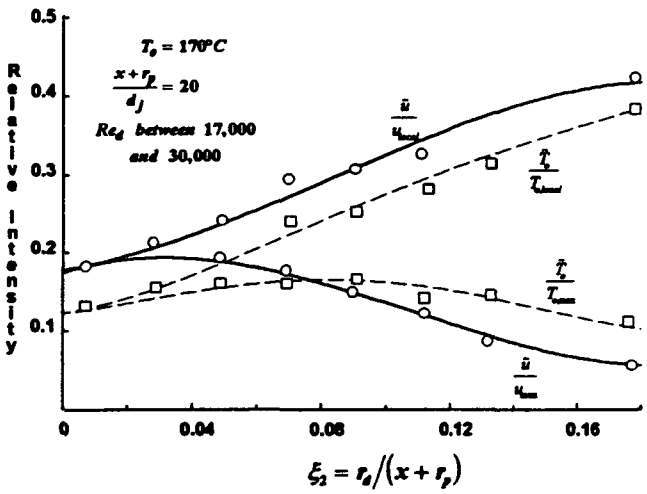

Figure 33. Distribution of Relative Intensity of Turbulent Velocity and Temperature Fluctuations in a Hot Round Free Jet; (ref. 157).

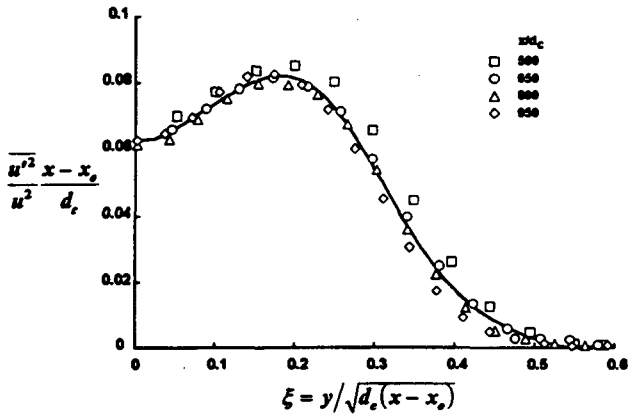

Figure 34. Relative Turbulence Intensity (u-component) in the Wake of a Circular Cylinder; Re_{d_c} = 1360; (ref. 43).

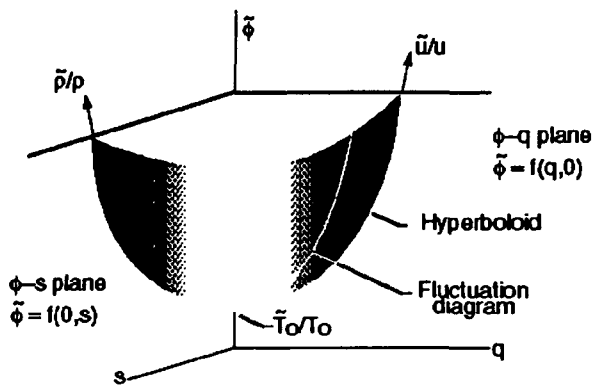

Figure 35. General Fluctuation diagram for Subsonic Compressible Flow; (ref. 168).

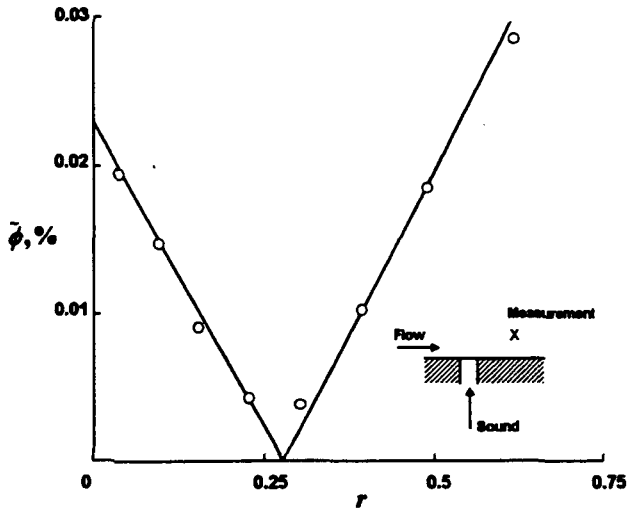

(a) Disturbances from Single Sound Source

Figure 36. Fluctuation Diagram; $M = 0.76$; (ref. 167).

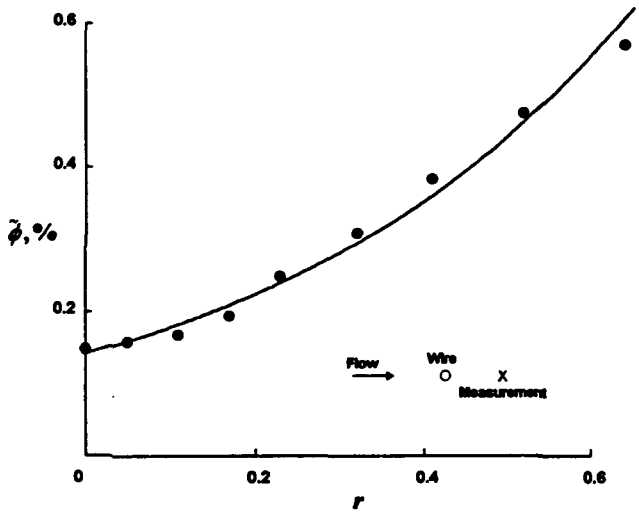

(b) Combination of Vorticity and Entropy Modes Downstream of a Cylinder

Figure 36. Concluded.

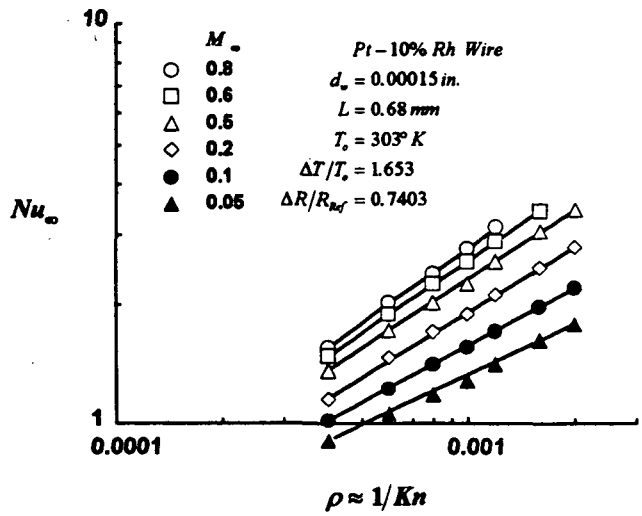

Figure 37. Nusselt Number as a Function of ρ; (ref. 110).

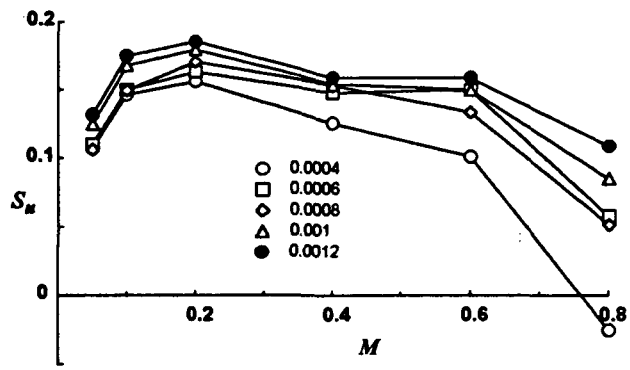

(a) Velocity Fluctuations; $T_o = 303°K$; $\tau_w = 0.672$.

Figure 38. Spangenberg Data; (ref. 163).

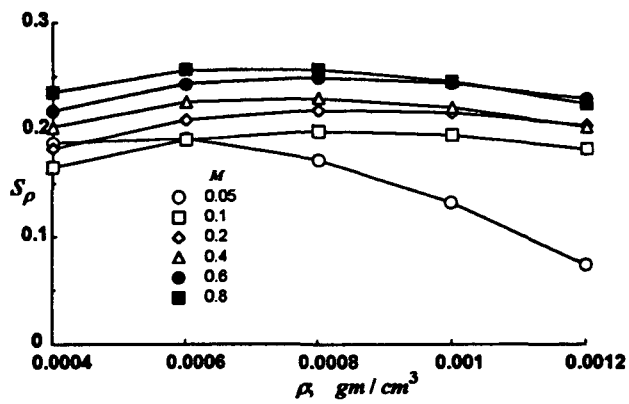

(b) Density Fluctuations; $T_o = 303°K$; $\tau_w = 0.672$.

Figure 38. Continued.

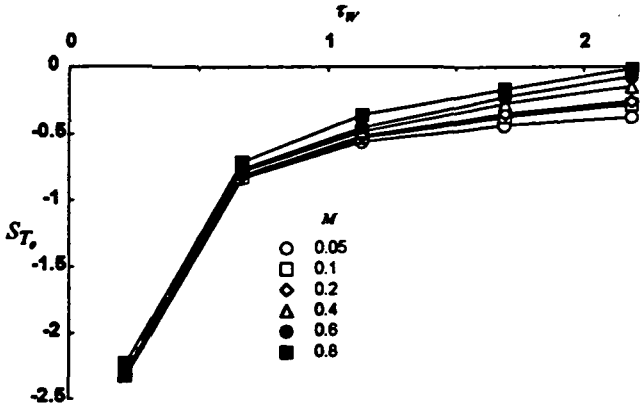

(c) Total Temperature Fluctuations $T_o = 303°K$; $\rho = 0.0008\ gm/cm^3$.

Figure 38. Concluded.

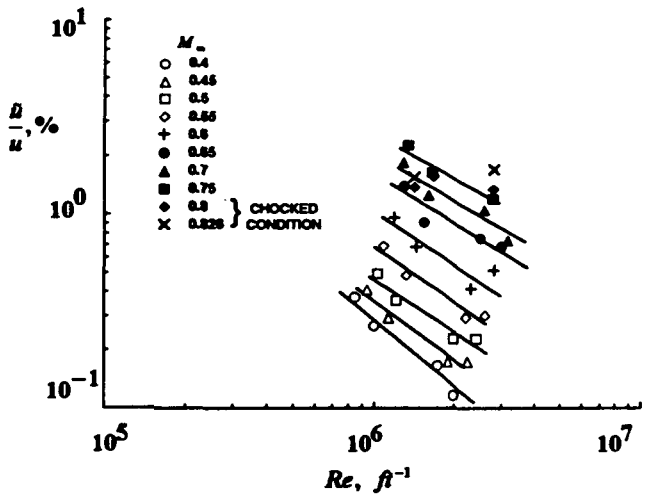

(a) Velocity Fluctuations

Figure 39. Disturbances Measured in the LaRC 8' Transonic Pressure Tunnel using a Three Element Hot-Wire Probe; (ref. 86).

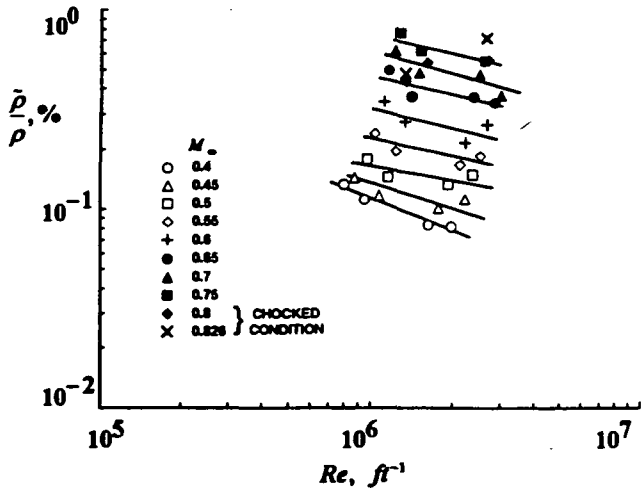

(b) Density Fluctuations

Figure 39. Continued.

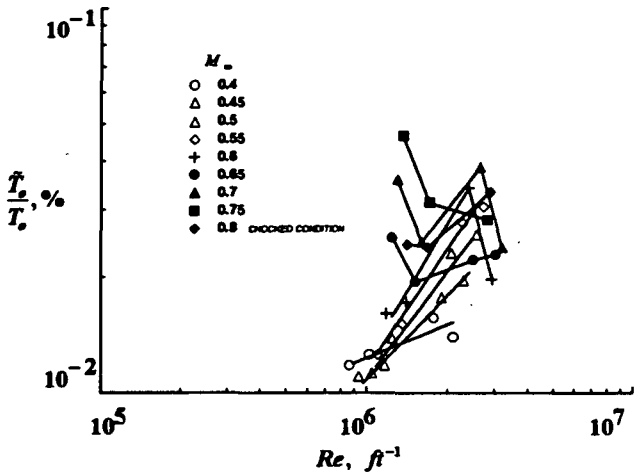

(c) Total Temperature Fluctuations

Figure 39. Continued.

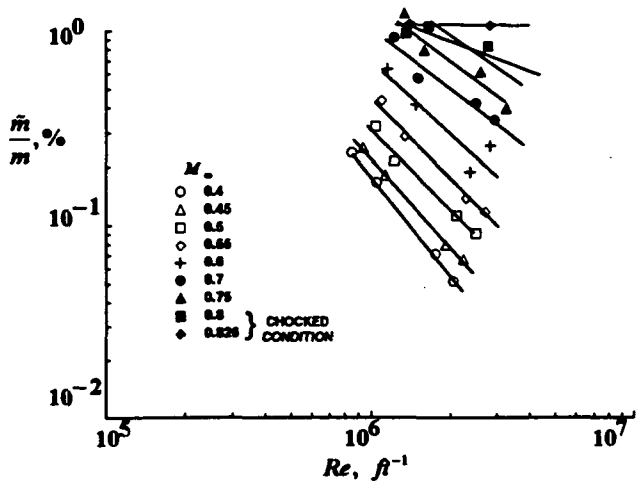

(d) Mass Flow Fluctuations

Figure 39. Concluded.

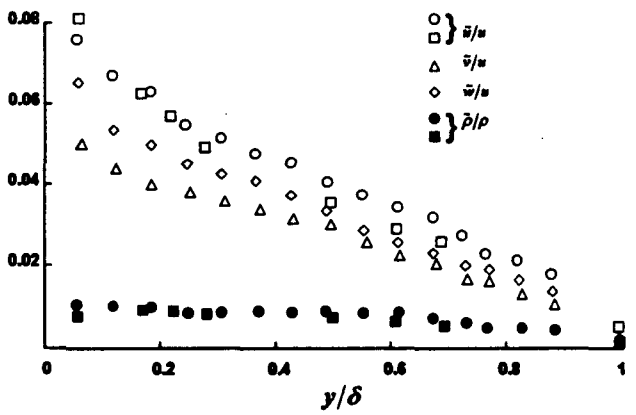

Figure 40. Normalized RMS Velocity and Density Fluctuation Distribution Across the Boundary Layer; (ref. 170).

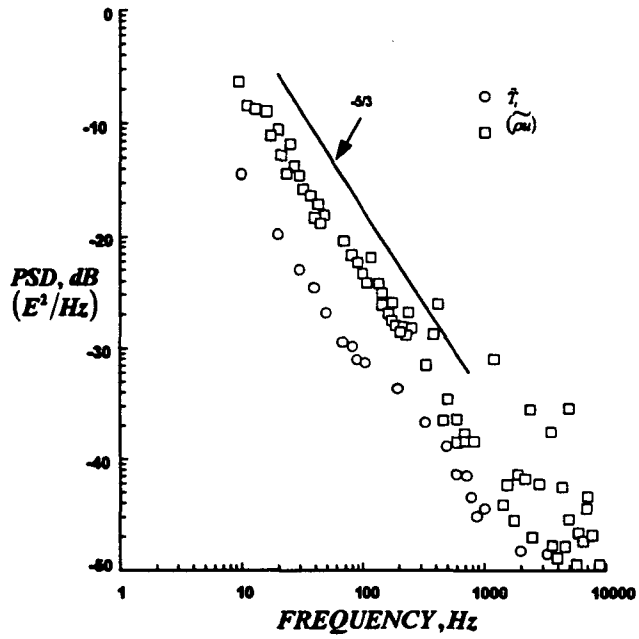

Figure 41. Spectra of Mass Flux and Total Temperature Fluctuations; 3.6 km; $M = 0.57$; Feb. 79; (ref. 49).

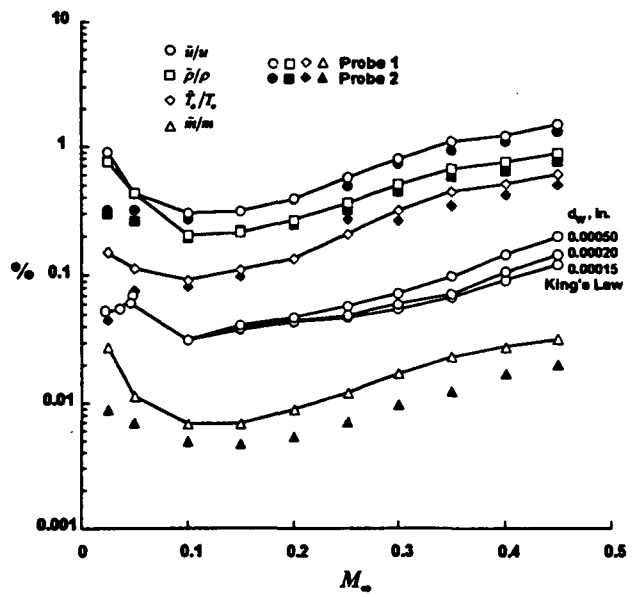

(a) Measured Fluctuations

Figure 42. Fluctuations Measured in the LaRC Low Turbulence Pressure Tunnel; $p_o = 15$ *psia*; (ref. 172).

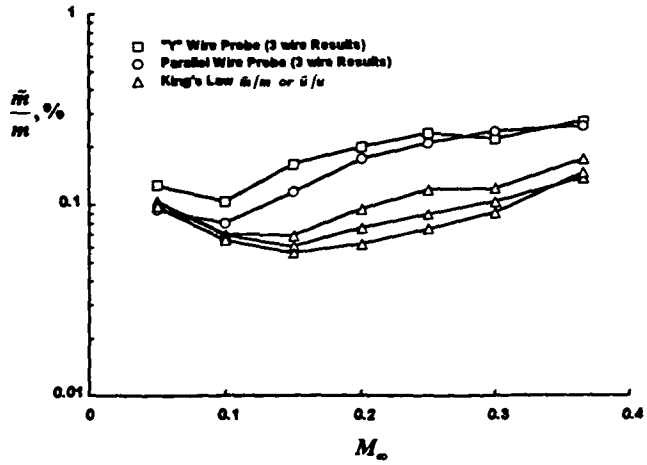

(b) Mass Flow Fluctuations

Figure 42. Concluded.

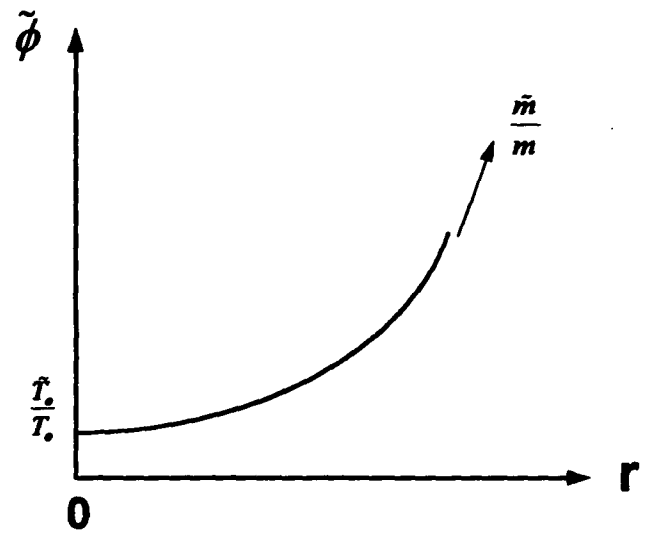

Figure 43. Generalized Fluctuation Diagram for Supersonic Flow.

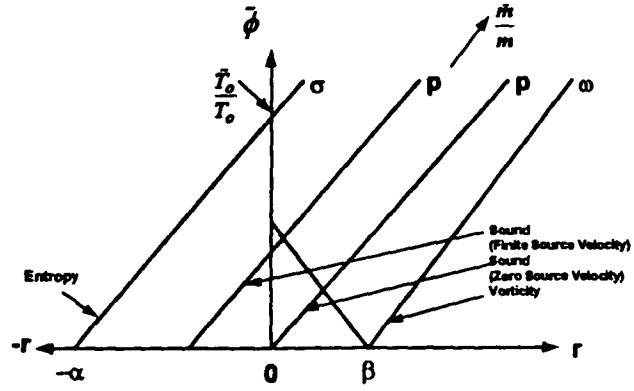

Figure 44. Generalized Mode Diagram for Supersonic Flow.

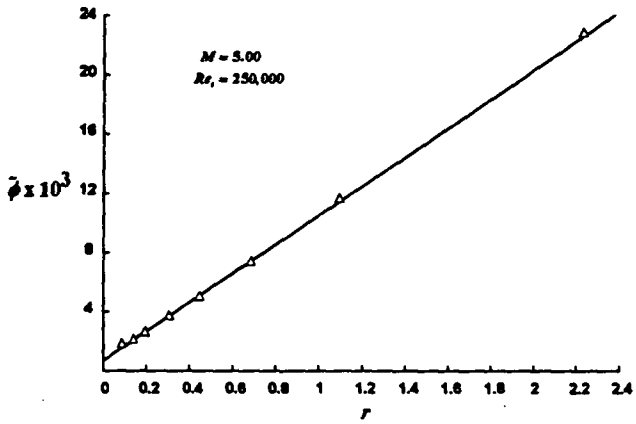

Figure 45. Mode Diagram Measured in Test Section for $M = 5.0$; (ref. 185).

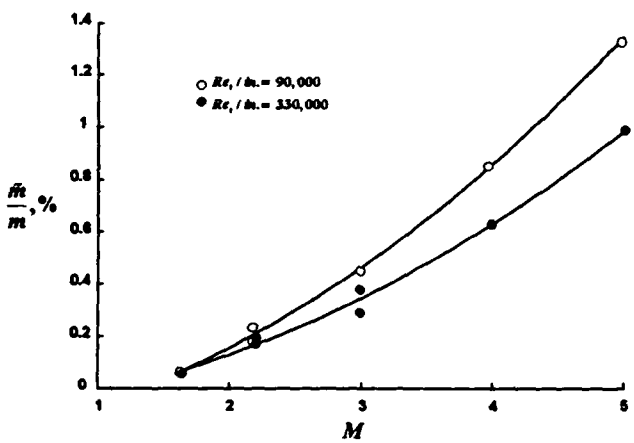

(a) Mass Flow Fluctuations

Figure 46. Variation with Tunnel Mach Number; (ref. 185).

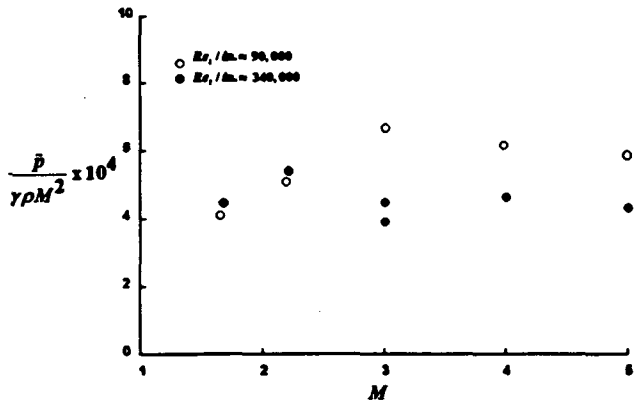

(b) Pressure Fluctuation

Figure 46. Concluded.

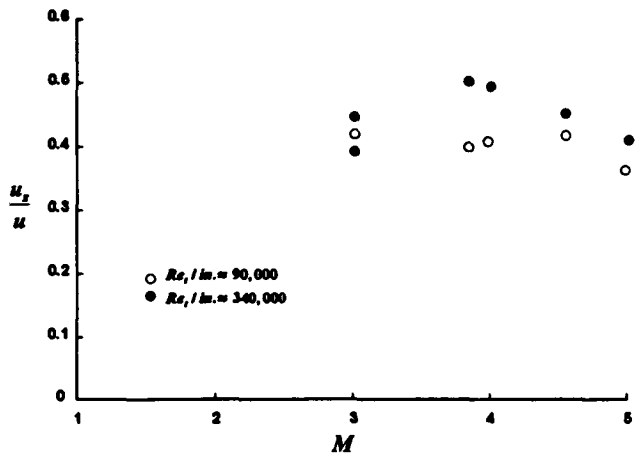

Figure 47. Variation of Source Velocity with Tunnel Mach Number; (ref. 185).

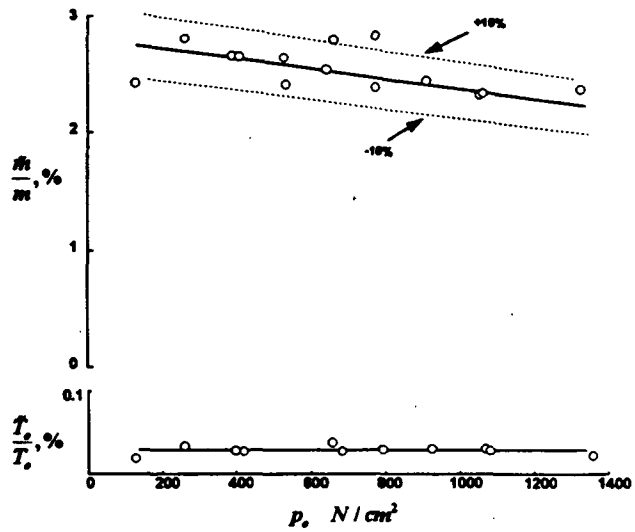

Figure 48. Root-Mean-Square Mass-Flow and Total-Temperature Fluctuations in the LaRC 22" Hypersonic Helium Tunnel; (ref. 181).

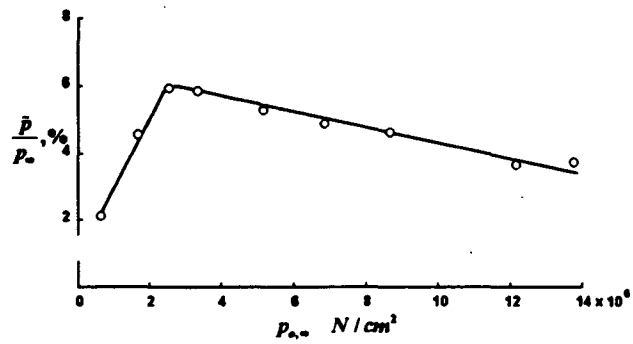

Figure 49. Pressure Fluctuation in the LaRC 22" Hypersonic Helium Tunne; (ref. 181).

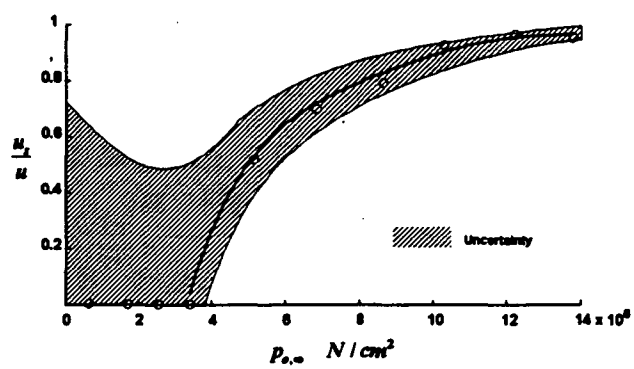

Figure 50. Relative Source Velocities in the LaRC 22" Hypersonic Helium Tunnel; (ref. 181).

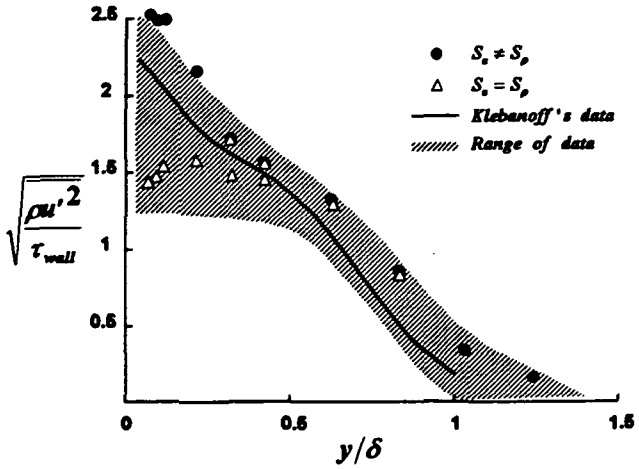

Figure 51. Velocity Fluctuation Measurements in Boundary Layer; Influence of the Sensitivity Coefficient to Mach Number; Shaded Zone - Range of the Available Velocity Fluctuation Data in Supersonic Boundary Layers, Including Hot-Wire and Laser-Doppler Measurements; (ref. 162).

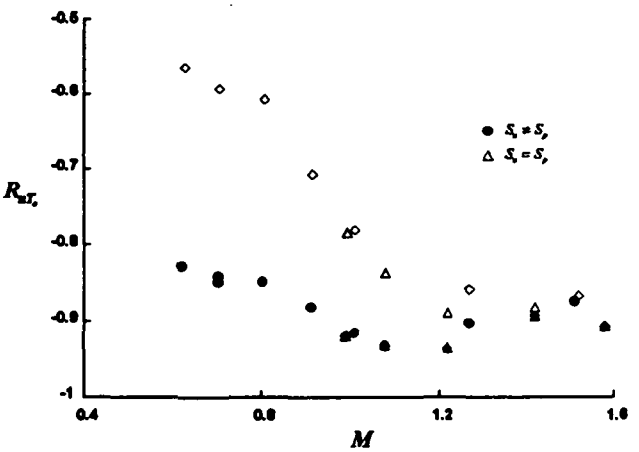

Figure 52. Variation of $R_{u\tau_t}$ with Mach Number Through Boundary Layer; (ref. 177).

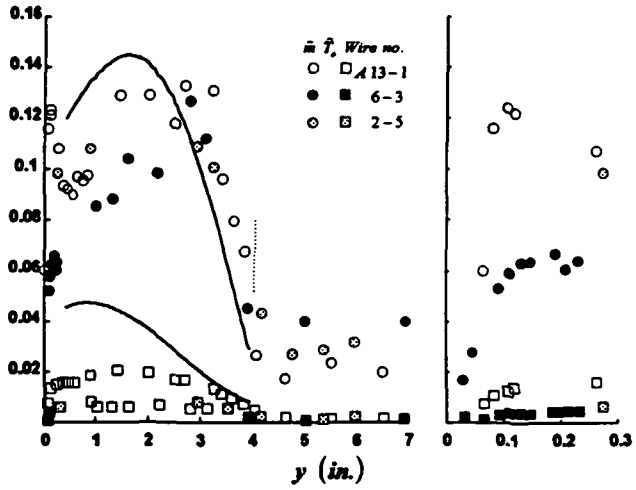

Figure 53. Variation of Wide-Band RMS Mass-Flux and Total-Temperature Fluctuations Across the Boundary Layer. Kistler's Results at $M = 4.76$ (Solid Line) are Included for Comparison; (ref. 188).

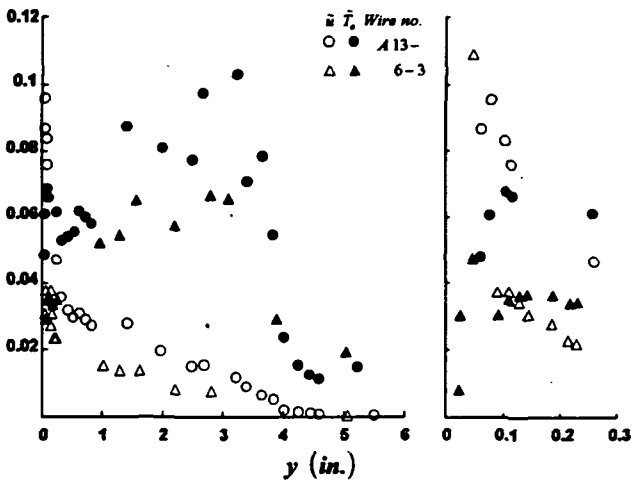

Figure 54. Variation of Wide-Band RMS Velocity and Static Temperature Fluctuations Across the Boundary Layer; $p' \neq 0$; (ref. 188).

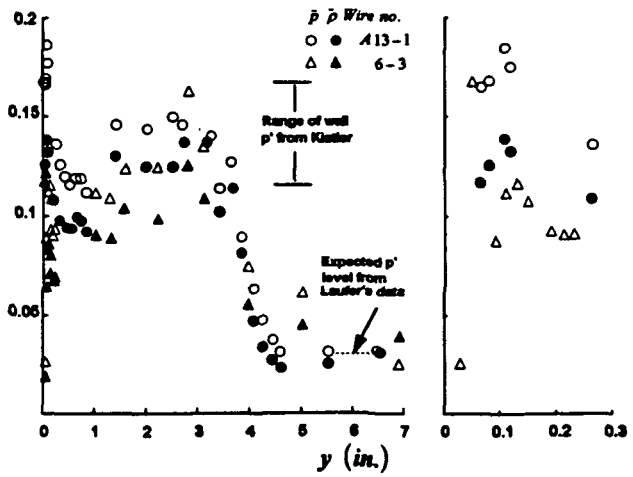

Figure 55. Variation of Wide-Band RMS Pressure and Density Fluctuations Across the Boundary Layer; $p' \neq 0$; (ref. 188).

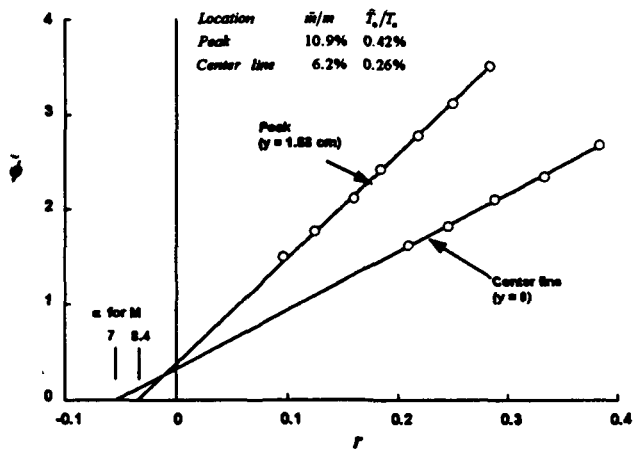

Figure 56. Mode Diagrams in Wake of 15° Half-Angle Wedge; (ref. 181).

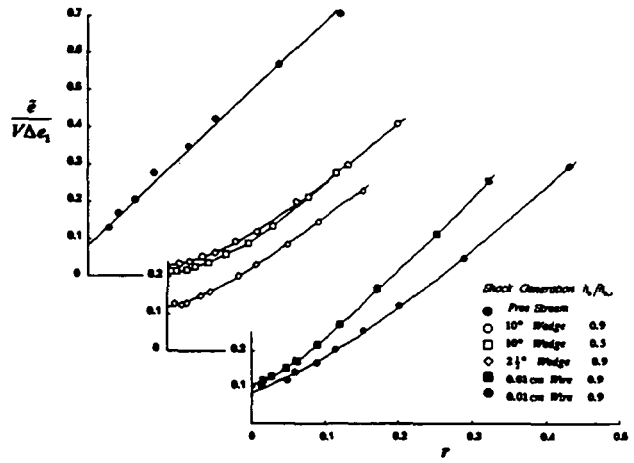

Figure 57. Fluctuation Mode Plots; $M \approx 21$; $p_o = 12.41 \times 10^6$ N/m^2; (ref. 48).

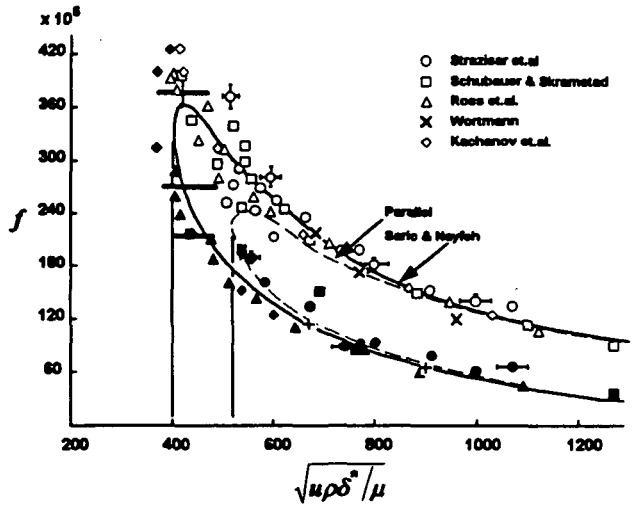

Figure 58. Neutral Disturbance in Studies of Laminar Boundary Layer Stability; (ref. 205).

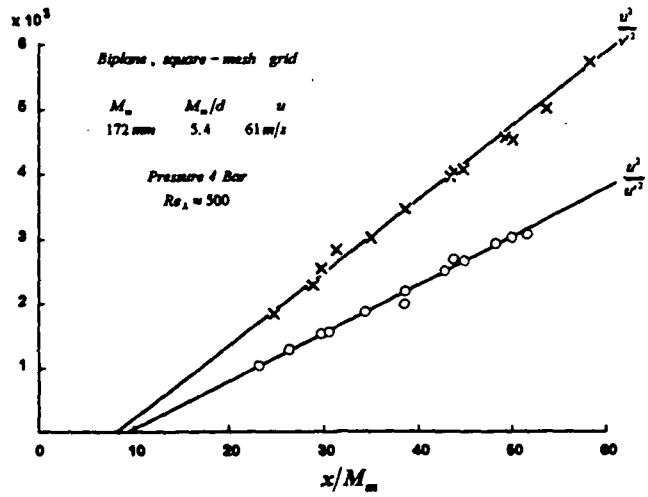

Figure 59. Decay of $\frac{u^2}{u'^2}$ and $\frac{u^2}{v'^2}$ Downstream of a Grid; (ref. 206).

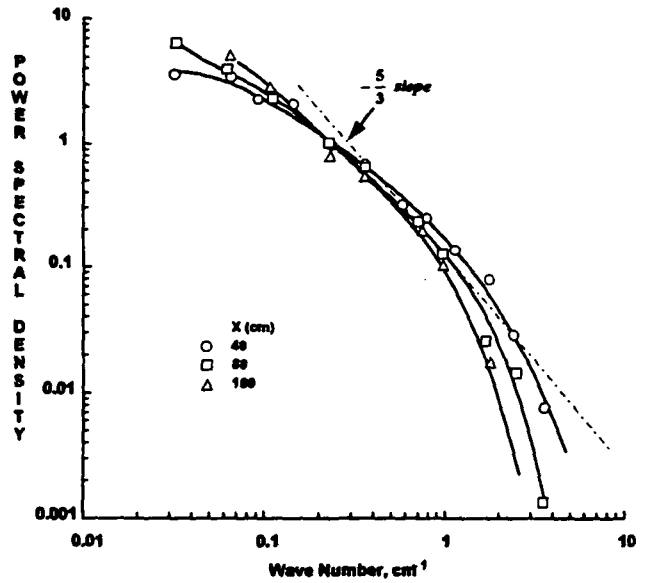

(a) Poser Spectral Density of u^2; $u = 10$ m/s; (ref. 88)

Figure 60. One-Dimensional Spectrum.

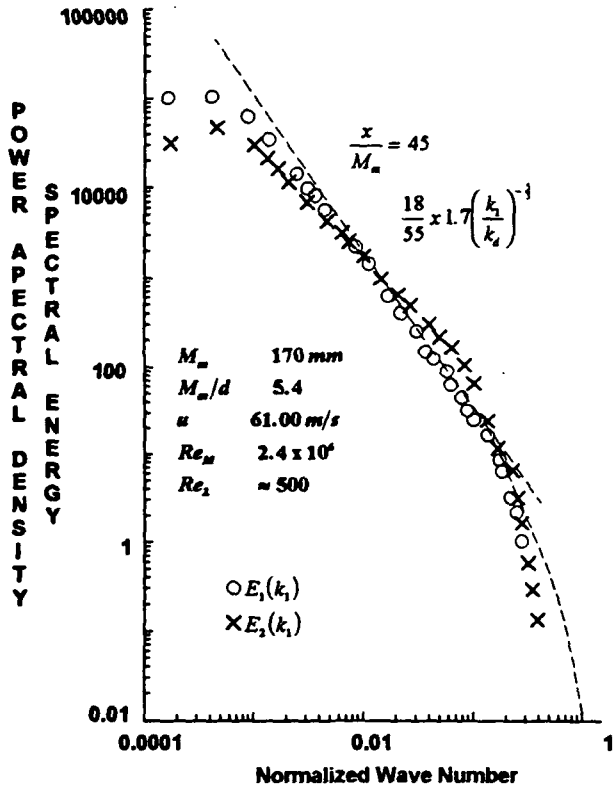

(b) Spectral Energy; (ref. 206)

Figure 60. Concluded.

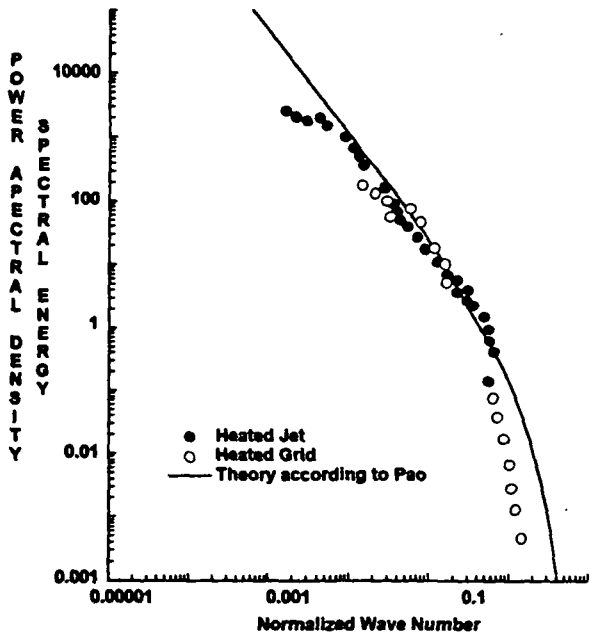

Figure 61. One-Dimensional Temperature Spectrum; (ref. 207).

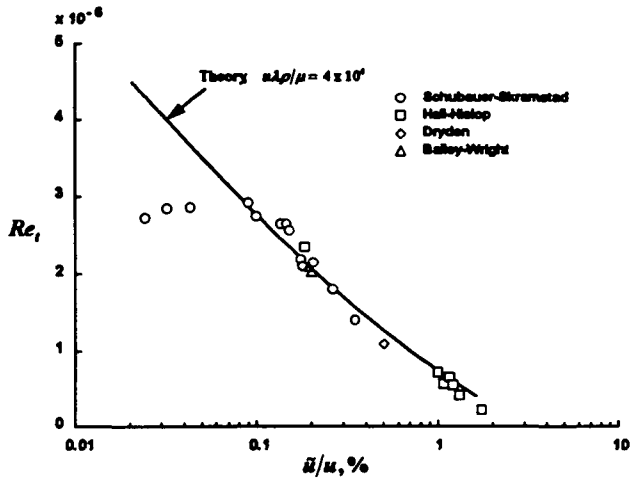

Figure 62. Effect of Free-Stream Turbulence on Boundary Layer Transition; (ref. 208).

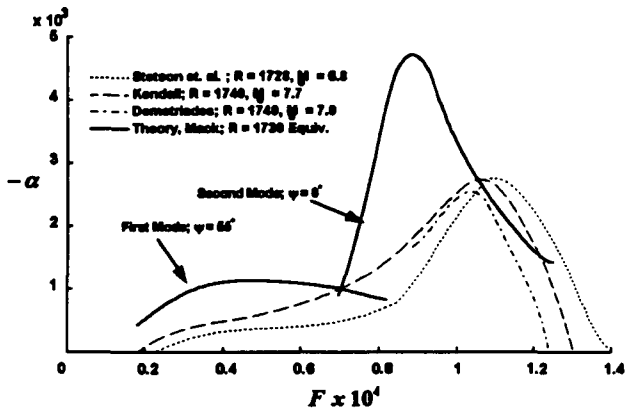

Figure 63. Amplification Rate vs. Frequency, Comparison with Others; (ref. 209).

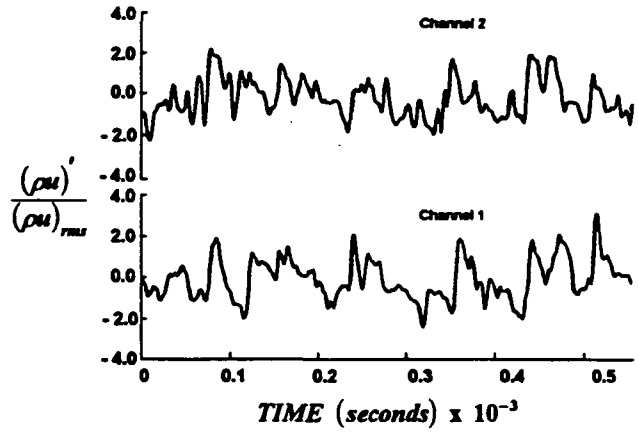

Figure 64. Typical Fluctuating Mass Flow Data from Two Hot-Wires Indicating Similarity Between the Signals; (ref. 226).

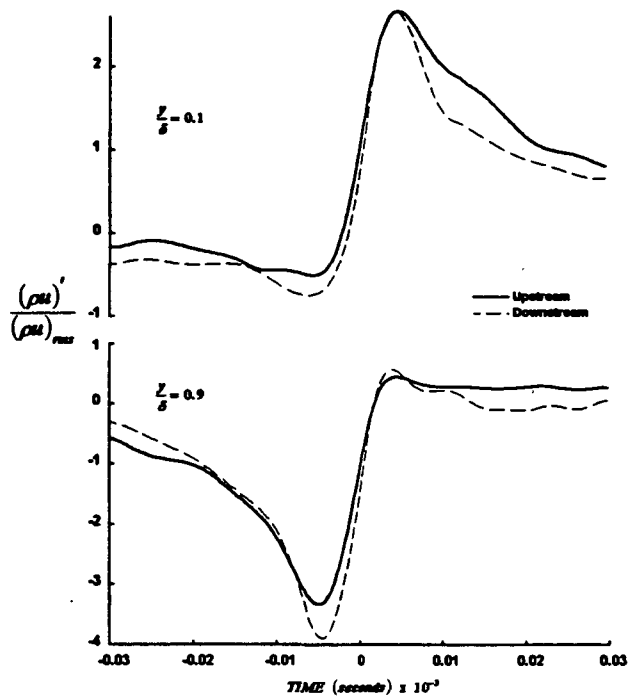

Figure 65. Ensemble Averaged Positive Events in the Weak Perturbation Case; (ref. 226).

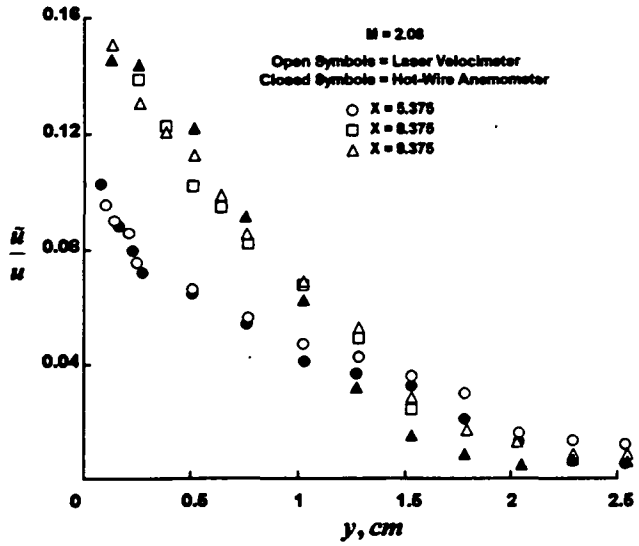

Figure 66. Comparision of Streamwise Velocity Fluctuations Measured by Hot-Wires and Laser Velocimeter; (ref. 227).

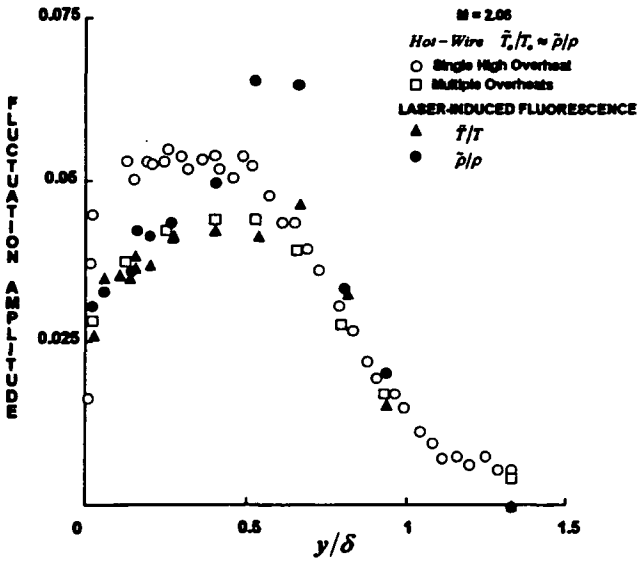

Figure 67. A Comparison of the Distribution of RMS Fluctuation Amplitudes in Static Temperature and Density within the Boundary-Layer obtained using a Hot-Wire at Single and Multiple Overheat Ratios with Direct Measurements Obtained using Laser-Induced Fluorescence (LIF). The LIF data have been Corrected for Instrument Noise; (ref. 229).

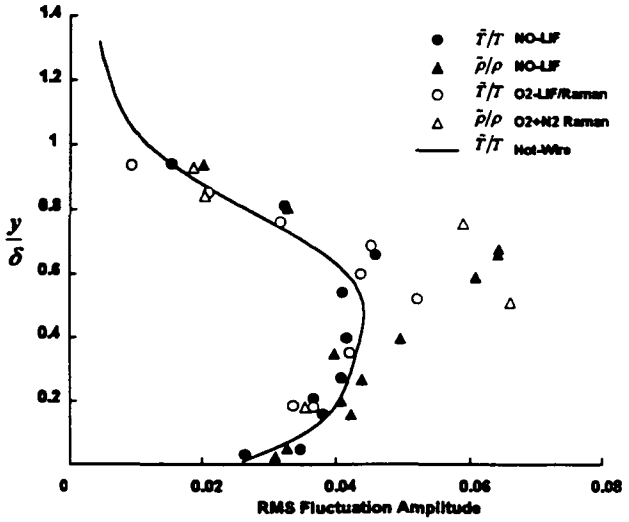

Figure 68. Comparisons of Temperature and Density RMS Fluctuation Amplitudes Obtained with LIF Techniques or Implied by Hot-Wire Anemometer Data. Flow Conditions are the Same as in Figure 66. For Each Variable, the Fluctuation Amplitude is Normalized by the Local Time-Averaged Value; (ref. 230).